Not in DRA

OCEAN DATA SYSTEMS, INC.

(NASA-CR-149213) ATMOSPHERIC ANALYSIS AND PREDICTION MODEL DEVELOPMENT, VOLUME 1 Final Report (Ocean Data Systems, Inc.) 117 p HC A06/MF A01 CSCL 04A

N77-14650

Unclas

G3/46 15446

[redacted]

Prepared For

Econ INCORPORATED

900 State Road

Princeton, NJ 08540

odsi

Contract No. NASW-2558

OCEAN DATA SYSTEMS, INC.
6000 EXECUTIVE BLVD., ROCKVILLE, MARYLAND 20852 • 301/881-3031

Submitted to
ECON, INC.
Princeton, New Jersey

Volume I

ATMOSPHERIC ANALYSIS AND PREDICTION MODEL DEVELOPMENT

Final Report

Prepared under
Contract No. NASW-2558
Modification 5

August 1976

Prepared by
Philip G. Kesel
Robert E. Wellck
Rodger A. Langland
Howard L. Lewit
OCEAN DATA SYSTEMS, INC.
Monterey, California

ABSTRACT

A set of hemispheric atmospheric analysis and prediction models was designed and tested by Ocean Data Systems, Inc. for ECON, Inc. under Contract NASW-2558 in support of SEASAT of the National Aeronautics and Space Administration.

All programs execute on either a 63 x 63 or 187 x 187 polar stereographic grid of the Northern Hemisphere. Parameters for objective analysis include sea surface temperature, sea level pressure, and twelve levels (from 1000 to 100 millibars) of temperatures, heights, and winds. Stratospheric extensions (up to 10 millibars) are also provided. Four versions of a complex atmospheric prediction model, based on the primitive equations, are programmed and tested. These models execute on either the 63 x 63 or 187 x 187 grid, using either five or ten computational layers. Complete descriptions of all models are provided in Volumes II and III of this Final Report.

The coarse-mesh (63 x 63) models are tested using real data for the period 21-23 April 1976. The fine-mesh (187 x 187) models were debugged, but insufficient computer resources precluded production tests. Preliminary test results for the 63 x 63 models are provided. Problem areas and proposed solutions are discussed. Complete test results will be documented at a later time.

TABLE OF CONTENTS

LIST OF TABLES

LIST OF FIGURES

Figure		Page

Figure		Page

Figure		Page

I. INTRODUCTION

This document describes the results obtained from Ocean Data Systems, Inc. (ODSI) analysis and prediction model development effort for ECON, Inc. under Contract No. NASW-2558, Modification 5, in support of SEASAT for the National Aeronautics and Space Administration (NASA). This is the first volume of three volumes comprising the final report on this contract.

For complete descriptions of the models, the reader is referred to Volumes II and III of this final report which are entitled "Meteorological Analysis Models" and "PECHCV, PECHFV, PEFHCV and PEFHFV - A Set of Atmospheric, Primitive Equation Models for the Northern Hemisphere", respectively.

The test results presented here are incomplete due to the lack of sufficient computer resources during the contract period to exercise most of the 187 x 187 analysis programs and the two 187 x 187 primitive-equation forecast models. Results are presented for the 63 x 63 analysis models and the five sigma layer - 63 x 63 and the ten sigma layer - 63 x 63 forecast models. Complete results for all the analysis and forecast models will be presented at a later date.

Section II describes the results of the analysis modeling including a brief description of the models, a description of the meteorological scenario chosen for the test, and the test results. The test results describe the production run organization, the vertical structure of the analyses, problems

and proposed solutions in the tropical area analysis, the effect of inclusion of lower level data in the refined vertical structure of the analysis, a comparison of the ODSI and FNWC analysis, and, finally, a comparison of a coarse mesh and fine mesh sea surface temperature analysis.

Section III describes the results of the forecast modeling, including a brief description of the forecast models and the test results. The test results include a discussion of the problems related to the use of realistic model terrain, the results of a 24-hour forecast with the five sigma layer - 63 x 63 forecast model (PECHCV), and the results of a 24-hour forecast for the same period with the ten sigma layer 63 x 63 forecast model (PECHFV).

Finally, it should be pointed out that the tables and figures pertaining to a given section appear at the end of that section.

II. ANALYSIS MODELING

This section describes the results, problem areas and solutions in some cases, of the analysis modeling effort. Section II-A gives a brief overview of the analysis models. Section II-B describes the meteorological scenario chosen as the test period.

Section II-C describes the test results obtained. Included are the production run organization describing the bootstrapping technique used to obtain analyses at 12-hour intervals, and problems arising from the inclusion of certain types of data in the tropics in the analysis. Also included are the method and effect of including lower level data in the analysis, a comparision of ODSI and FNWC analyses, and a comparision of a fine mesh and coarse mesh sea surface temperature analysis.

A. Model Descriptions

The analysis portion of this project involved developing two sets of analysis programs, one set on the 63 x 63 polar stereographic grid and the other on the one-third mesh 187 x 187 grid. Each set of analyses involves numerous programs, each analyzing a different parameter. These parameters are sea level pressure, sea surface temperature, and ten or twelve levels of upper air temperatures, heights

and winds. The theory behind the analysis scheme called the Pattern Conservation Technique along with descriptions of the various programs is described in Volume II of this final report entitled "Meteorological Analysis Models".

B. Meteorological Scenario

The synoptic situation on 22 April 1976 at 1200 Z was picked as the date-time-group to initialize the forecast model. This particular initial condition was picked because active cyclogenesis occurred in the next 24 hours in many systems distributed around the world. Figure II-9 shows the surface pressure analysis that was used to initialize the forecast model. The surface pressure analysis that verifies the 24-hour forecast is shown in Figure II-15. Notice the deepening of the surface low pressure systems initially located north of Korea, east of Kamchatka, in the Gulf of Alaska and over the North Atlantic. The rapid development of these systems should provide a challenging test of the forecast model performance. Similar analyses for the 500 mb level are shown by Figures II-12 and II-18.

The fields are not displayed equatorward of 20 degrees latitude because of their unmeteorological appearance. The cause of this problem will be discussed later.

C. Test Results

1. Production Run Organization

The analysis models were initialized from the FNWC 4/21/76 12Z fields. The initial analysis linearly interpolates the 950- and 900-mb temperature first guess fields using 1000- and 850-mb information. The initial wind analysis does not include divergence.

Subsequent analysis cycles (of 12-hour forecasts used to initialize the next analysis) are performed to analyze through the 4/23/76 12Z date-time group. (See Figure II-1.) In these cycles, the divergence in the 12-hour forecast wind fields is used as a constraint in the upper air wind analyses. The five-level 63 x 63 PE model (PECHCV) was used to produce these forecast guess fields.

The sea level pressure and 500 mb fields for each date-time group along with the corresponding FNWC analyses and comparisons of the ODSI and FNWC analyses are shown in Figures II-2 through II-19.

Table II-1 on page II-12 lists both the types of observations included in each analysis and a typical number of observations of each type (in parentheses). One should keep in mind that satellite retrieved heights and temperatures are restricted to poleward of 20 degrees latitude. The reason is described in Secton II-C-3.

2. Vertical Structure of the Analyses

A series of charts for 4/22/76 12 Z (Figures II-20 through II-30) is included to illustrate the vertical variations of the horizontal sections of the atmosphere. The analysis sequence has been specifically designed to produce a hydrostatically consistent set of analyses. This is a prerequisite for initialization of a primitive equation forecast model.

Once first guess fields for the sea level pressure and upper air temperatures are obtained, independent analyses of these parameters is done. These analyses are used to calculate height analysis first guess fields using the hydrostatic equation. Next the height analysis is performed. The altering of the height fields to agree with the new observations leaves the height and temperature fields hydrostatically inconsistent. Therefore, the height fields are transformed to stability fields, the stabilities are set to zero if they are negative, and the resulting stabilities are then transformed back to heights. Next, a set of consistent temperature fields is generated using a linear transformation to convert heights to temperature.

Notice that the lower troposphere is composed of numerous closed cellular circulations. These give way to (open) wave structures in the mid and upper troposphere. The troposphere is characterized by decreasing temperatures

toward the pole while the stratosphere is just the opposite. Notice also that the majority of tropospheric low pressure systems are characterized by cold centers or troughs of cold air.

3. Tropical Area Analysis

The first analysis runs attempted to use <u>all</u> available data. It soon became evident that data in the tropics, particularly satellite retrieved data, produced unmeteorological features. (See Figure II-32.) FNWC has experienced similar problems. Satellite retrieved parameters, especially heights, are sometimes in disagreement with conventional observations. Some of the contributing reasons are: a different reference level is used for determining the heights, inversions in the lower troposphere are not detected, and cloud contamination leads to incorrect retrievals. These unmeteorological features must be removed in some manner because the forecast model attempts to predict their time changes. This results in amplified noise in the tropics. These forecasts are used as first guess fields for the next analysis cycle which further compounds the problem. The ODSI forecast model uses rigid, insulated, slippery-wall boundary conditions which are not as effective as the FNWC restoration type boundaries in handling this tropical problem. FNWC (as a result of years of experimentation) imposes severe restrictions on the character of the upper air analysis

in the tropical regions. These include: 1) Small reject tolerances in the tropics as compared to mid latitudes resulting in rejection of many questionable observations; 2) Heavy filtering of the final analysis in the tropics to remove small scale features; and 3) Use of a special procedure to derive "balanced" winds and heights in the equatorial regions, leading to modifications in the lateral boundary conditions in a manner consistent with conditions in the extratropics.

The ODSI analysis procedure places restrictions as to the stage at which filtering of the tropical regions can be performed. (See Figure II-31.) Smoothing of the first guess forecast fields would be ineffective because analysis of data in the tropics would reintroduce the unwanted features. As a partial solution, satellite retrieved heights and temperatures are only introduced north of 20 degrees north.

Other types of conventional data can cause features in the tropics that are undesirable. Therefore a filter, effective only in the tropical areas, was applied after the surface pressure, upper air temperature and upper air height analyses. Filtering of the retrieved temperatures or wind analyses destroys the balance between the mass and the motion fields and is unacceptable for initializing the forecast model.

First attempts at filtering the tropics used a Laplacian type filter applied equatorward of 20 degrees latitude. These results were better than those obtained when no filtering was done, but were still unacceptable. Tests are continuing to find an acceptable way of removing this noise.

4. Inclusion of Lower Level Data

The 950 and 900 mb levels were included in the vertical structure to better specify the lower troposphere. Since these are not mandatory reporting levels, the radiosonde checking program generates these levels by interpolation from the merged mandatory and significant level information.

In the absence of this data, the 950 and 900 mb analysis fields would either be an interpolation between the 1000 and 850 mb levels or the first guess obtained from the forecast model. Figures II-33, through II-36 show the 900 mb temperature and height fields with and without the additional data. Considerable detail is included in the fields as a result of the additional data. In the temperature analysis, notice the change of the temperature trough off the east coast of the United States, and the sharpening of the trough in the Gulf of Alaska. Disregard the centers over the Himalayas. These are a result of a deficiency in the forecast model outputs at this stage of the project which

will be discussed separately in Section III.

In the height analysis notice the change in the central values of the low centers as a result of data.

Figure II-37 shows the 900 mb temperature field which was retrieved from the final 900 mb height analysis using the linear transforms. Focusing on the features along the east coast of the United States, one can see that the retrieved temperatures have lost some of the detail obtained earlier in the temperature analysis. The causes for this will be investigated further. An attempt to initialize the forecast model with the analysis temperatures as opposed to the retrieved temperatures will be made to see how it affects the forecast.

Table II-2 shows a distribution by layer of the number of grid points at which stability corrections had to be made. The first column is the total number of points at which the analyzed heights had to be altered to obtain a stable profile. The next columns provide a latitudinal breakdown of the total. The large number of changes in the band from the equator to 30°N are a result of the heavy filtering done in the tropics. Notice that the distribution in the vertical is concentrated in the lower layers and around layers 7 and 8. These layers are relatively thin. In the lower layers the additional resolution allows for better depiction of the observed vertical variations. In the upper troposphere the resolution allows for the specification of the

tropopause. Small changes or inconsistencies in height can produce large changes in the value of stability -- resulting in many layers that are unstable. Further investigation of the retrieval procedure is also underway.

5. Comparison of ODSI and FNWC Analyses

Figures II-8 and II-9 show the FNWC and ODSI 4/22/76 12Z sea level pressure analyses. Figure II-10 shows their difference. Figures II-11, II-12 and II-13 show the same information for the 500 mb height field.

The differences between ODSI and FNWC analyses are relatively small except for a few isolated centers, especially at 500 mb. There are many explanations for the differences. Probably the largest contributor is the different source of the first guess field for the two different analyses. The ODSI forecast model is the source for both the surface and 500 mb ODSI analyses. The FNWC first guess fields, in contrast, are obtained through extrapolation or barotropic model prognosis. These differences can, in certain synoptic situations, and through deficiencies in one method or the other, lead to considerably different (analysis) first guess fields. In the absence of current data to correct the situation this can produce the differences shown. The 500 mb and sea level difference east of Greenland is a good example of this variation. Other sources of the difference between the analyses are: different amounts of data available at analysis time and different

relative weights given to different sources of data, different types of analysis programs and different tuning of similar analysis schemes (including the filtering of the output fields).

The large centers of difference noted around the Himalayas are a result of an ODSI forecast model deficiency related to terrain which has since been corrected.

6. Comparison of Coarse Mesh and Fine Mesh Sea Surface Temperature Analyses

Figure II-39 shows the ODSI 63 x 63 SST analysis, II-38 the FNWC analysis, and II-40 the ODSI 187 x 187 analysis. It should be pointed out that the FNWC analysis is produced on a 125 x 125 grid from which the 63 x 63 is extracted.

The differences between the ODSI and FNWC 63 x 63 analyses are a result of many causes. Each analysis uses its last analysis as a first guess. Therefore differences are cumulative. Both analyses are done with the same basic technique but data weights and tuning are different. The ODSI analysis has the advantage of all available conventional ship observations while the FNWC analysis, due to operational necessity, was produced before all the data was available. The FNWC analysis, on the other hand, uses satellite derived observations which were not included in the ODSI analysis.

The ODSI 187 x 187 analysis uses the same data as the 63 x 63 analysis. Two characteristics of the 187 analysis

have been noted:

- Spreading of data is a function of a number of grid intervals. Since the 187 analysis has three intervals for the same earth distance as one interval on the 63 grid, the spreading on the 187 analysis is restricted to a smaller geographical region. This points out the advantage of having numerous equally spaced observations as SEASAT would provide.

- The available display program performs a three subinterval interpolation on the 63 x 63 analysis in order to achieve smooth contours. Otherwise the contours would appear as a series of connected straight lines. The 187 display however does not use the subinterval interpolation. This implies that the 187 analysis is as smooth as it is displayed, an added advantage of the increased resolution.

Charts II-41 and II-42 show the 63 X 63 and 187 x 187 SL field respectively and II-45 and II-46 show similar SD fields. These fields are produced by a scale separation program. The SL field depicts the long-wave disturbance pattern and the SD field the short wave disturbances. It should be pointed out that the 187 output is obtained by using the 63 x 63 separation program after extracting every third grid point. A program is being written to operate on the large field which should produce more valid comparisons.

One would expect the long wave features to be the same on the two resolutions. However, the SD fields obtained from the 187 grid should be able to better depict the small scales implied by the observations. Notice that the SL fields are almost identical but there is considerably more difference in the SD fields.

TABLE II-1

TYPICAL DATA SAMPLES

ANALYSIS

SST	SHIPS (400)
SURFACE PRESSURE	SHIPS (500), LAND (4200)
TEMPERATURE	RADIOSONDES (550), SIRS (150)
HEIGHT	RADIOSONDES (550), SIRS (150) WINDS FOR GRADIENTS: AIREPS (200), PIBALS (150), RADIOSONDES (500), SATELLITE (350 LOW) (200 UPPER)
WIND	AIREPS (200), PIBALS (150), RADIOSONDES (500), SATELLITE (350 LOW) (200 UPPER)

TABLE II-2

STABILITY CORRECTIONS

LAYER	TOTAL NUMBER	(EQ-30N)	(30N-45N)	(45N-60N)	(60N-90)
1	1007	488	255	145	118
2	1136	408	379	207	141
3	783	211	269	188	114
4	326	77	147	69	33
5	48	21	19	7	1
6	155	37	58	40	20
7	215	139	48	21	7
8	286	115	151	20	0
9	48	45	3	0	0
10	9	9	0	0	0

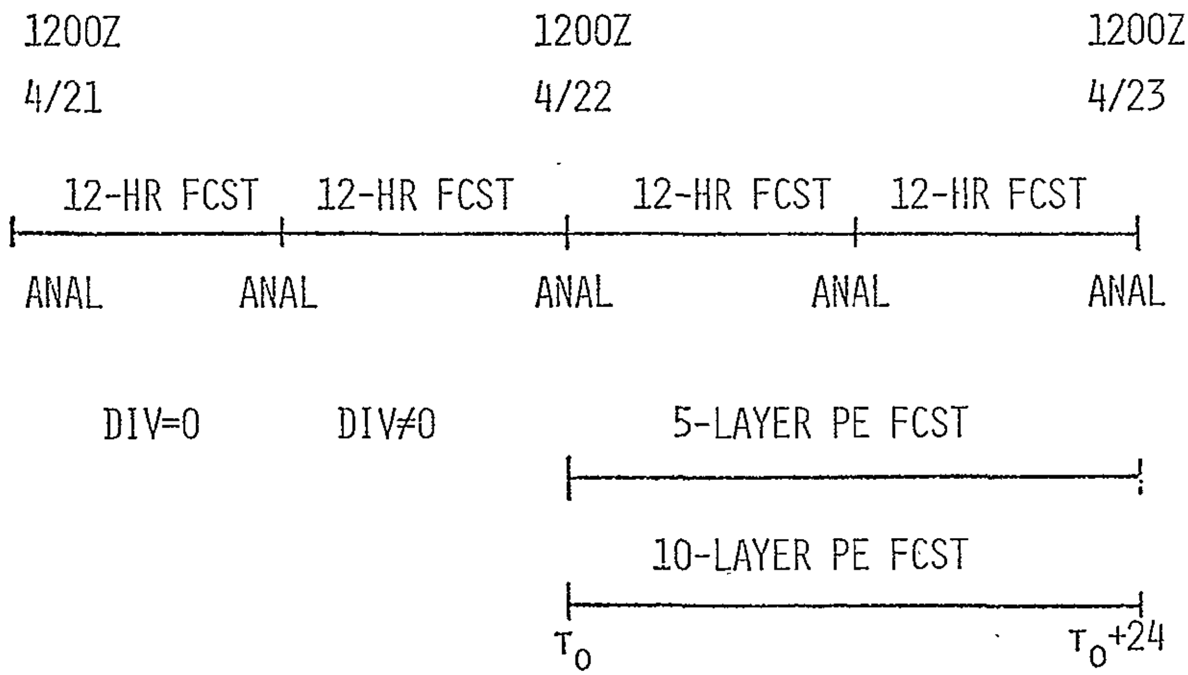

FIGURE II-1: DIAGRAM OF METEOROLOGICAL SCENARIO

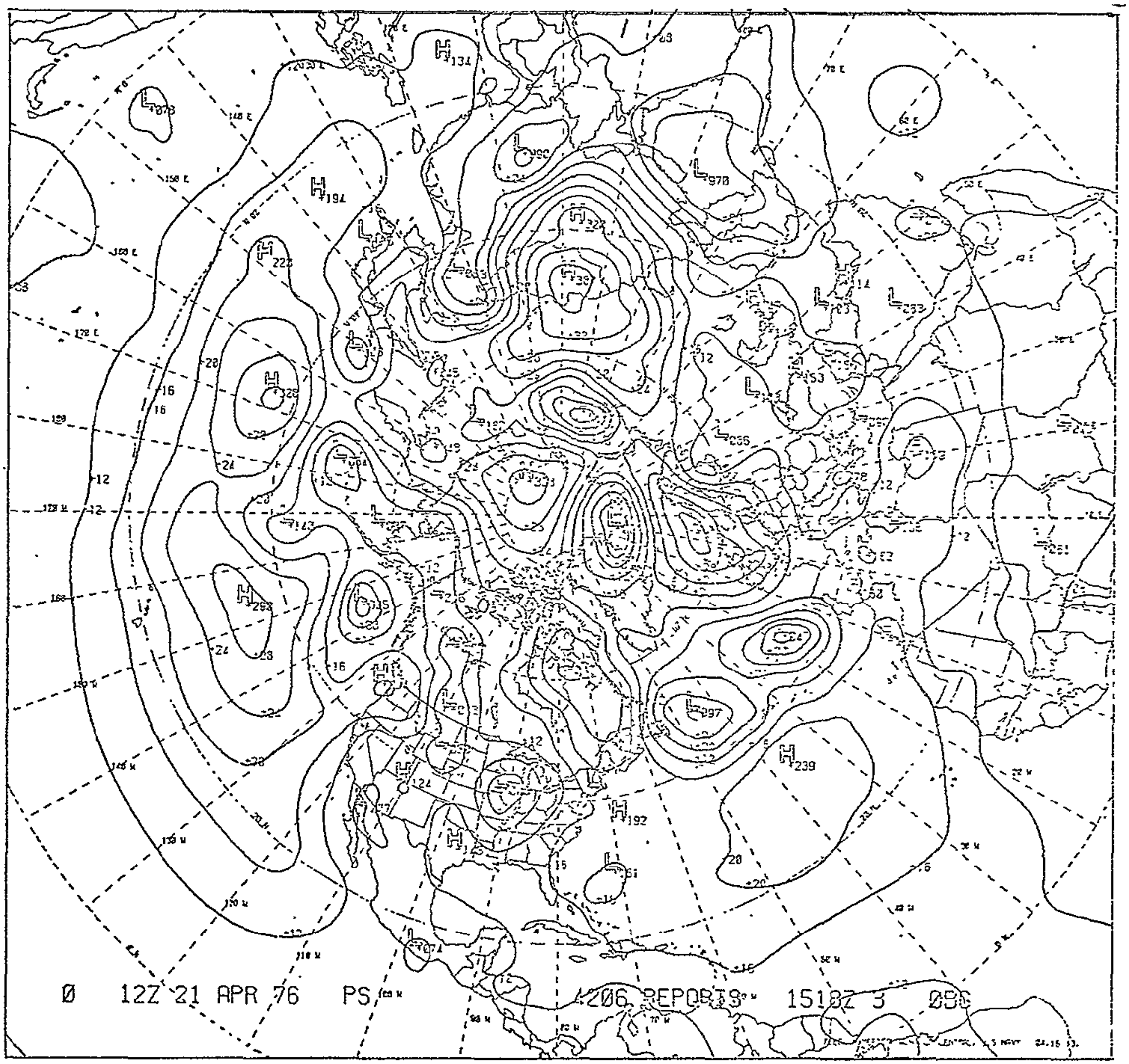

FIGURE II-2: FNWC SURFACE ANALYSIS
4/21/76 1200Z

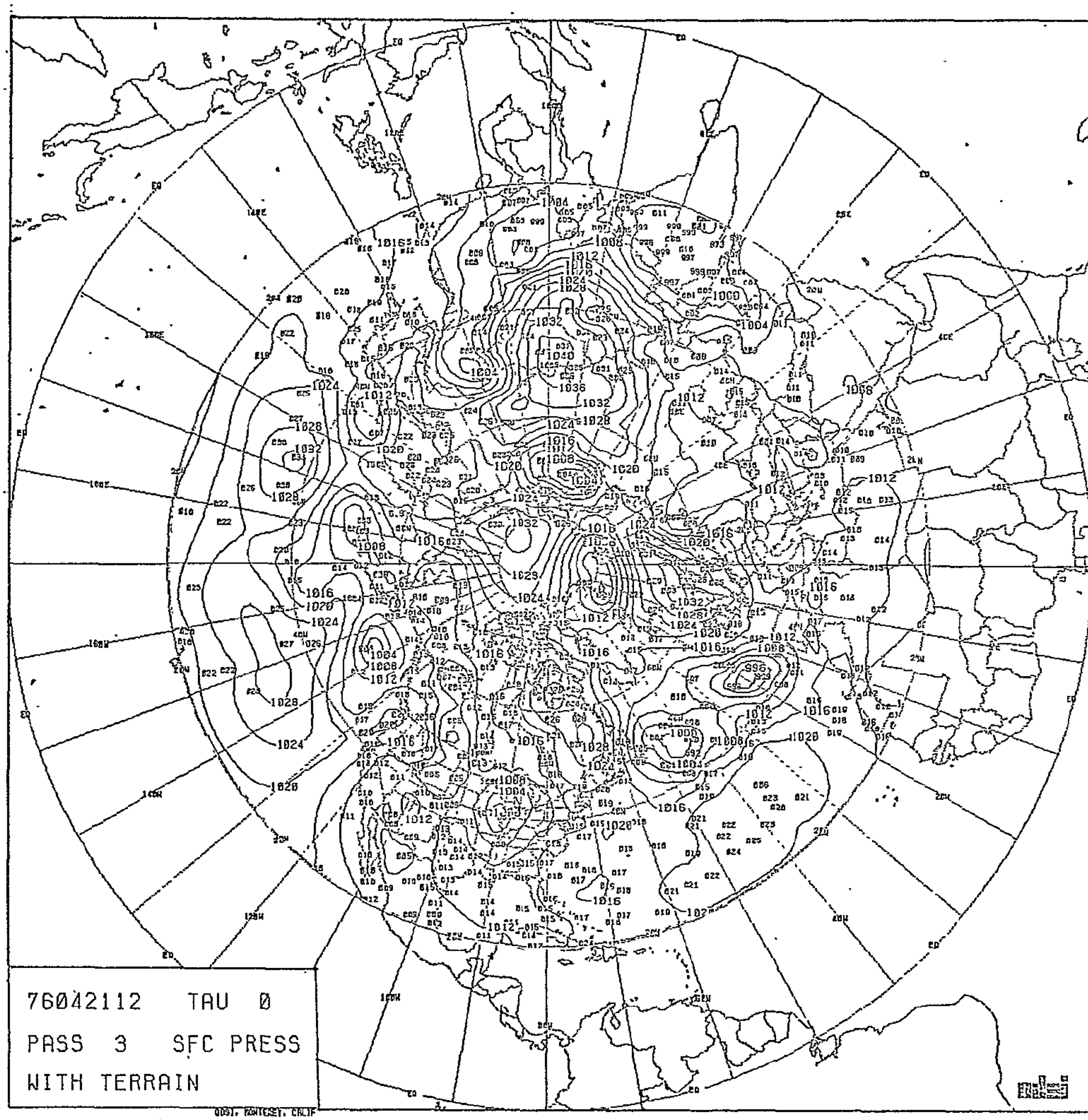

FIGURE II-3: ODSI SURFACE ANALYSIS
4/21/76 1200Z

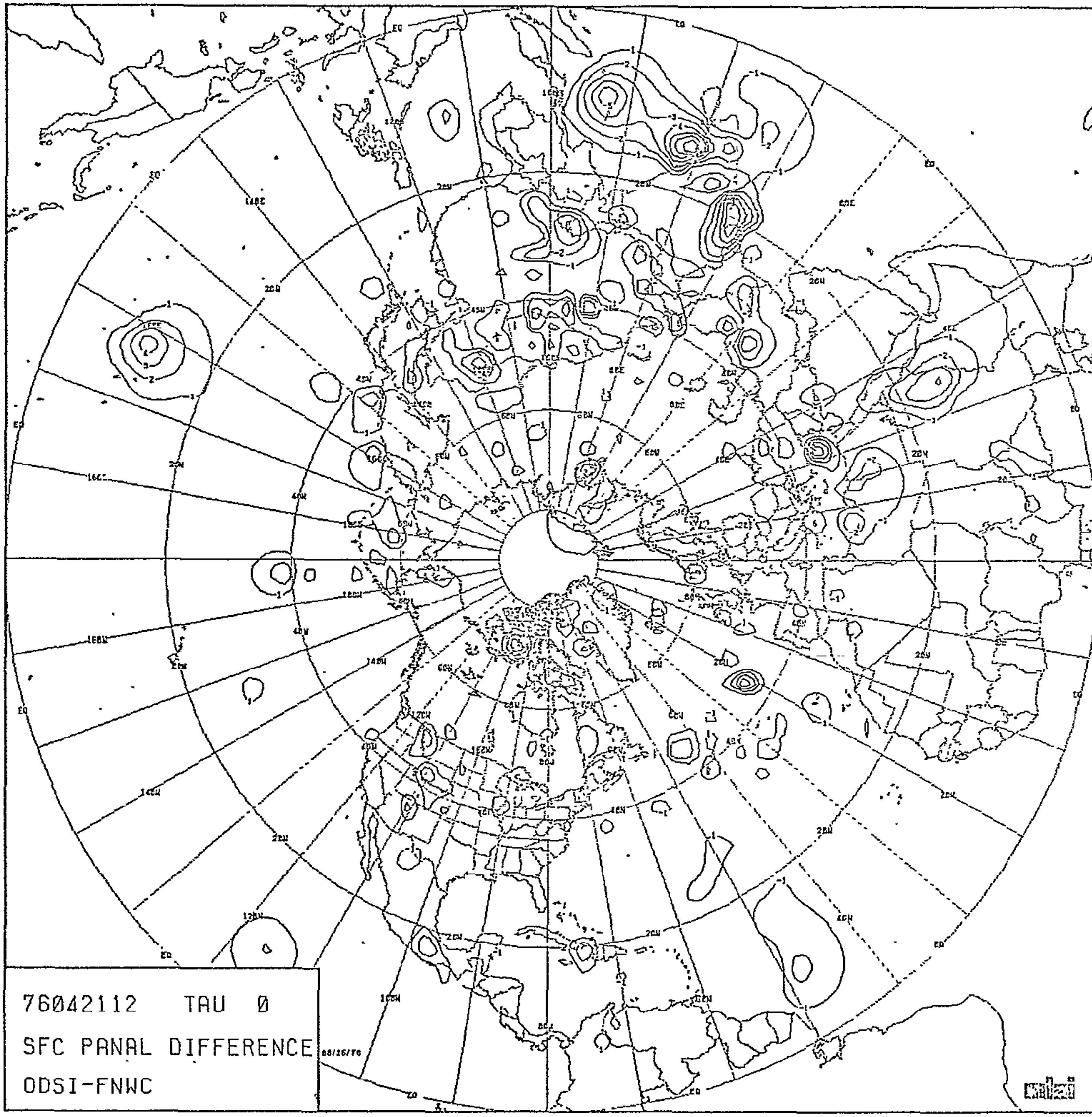

FIGURE II-4: ODSI-FNWC SURFACE ANALYSIS DIFFERENCE 4/21/76 1200Z (1-mb contour interval)

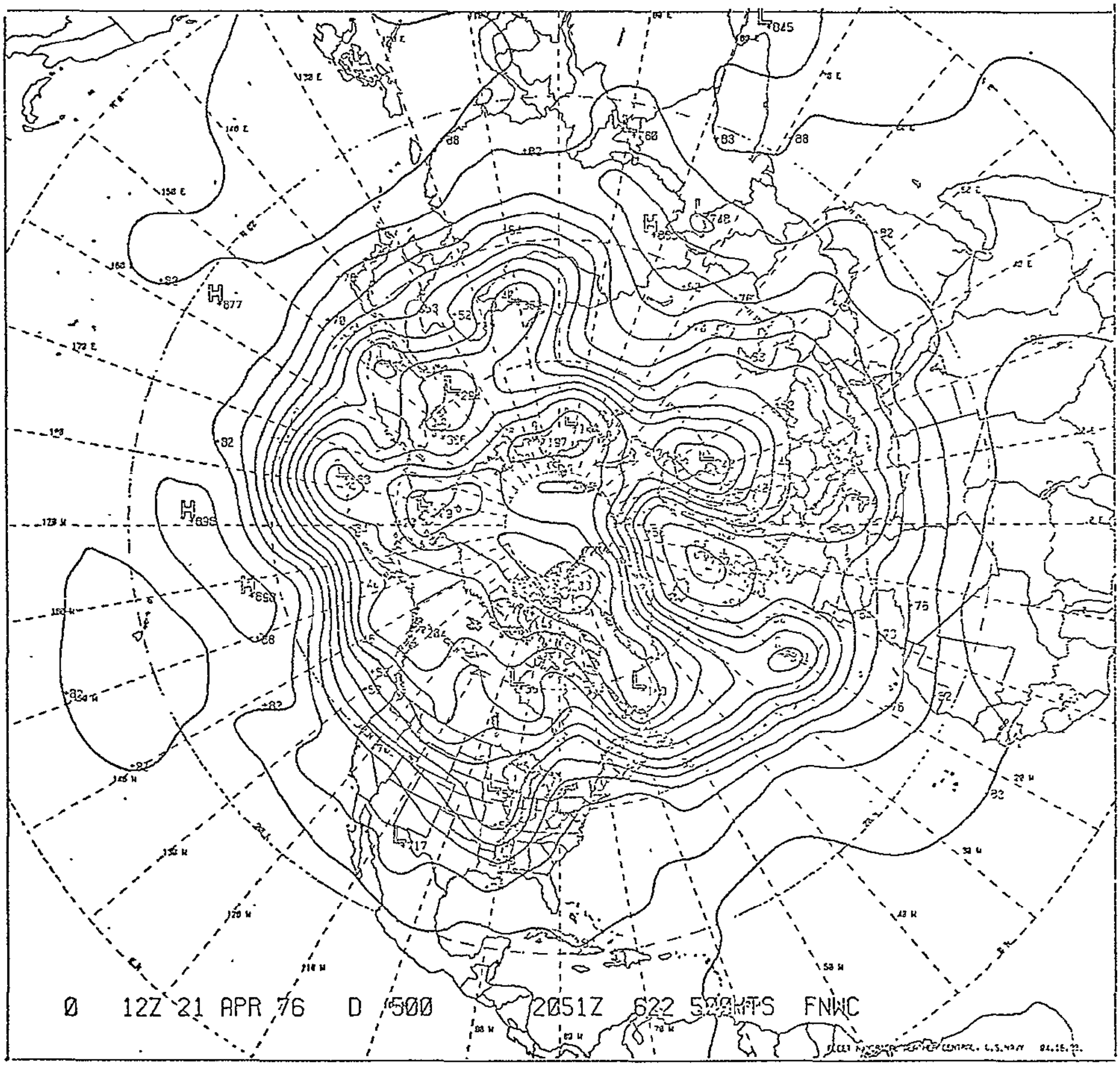

FIGURE II-5: FNWC 500mb ANALYSIS
4/21/76 1200Z

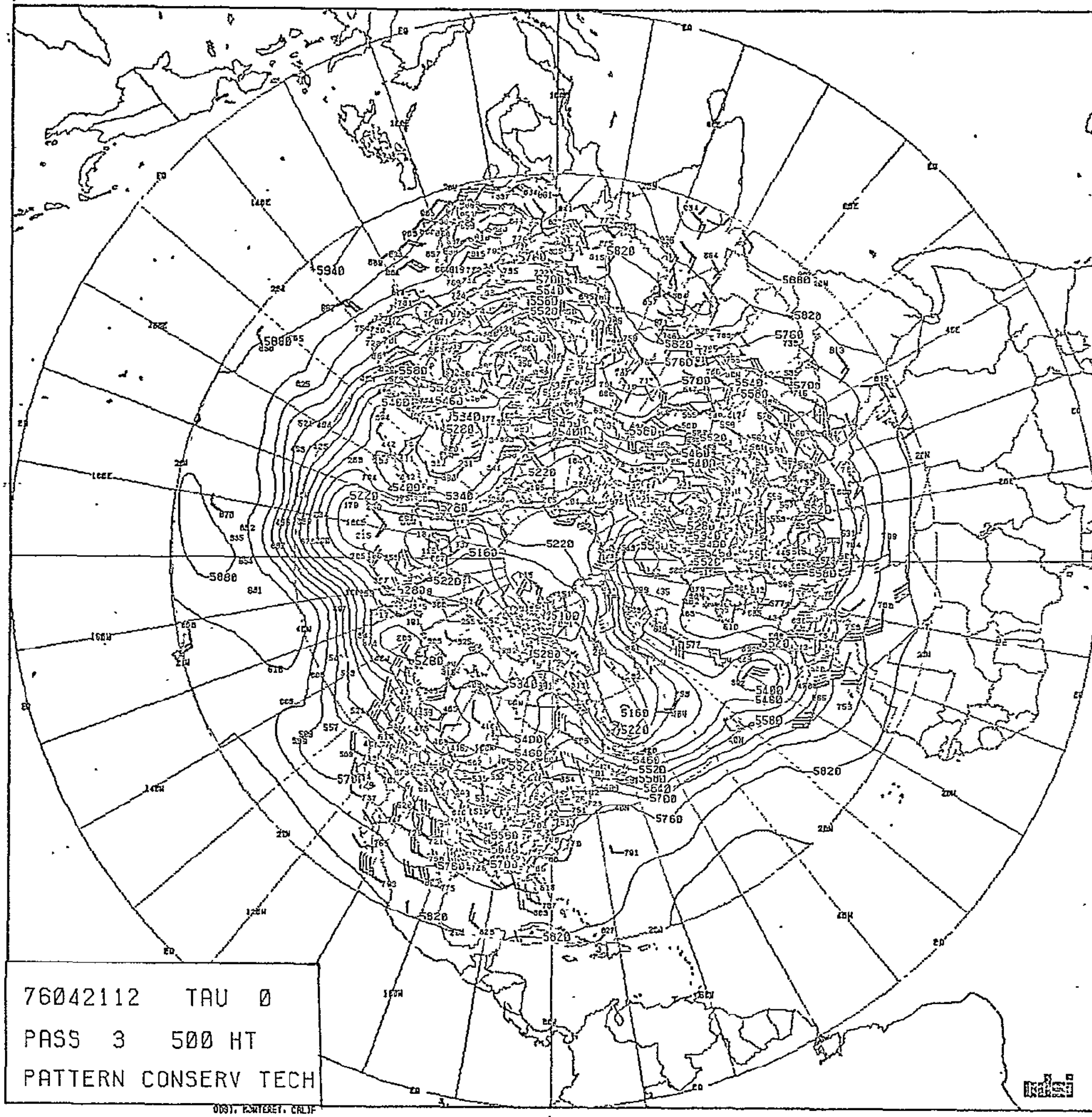

FIGURE II-6: ODSI 500mb ANALYSIS
4/21/76 1200Z

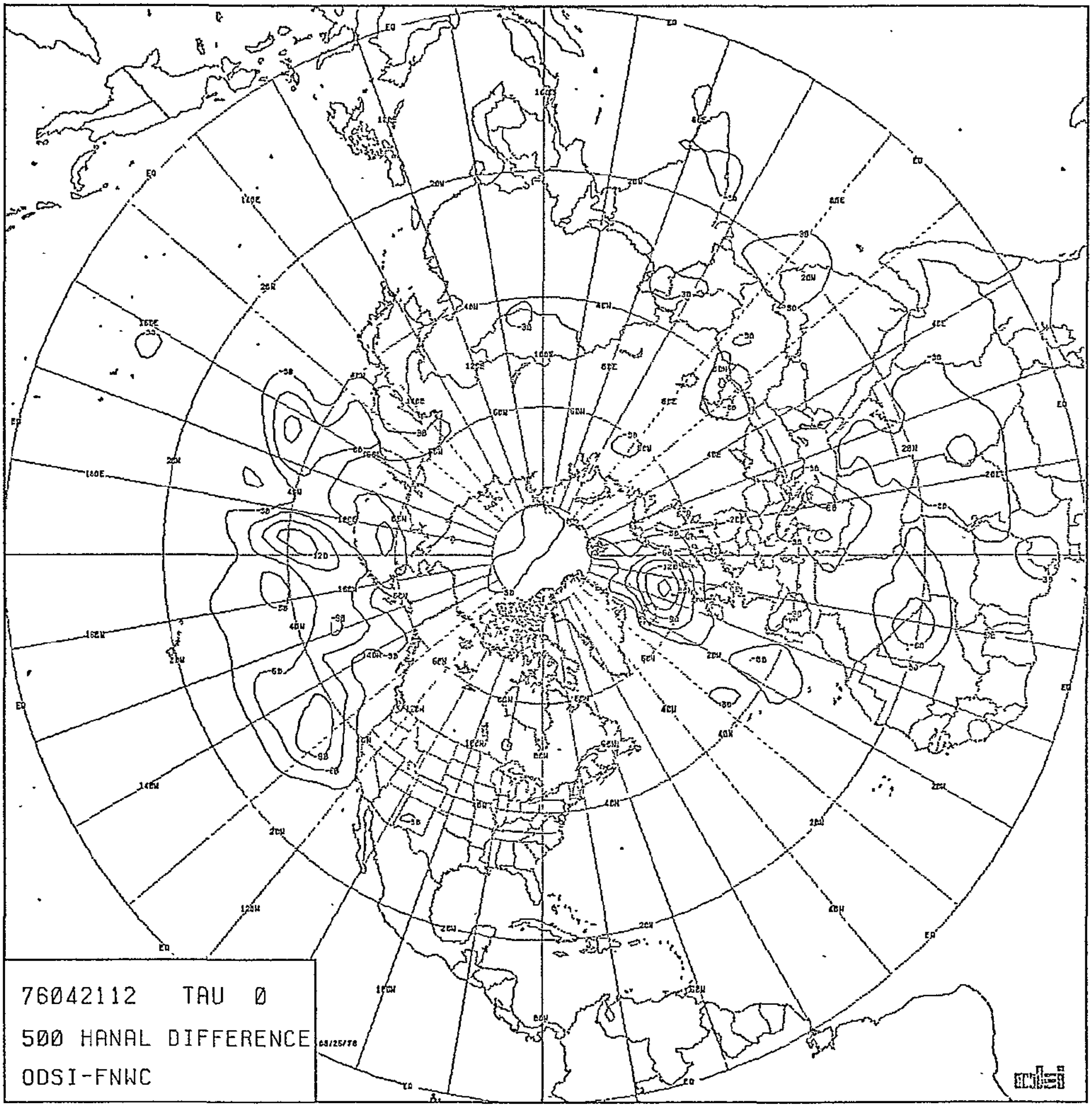

FIGURE II-7: ODSI-FNWC 500mb ANALYSIS
DIFFERENCE 4/21/76 1200Z
(30 meter contour interval)

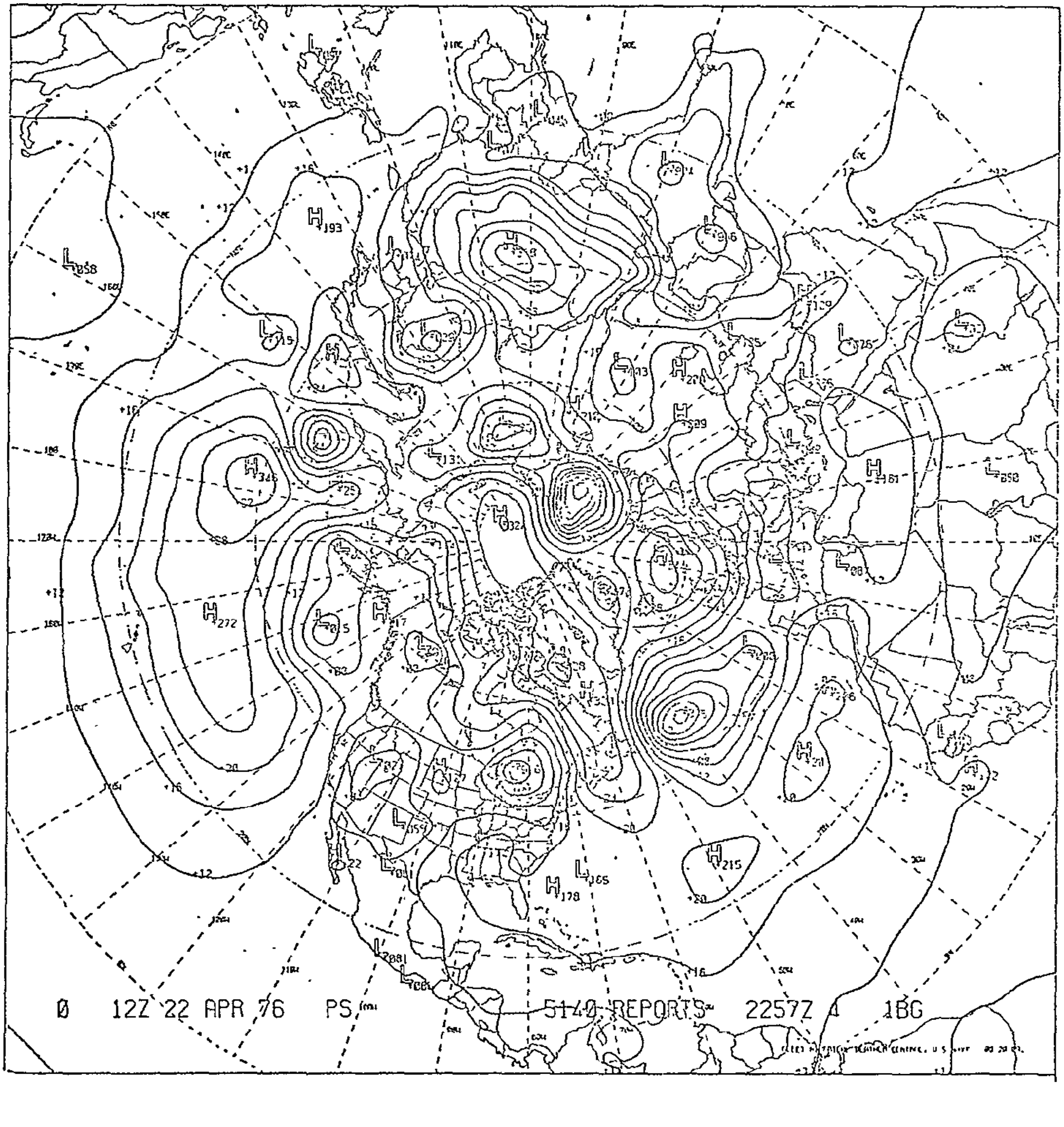

FIGURE II-8: FNWC SURFACE ANALYSIS
4/22/76 1200Z

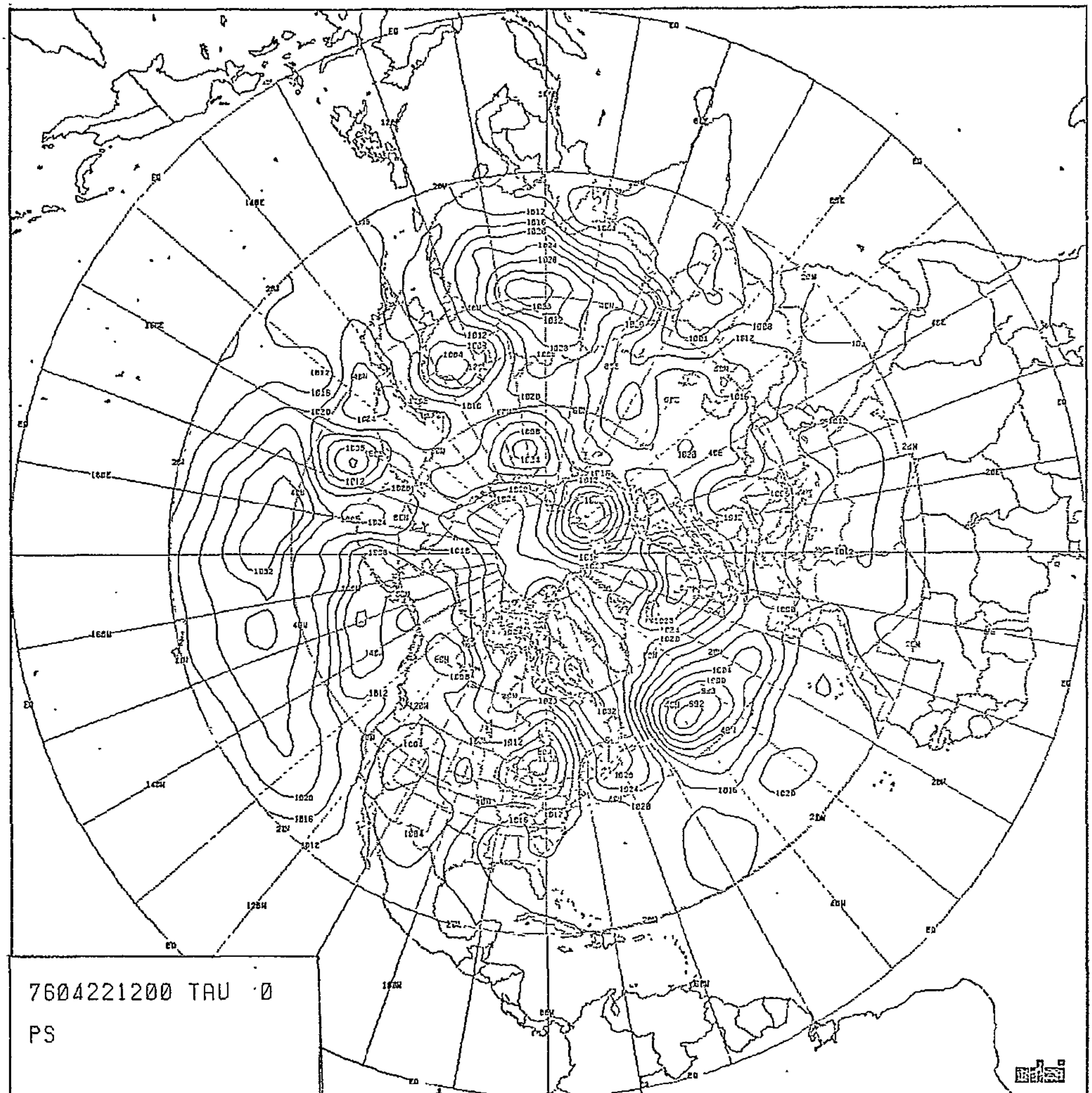

FIGURE II-9: ODSI SURFACE ANALYSIS
4/22/76 1200Z

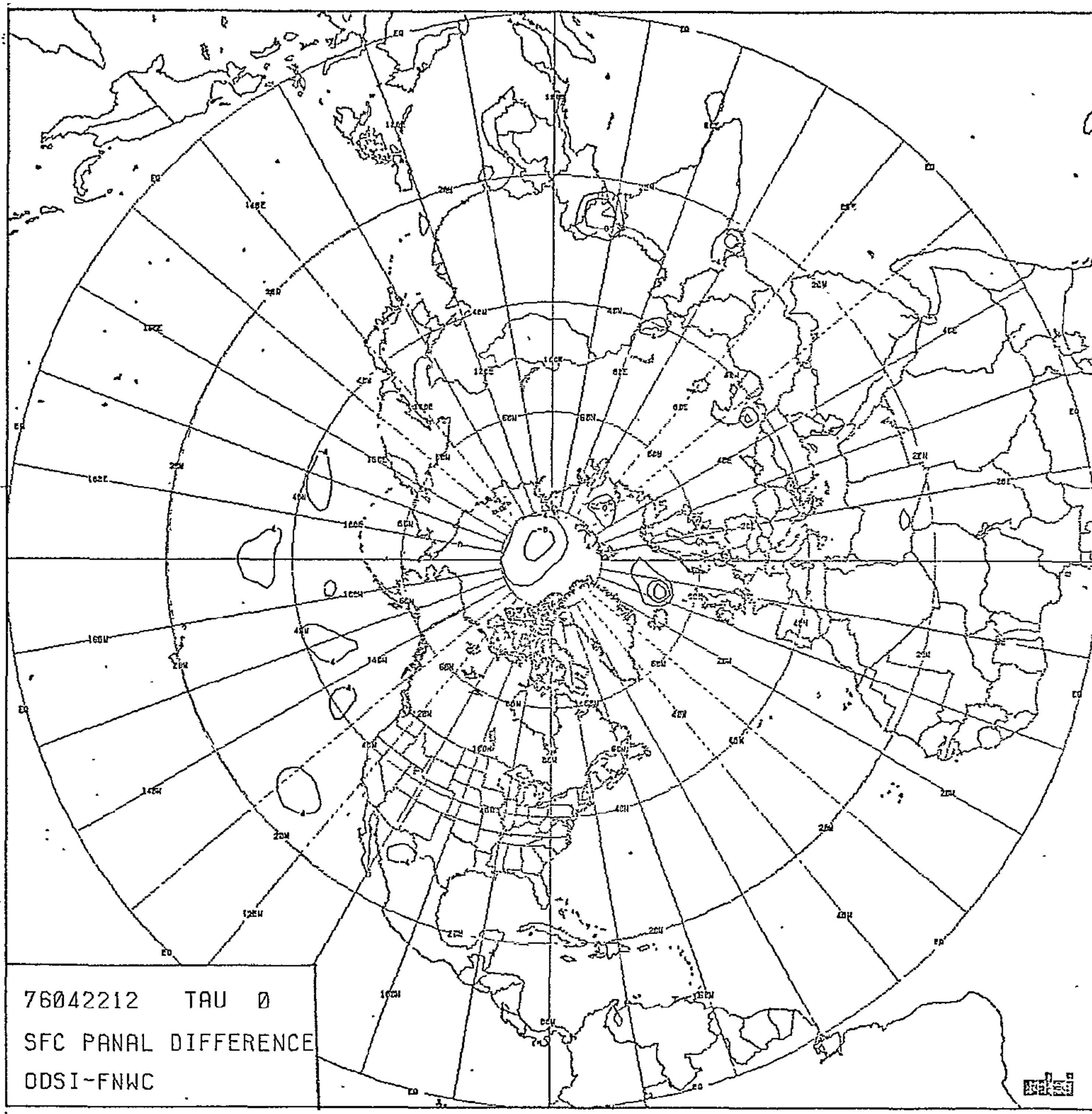

FIGURE II-10: ODSI-FNWC SURFACE ANALYSIS DIFFERENCE 4/22/76 1200Z (4-mb contour interval)

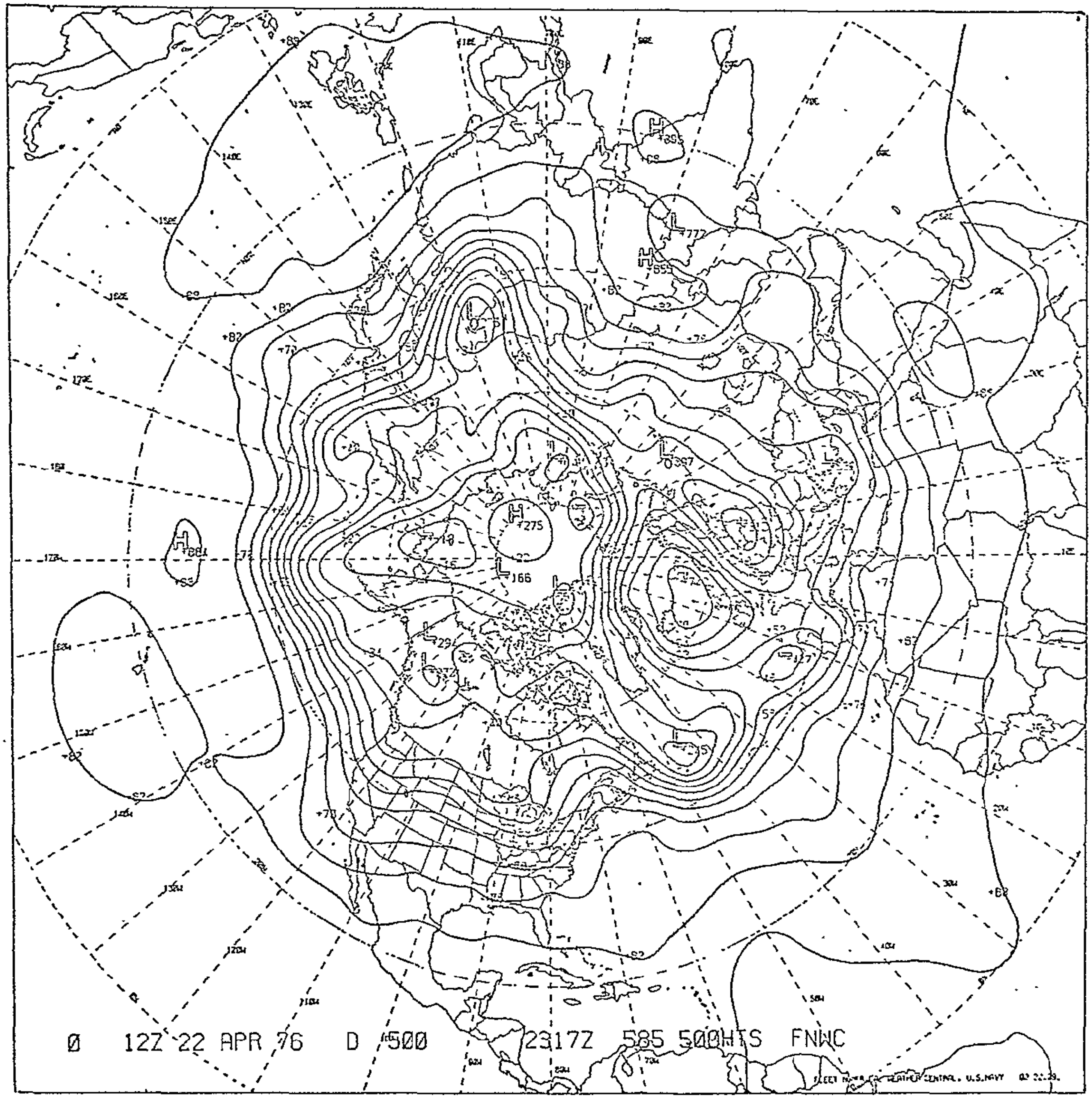

FIGURE II-11: FNWC 500mb ANALYSIS
4/22/76 1200Z

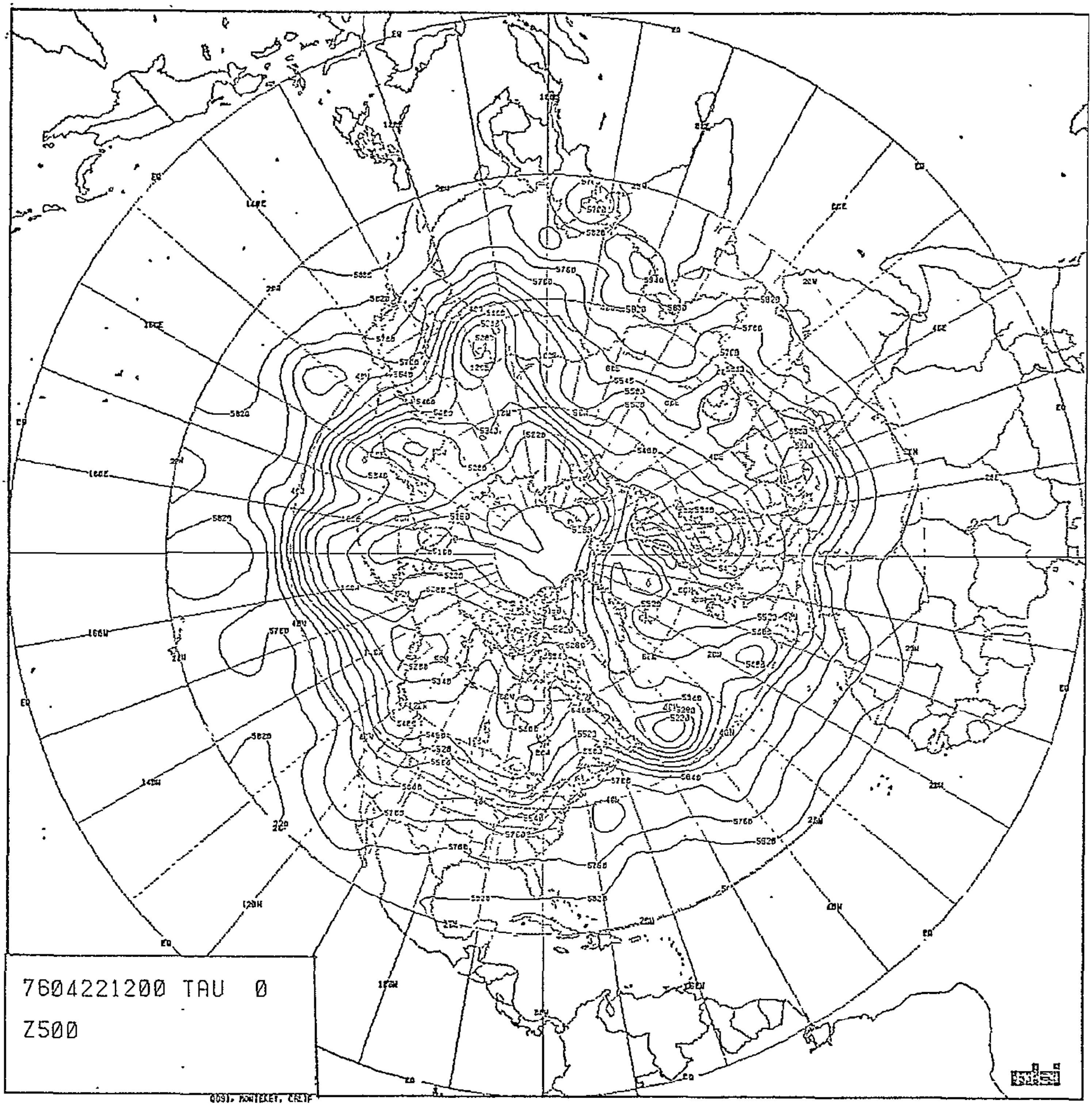

FIGURE II-12: ODSI 500mb ANALYSIS
4/22/76 1200Z

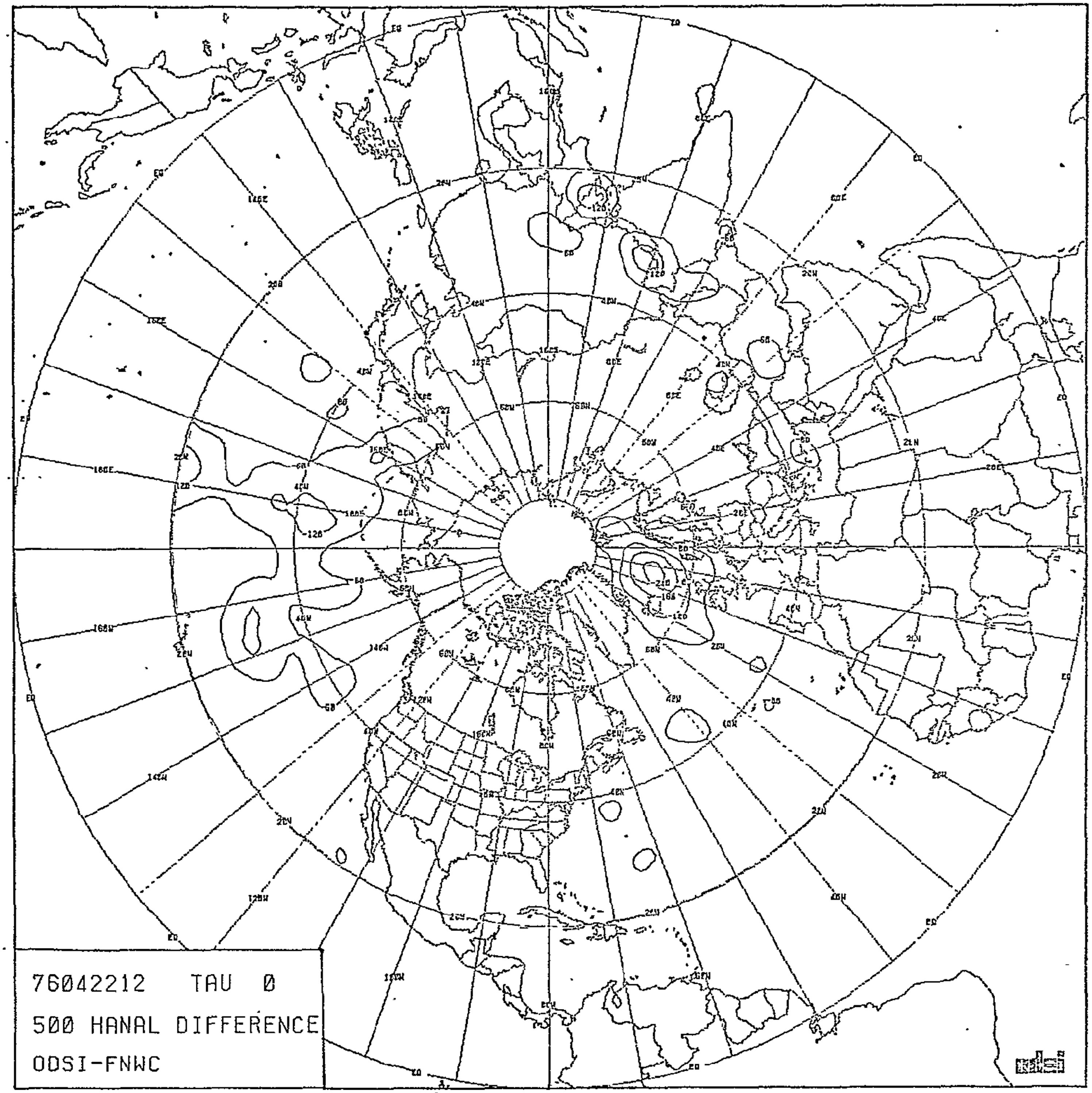

FIGURE II-13: ODSI-FNWC 500mb ANALYSIS DIFFERENCE 4/22/76 1200Z (60 meter contour interval)

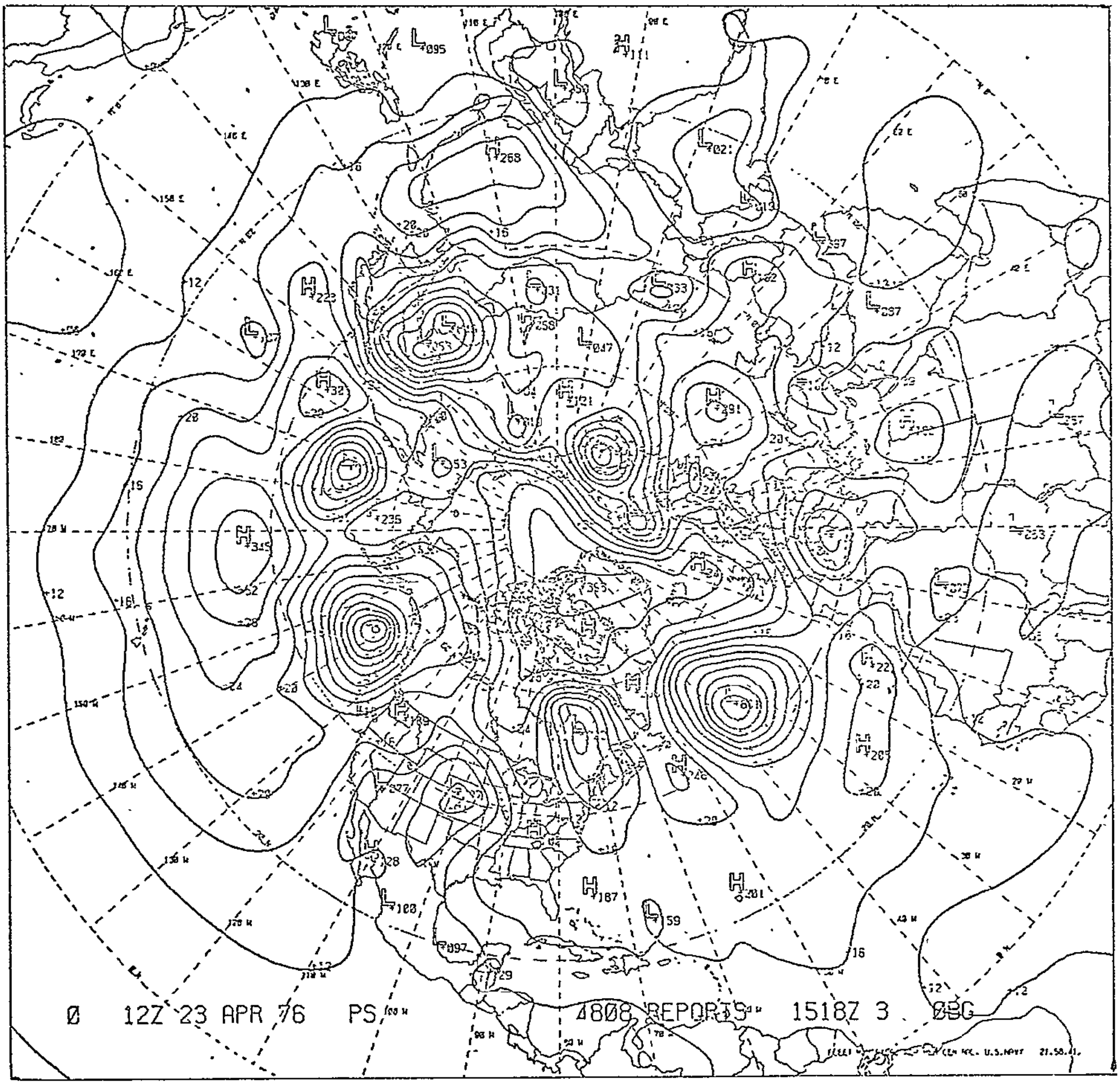

FIGURE II-14: FNWC SURFACE ANALYSIS
4/23/76 1200Z

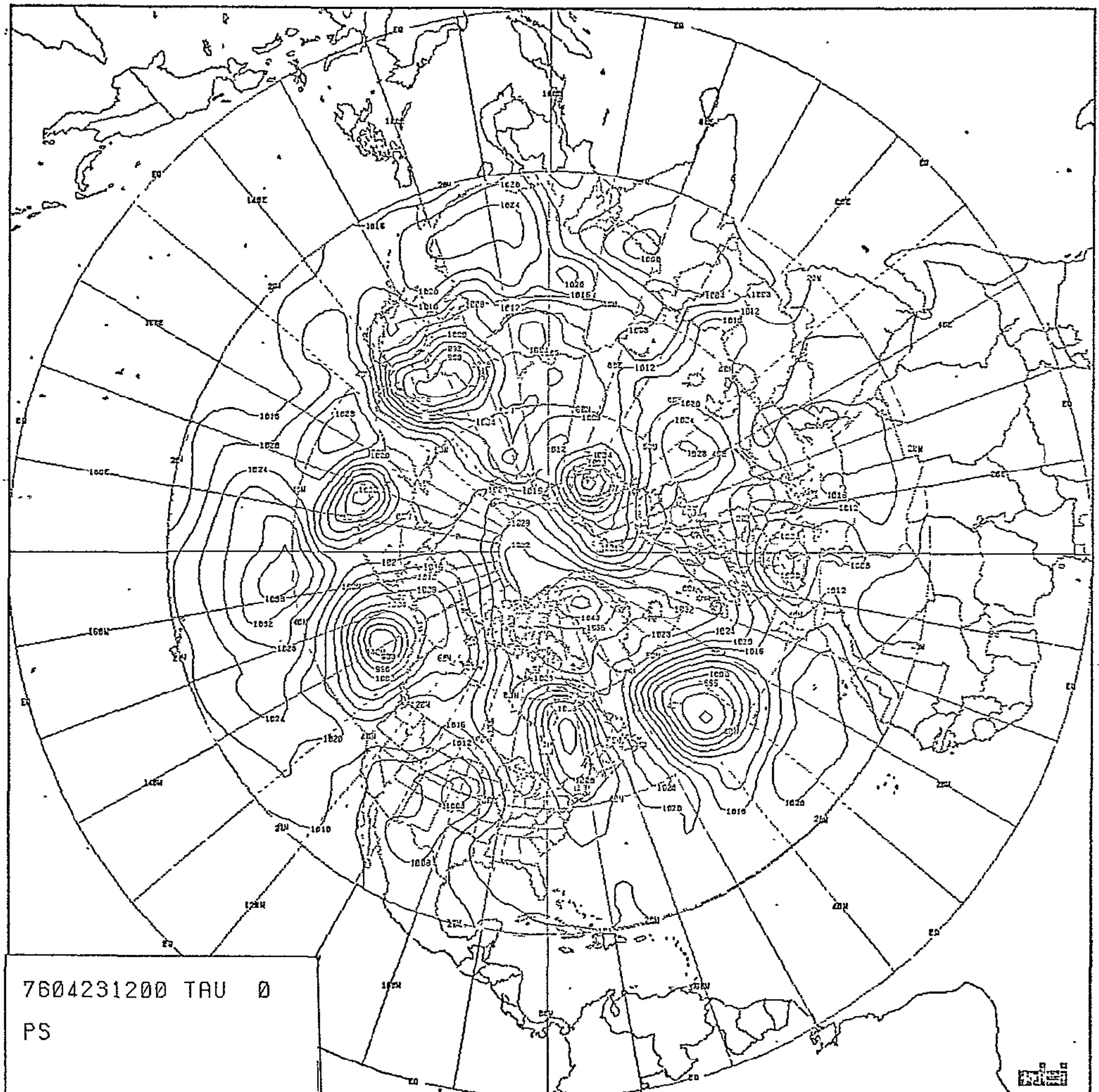

FIGURE II-15: ODSI SURFACE ANALYSIS
4/23/76 1200Z

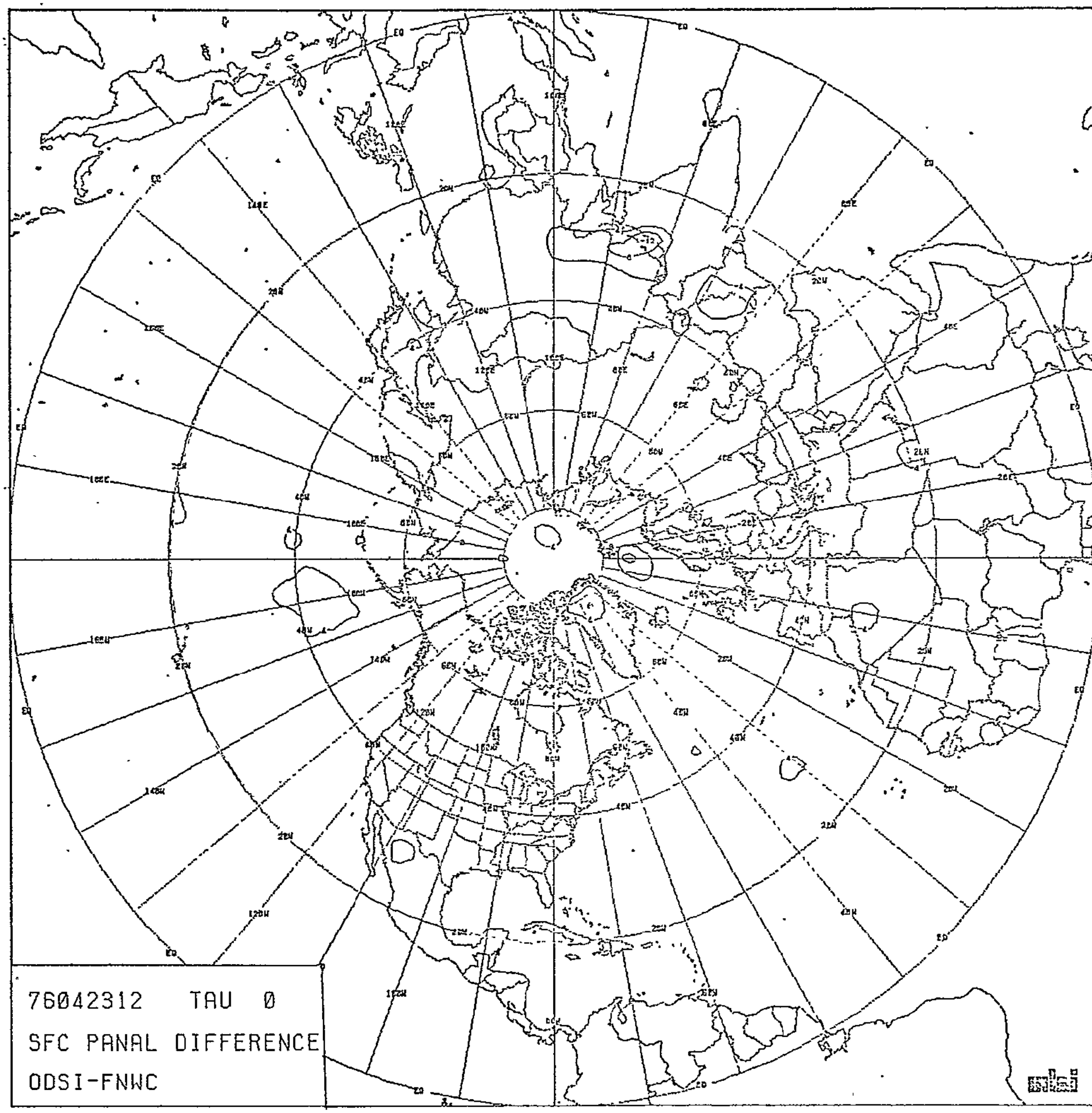

FIGURE II-16: ODSI-FNWC SURFACE ANALYSIS DIFFERENCE 4/23/76 1200Z

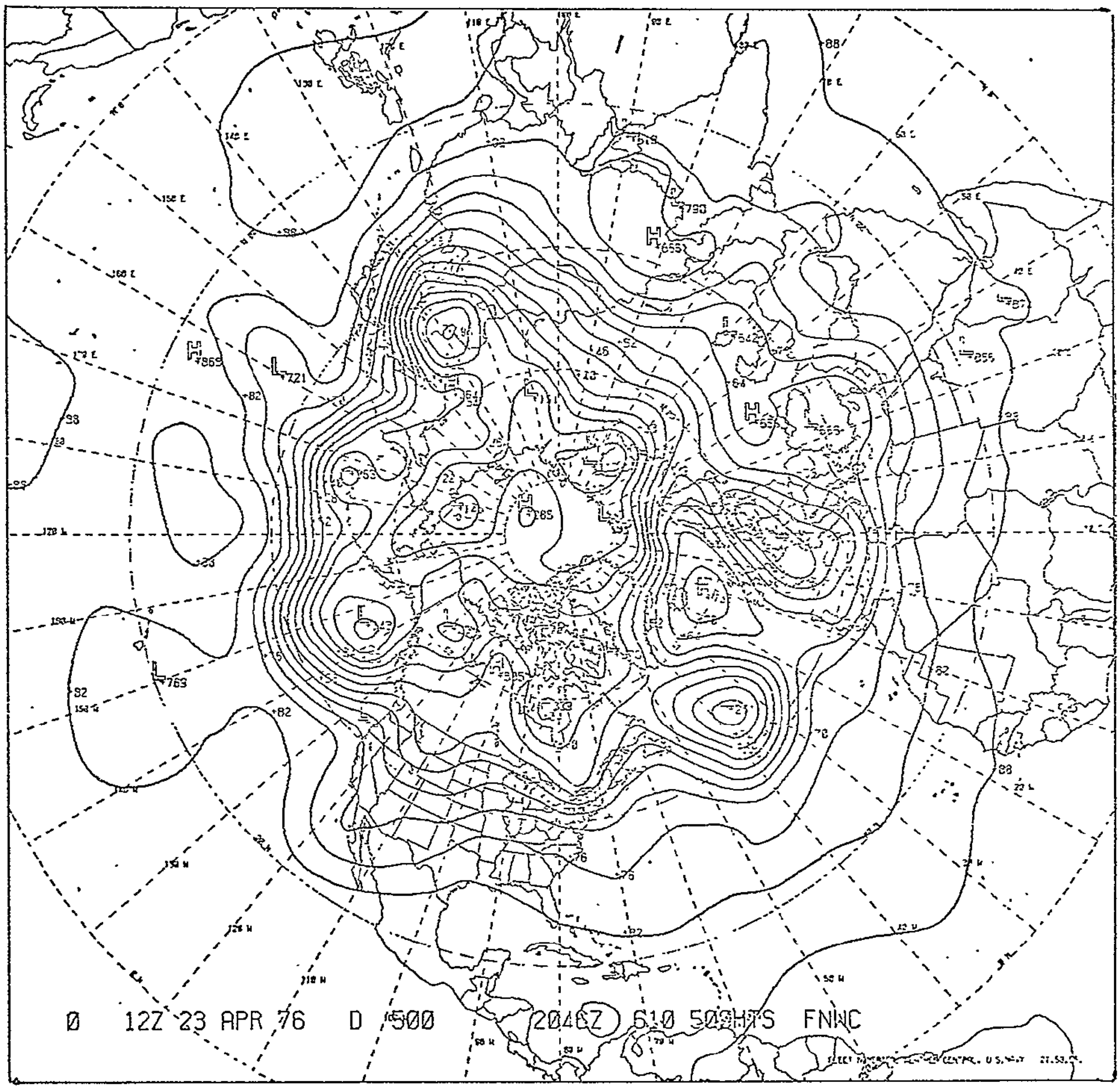

FIGURE II-17: FNWC 500mb ANALYSIS
4/23/76 1200Z

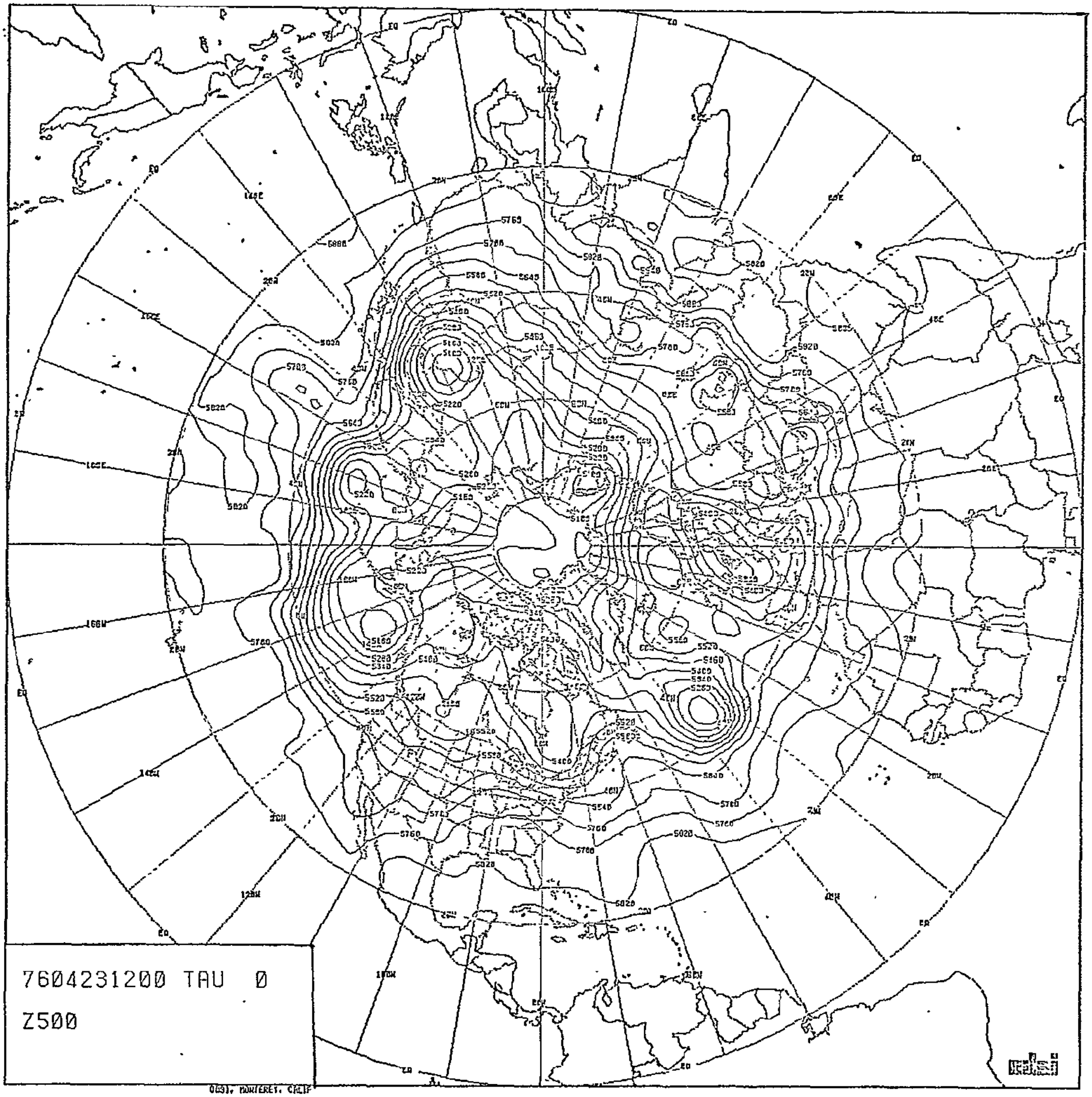

FIGURE II-18: ODSI 500mb ANALYSIS
4/23/76 1200Z

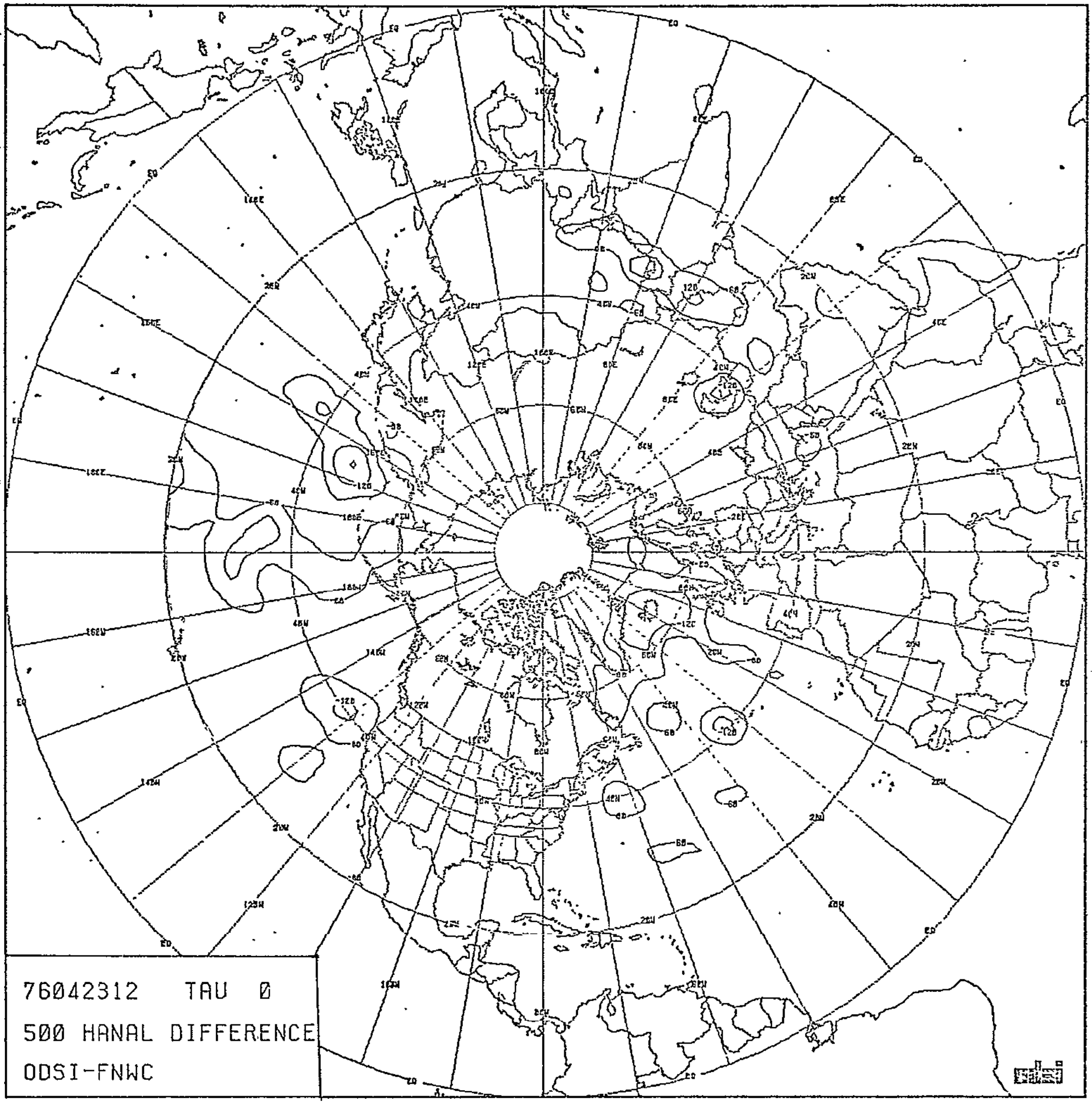

FIGURE II-19: ODSI-FNWC 500mb ANALYSIS DIFFERENCE 4/23/76 1200Z (60 meter contour interval)

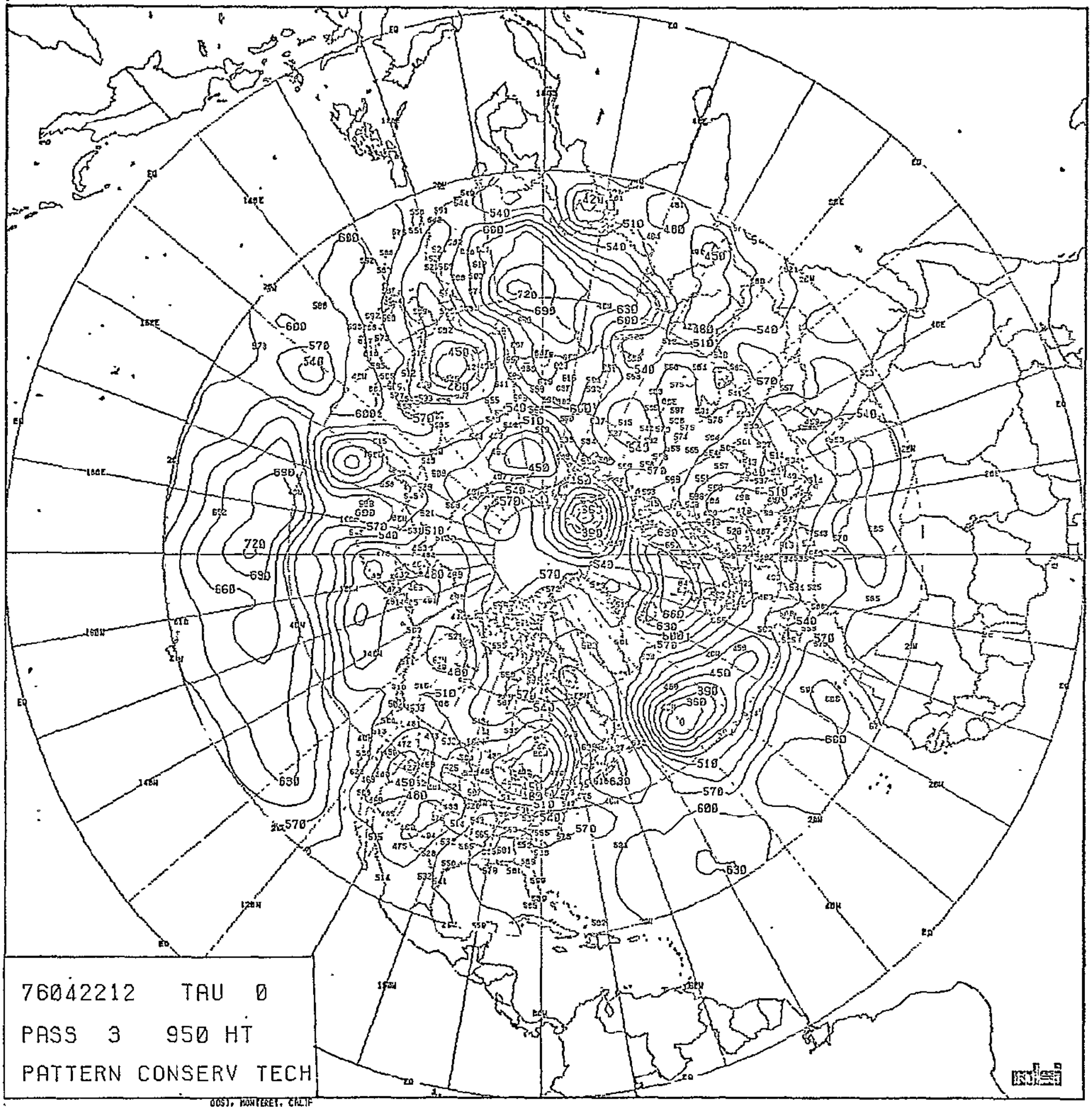

FIGURE II-20: ODSI 950mb HEIGHT ANALYSIS
4/22/76 1200Z

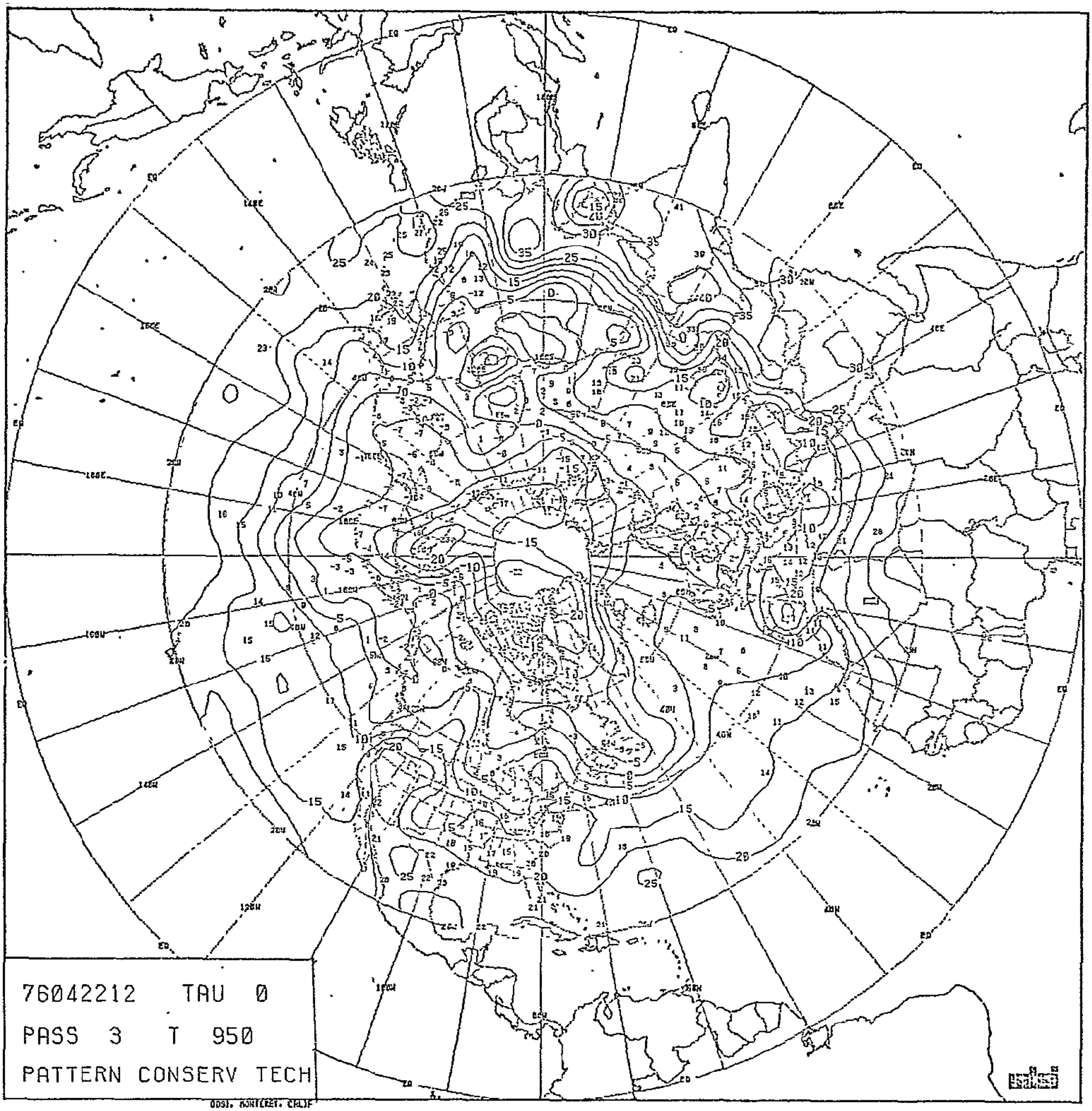

FIGURE II-21: ODSI 950mb TEMPERATURE
ANALYSIS 4/22/76 1200Z

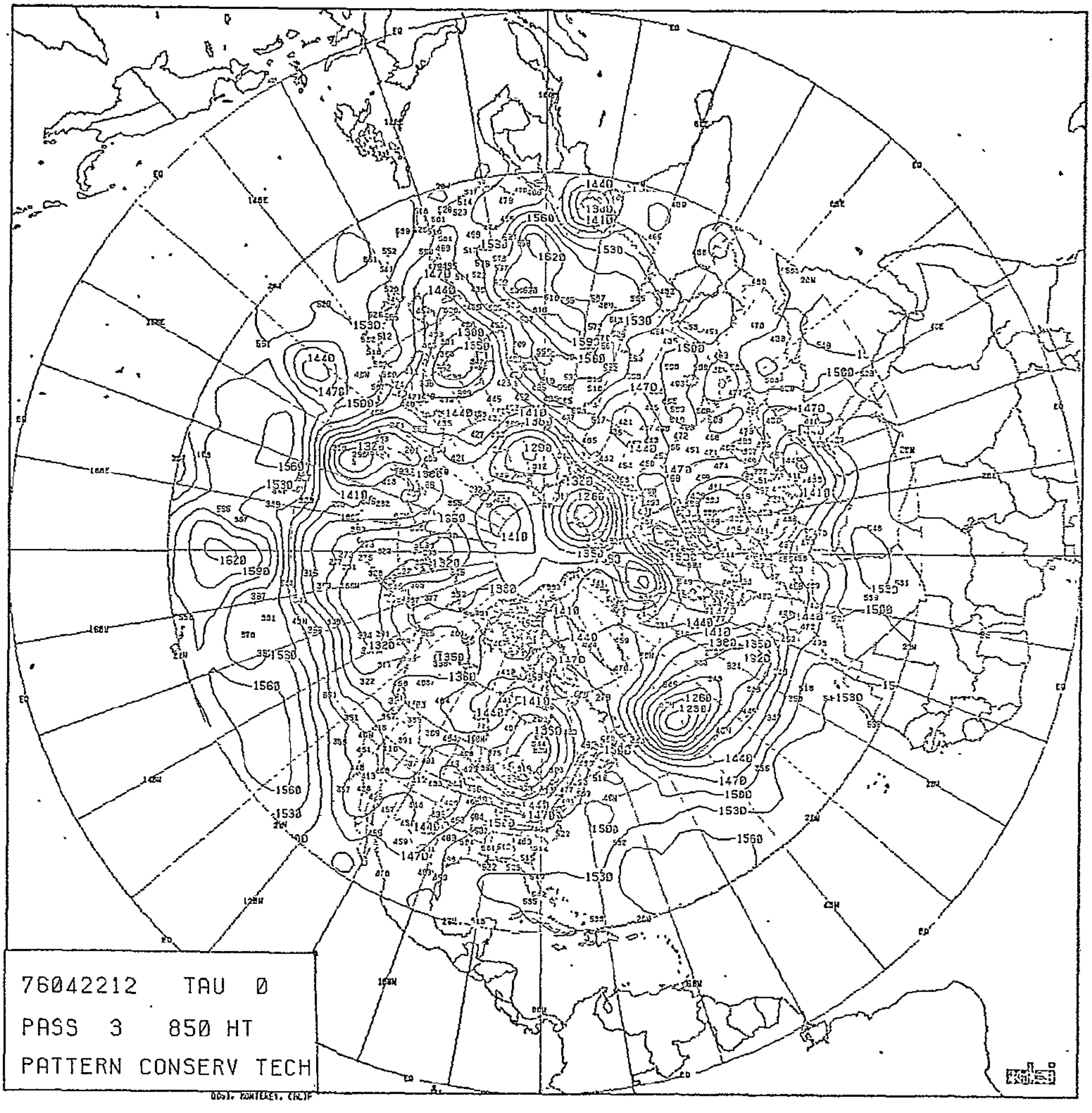

FIGURE II-22: ODSI 850mb HEIGHT ANALYSIS
4/22/76 1200Z

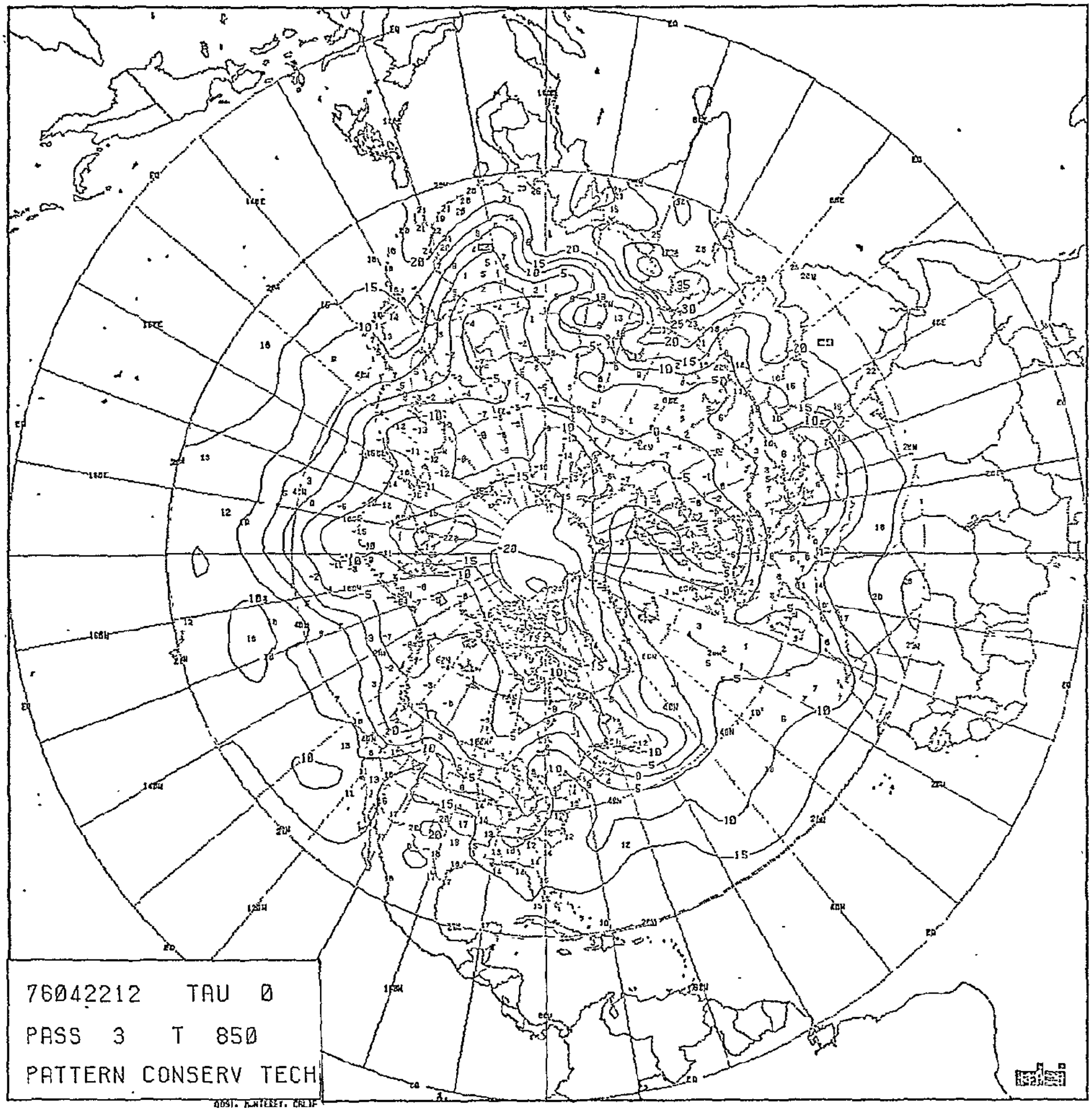

FIGURE II-23: ODSI 850mb TEMPERATURE ANALYSIS
4/22/76 1200Z

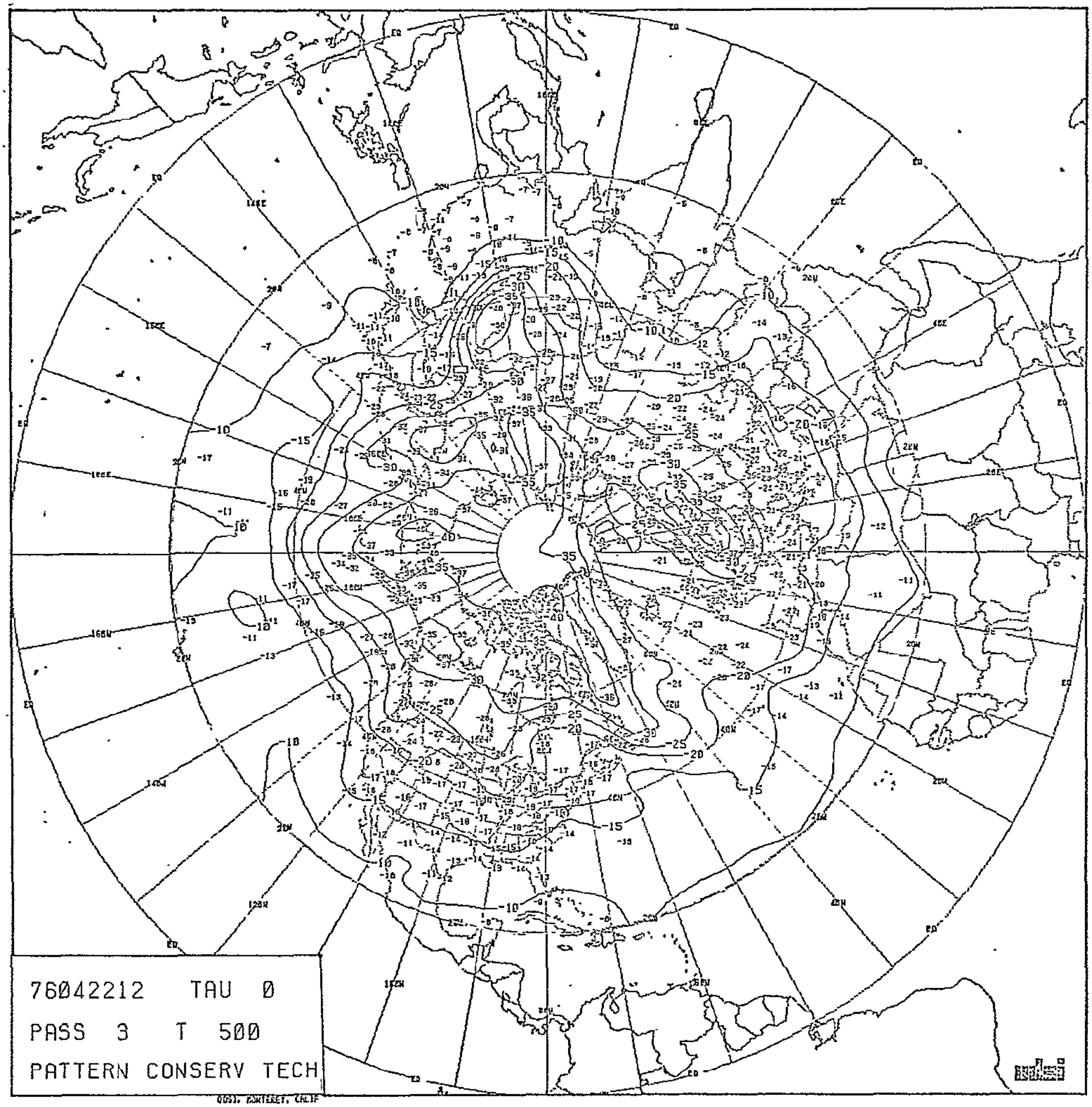

FIGURE II-24: ODSI 500mb TEMPERATURE ANALYSIS
4/22/76 1200Z

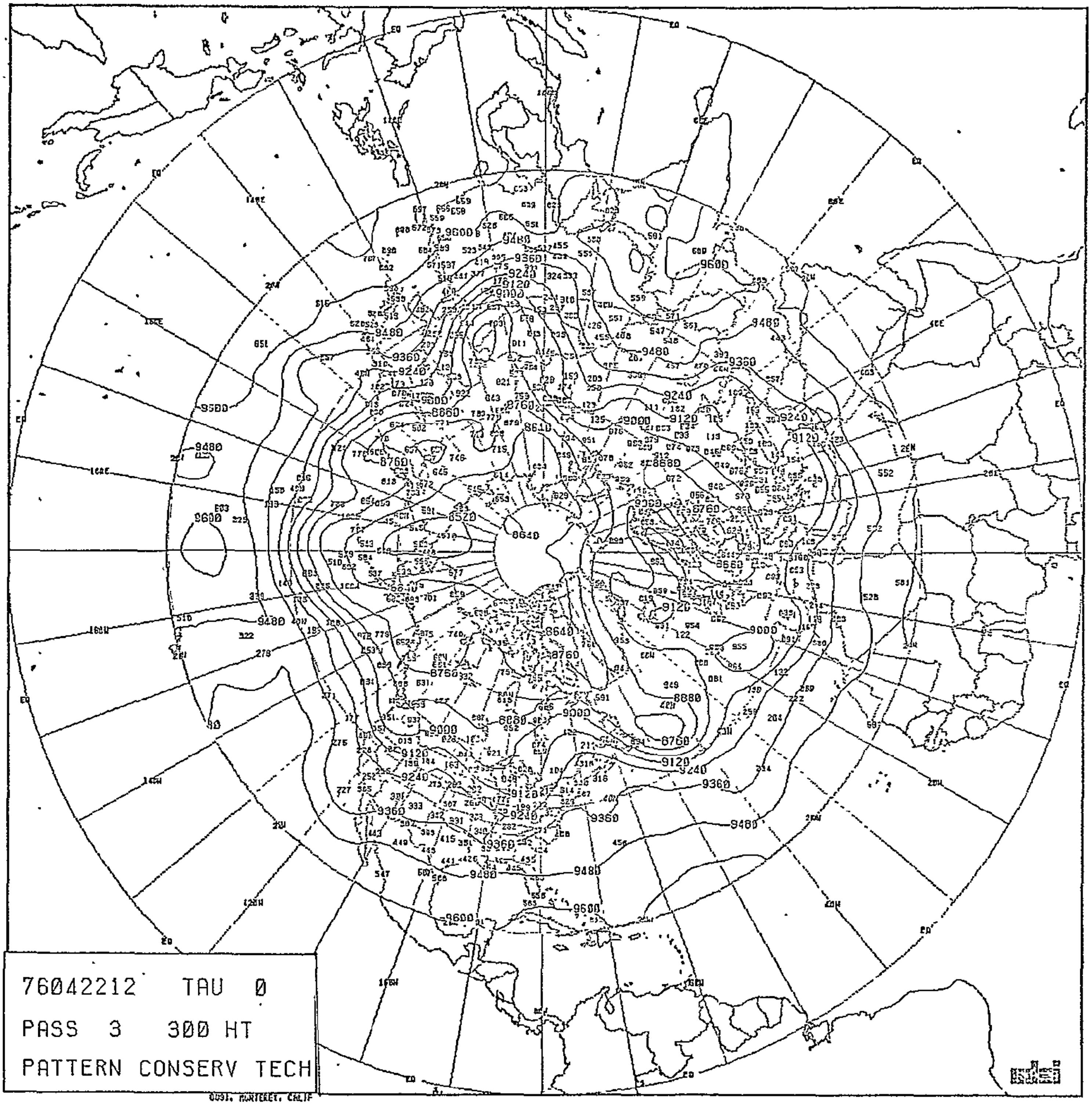

FIGURE II-25: ODSI 300mb HEIGHT ANALYSIS
4/22/76 1200Z

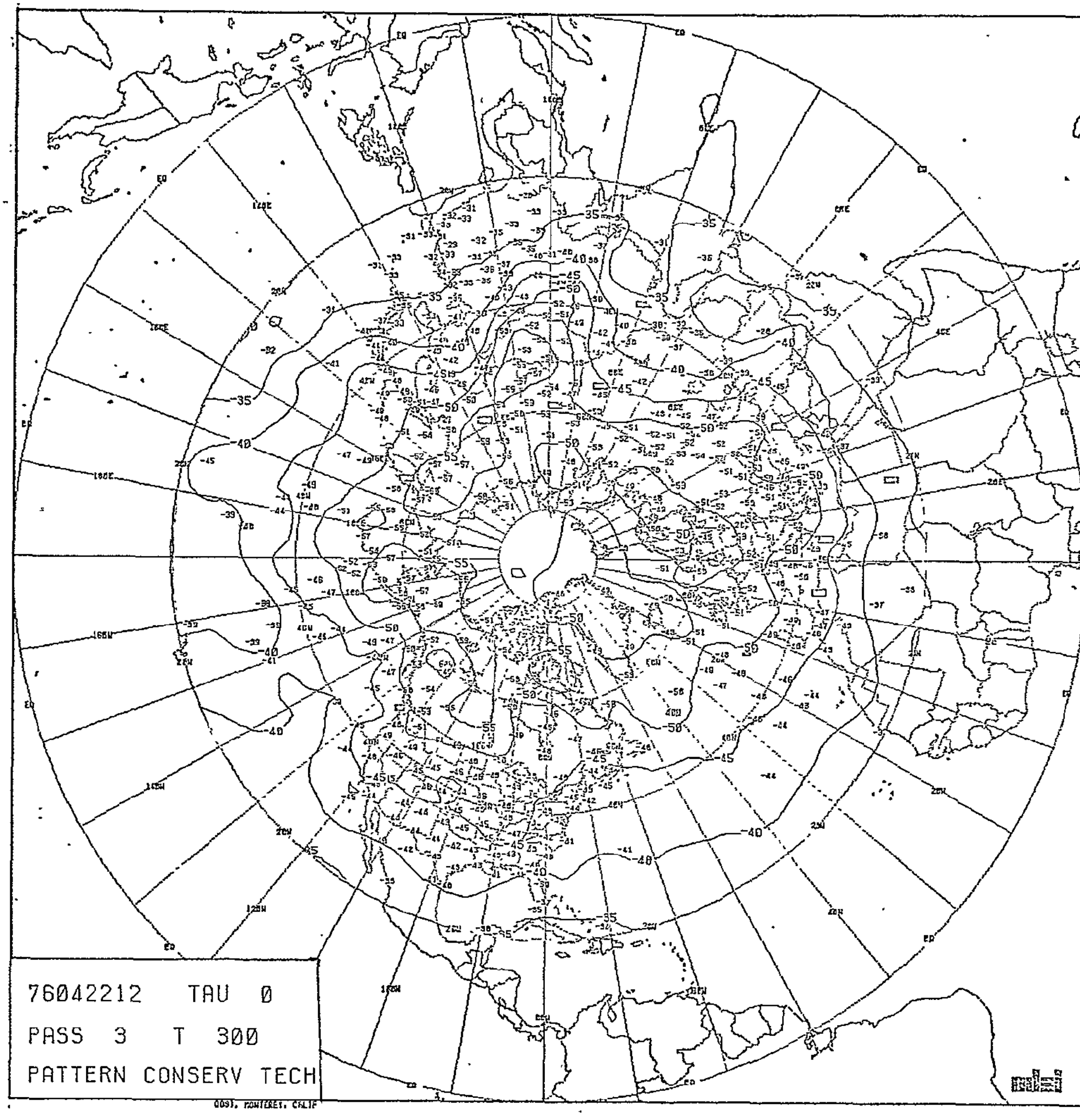

FIGURE II-26: ODSI 300mb TEMPERATURE ANALYSIS 4/22/76 1200Z

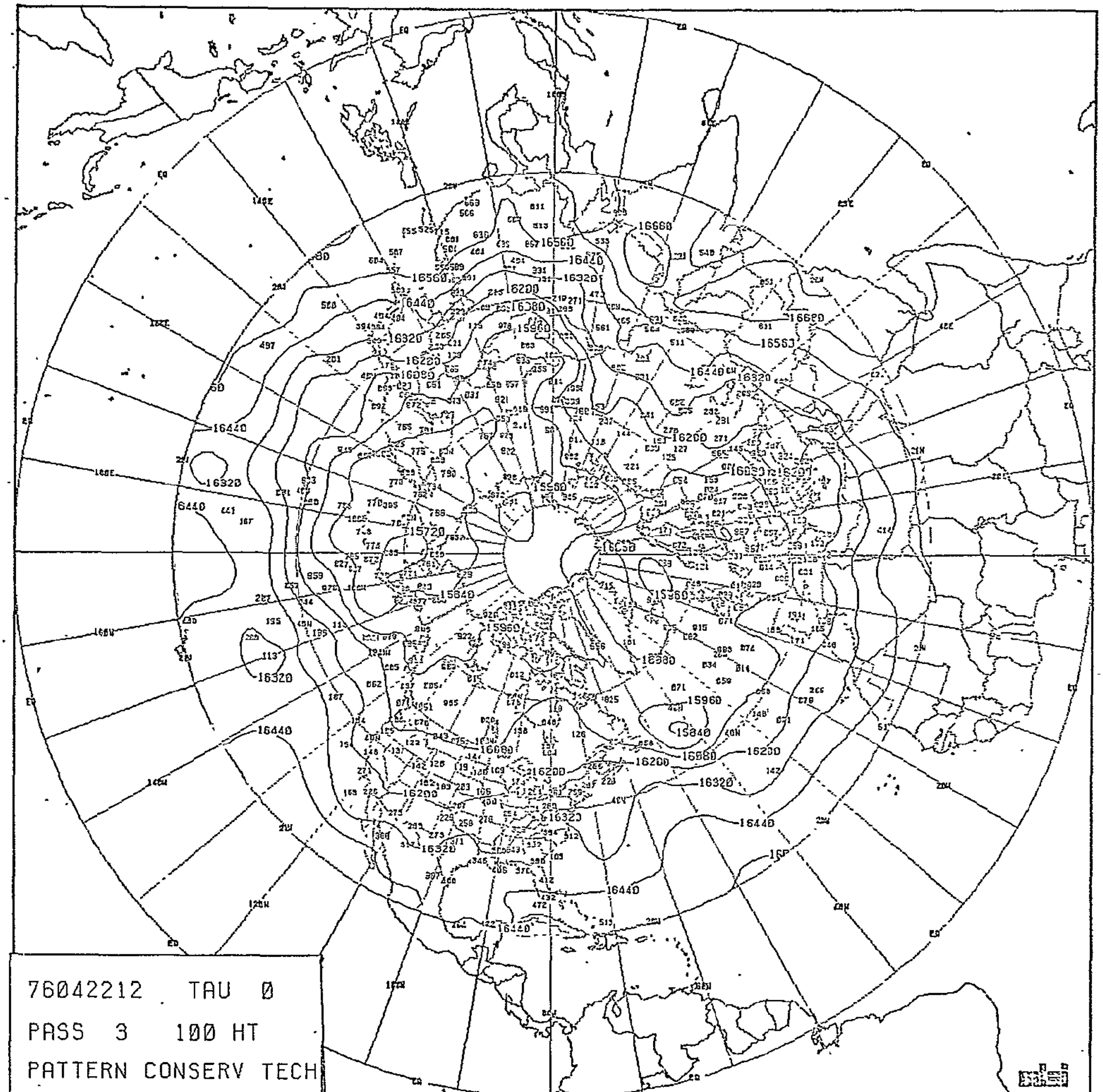

FIGURE II-27: ODSI 100mb HEIGHT ANALYSIS
4/22/76 1200Z

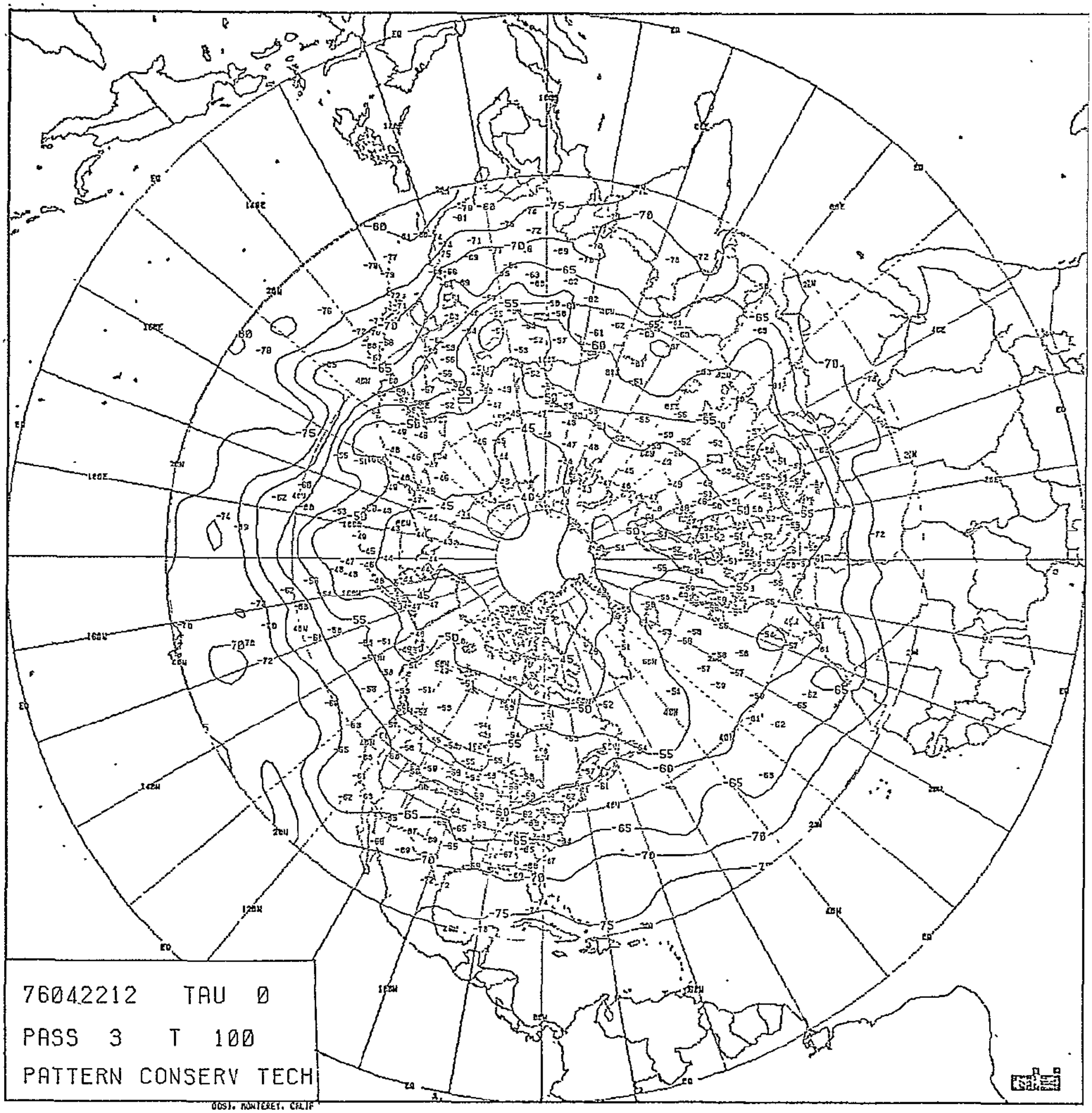

FIGURE II-28: ODSI 100mb TEMPERATURE ANALYSIS 4/22/76 1200Z

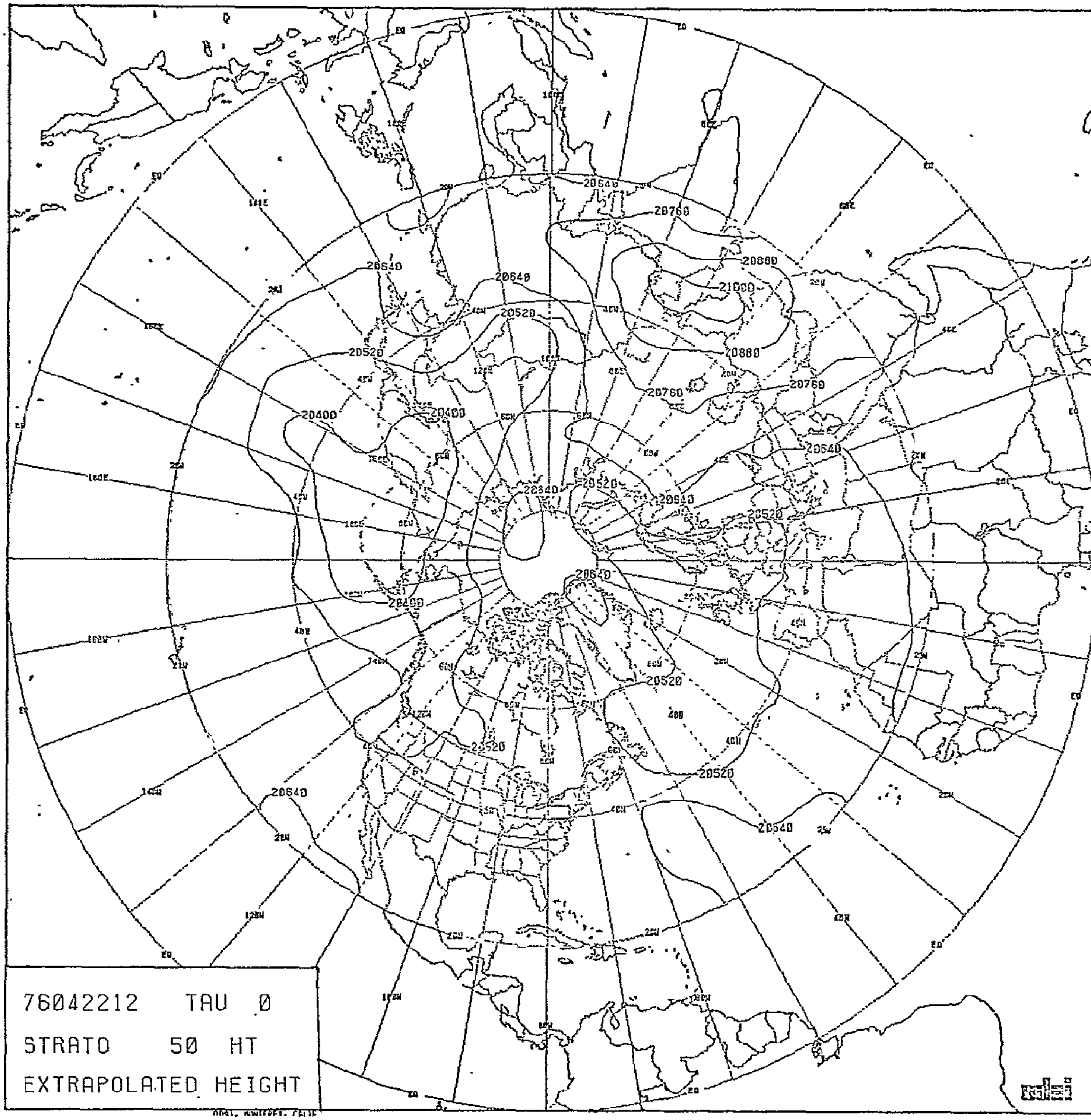

FIGURE II-29: ODSI 50mb HEIGHT ANALYSIS
4/22/76 1200Z

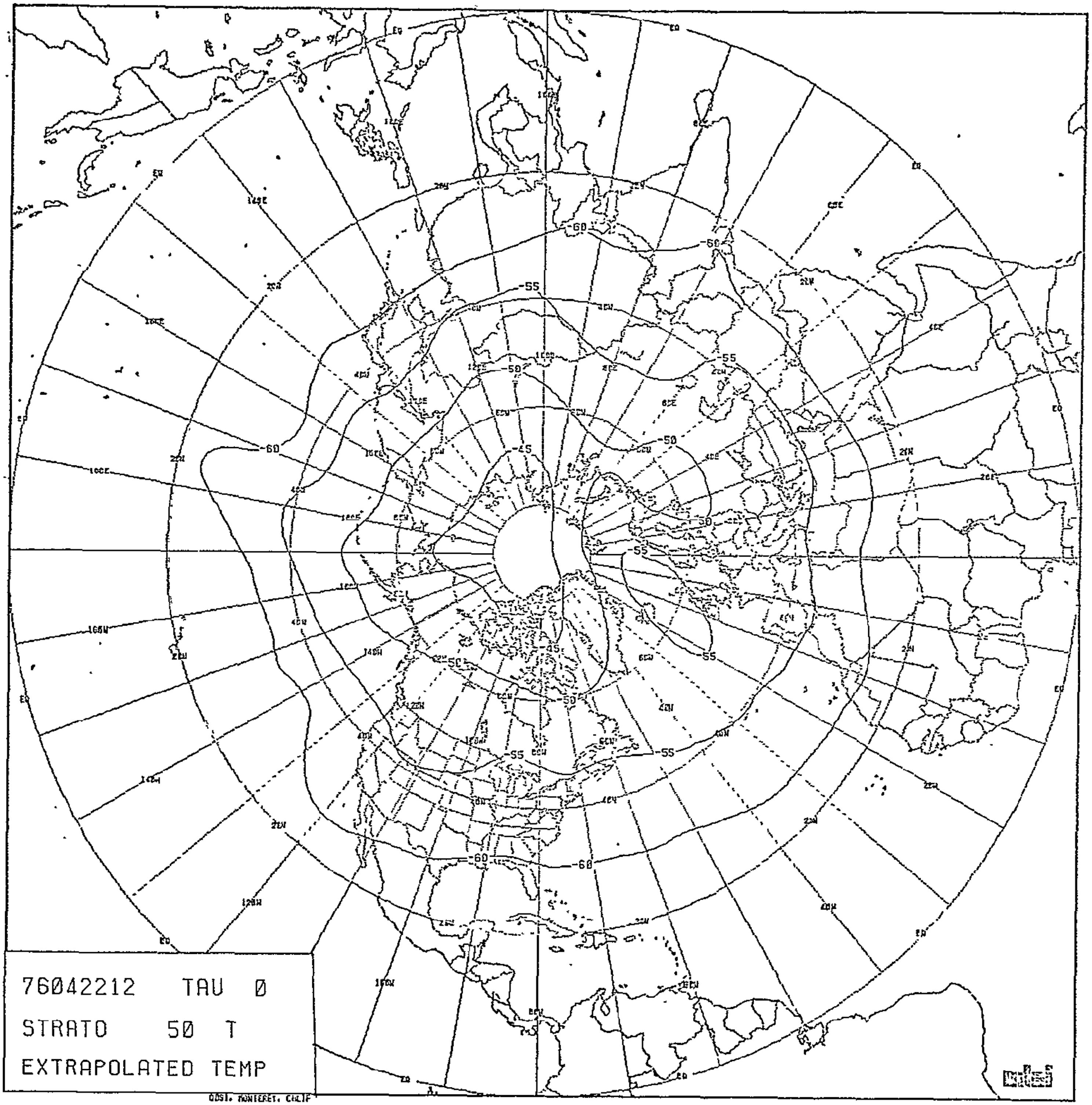

FIGURE II-30: ODSI 50mb TEMPERATURE
ANALYSIS 4/22/76 1200Z

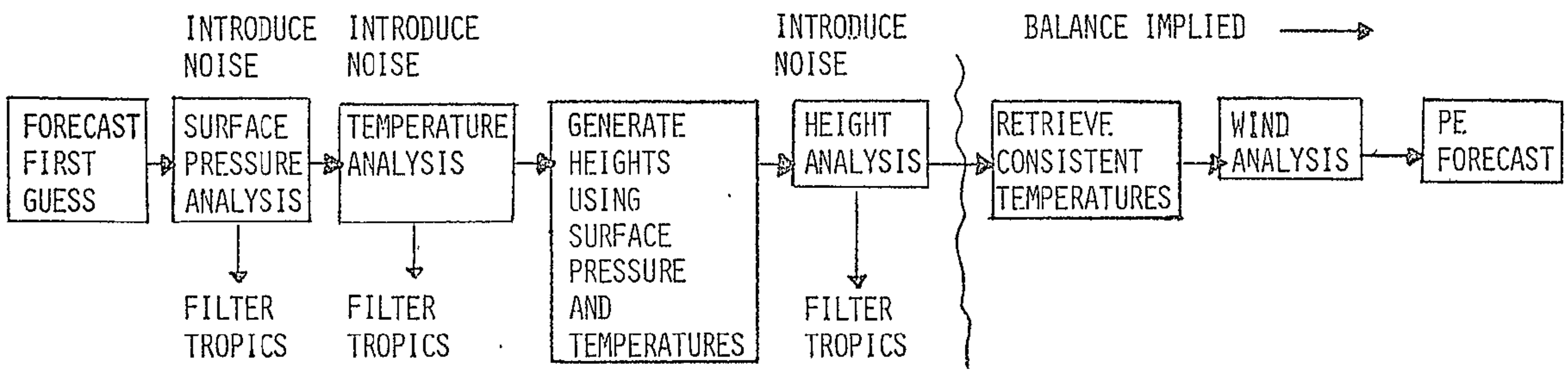

FIGURE II-31: DIAGRAM OF TROPICAL REGION SMOOTHING

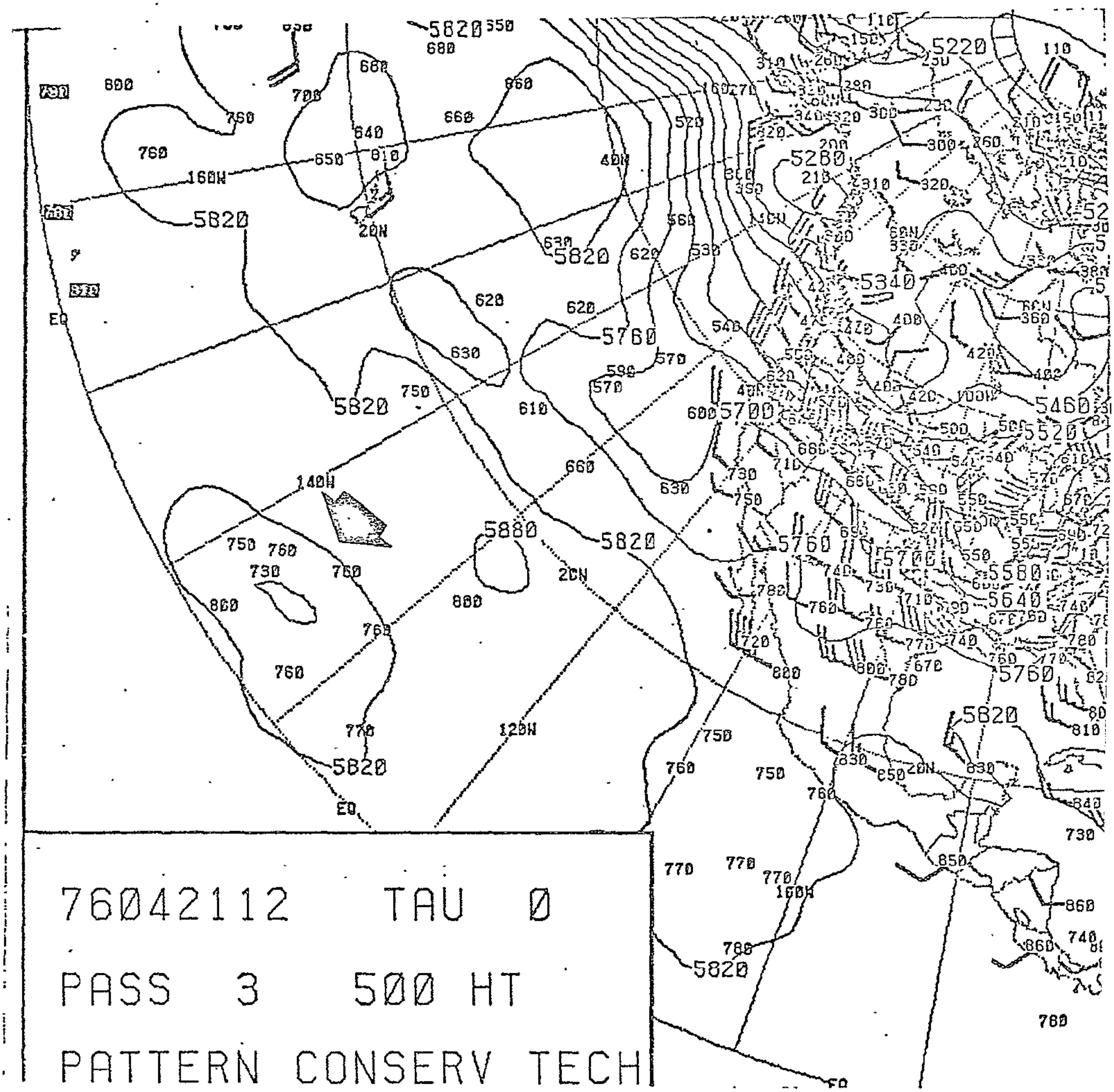

FIGURE II-32: ODSI 500mb HEIGHT ANALYSIS SHOWING NON-METEOROLOGICAL FEATURES IN THE TROPICS 4/21/76 1200Z

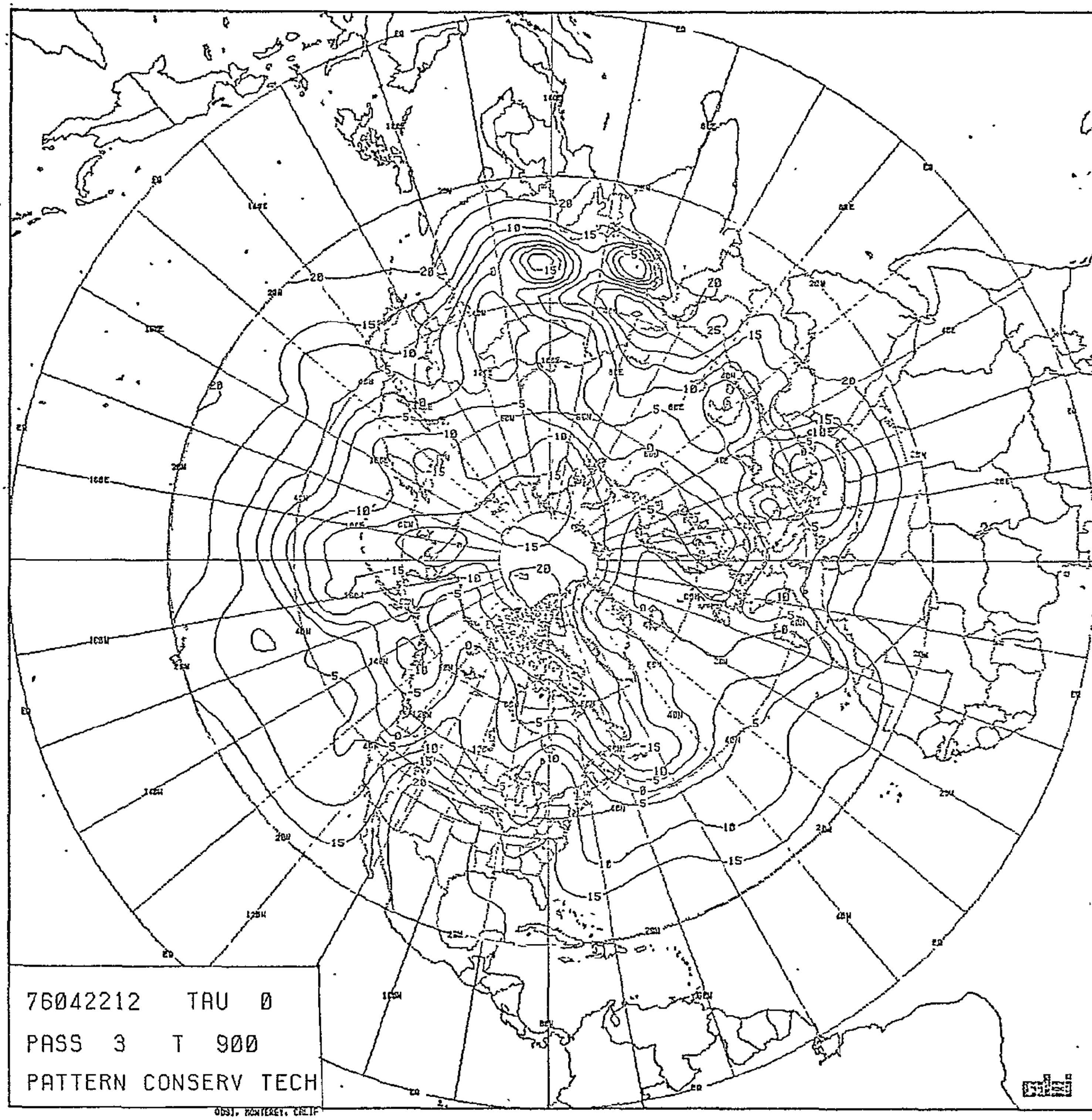

FIGURE II-33: ODSI 900mb TEMPERATURE ANALYSIS
WITHOUT DATA 4/22/76 1200Z

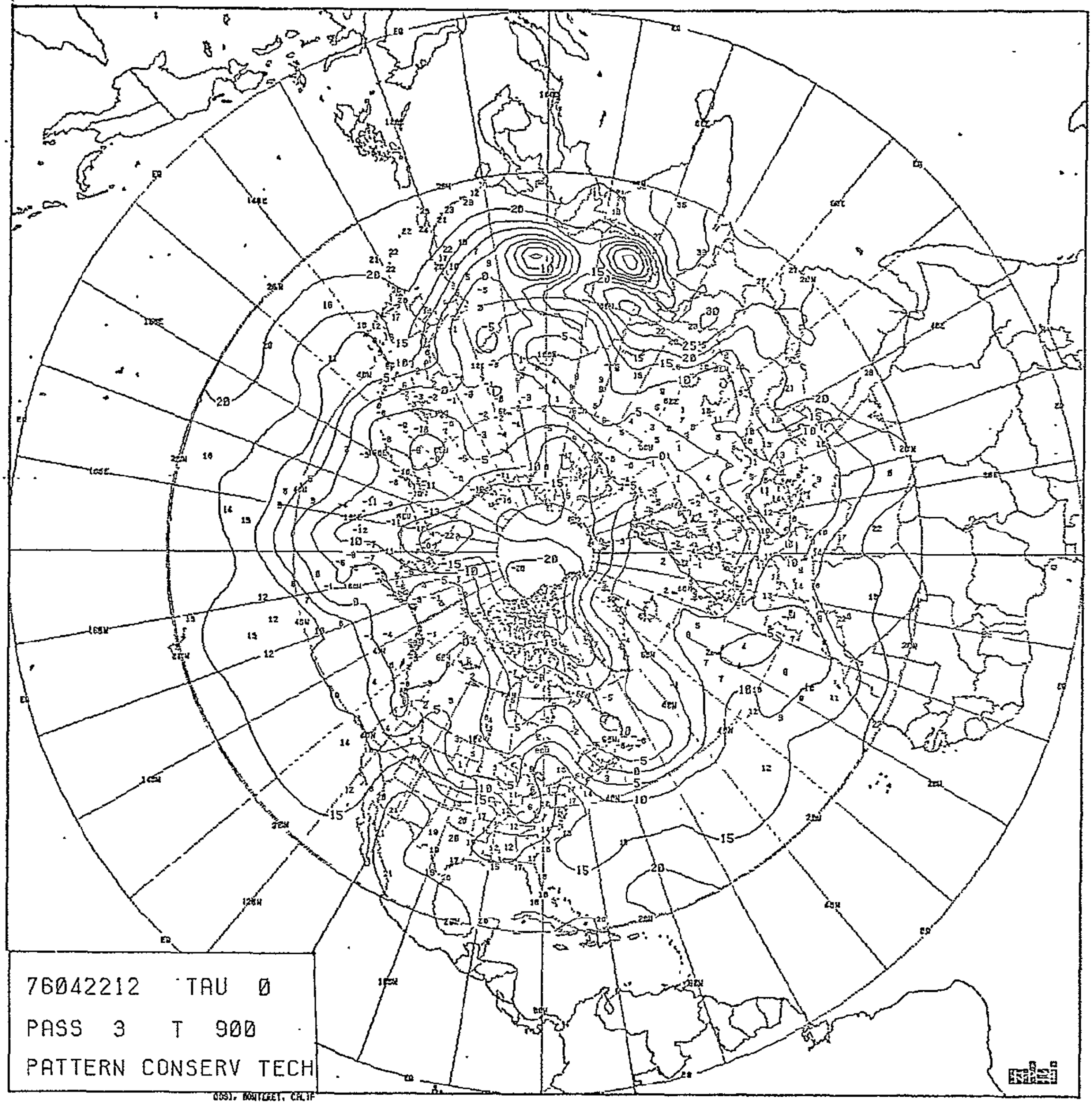

FIGURE II-34: ODSI 900mb TEMPERATURE ANALYSIS
WITH DATA 4/22/76 1200Z

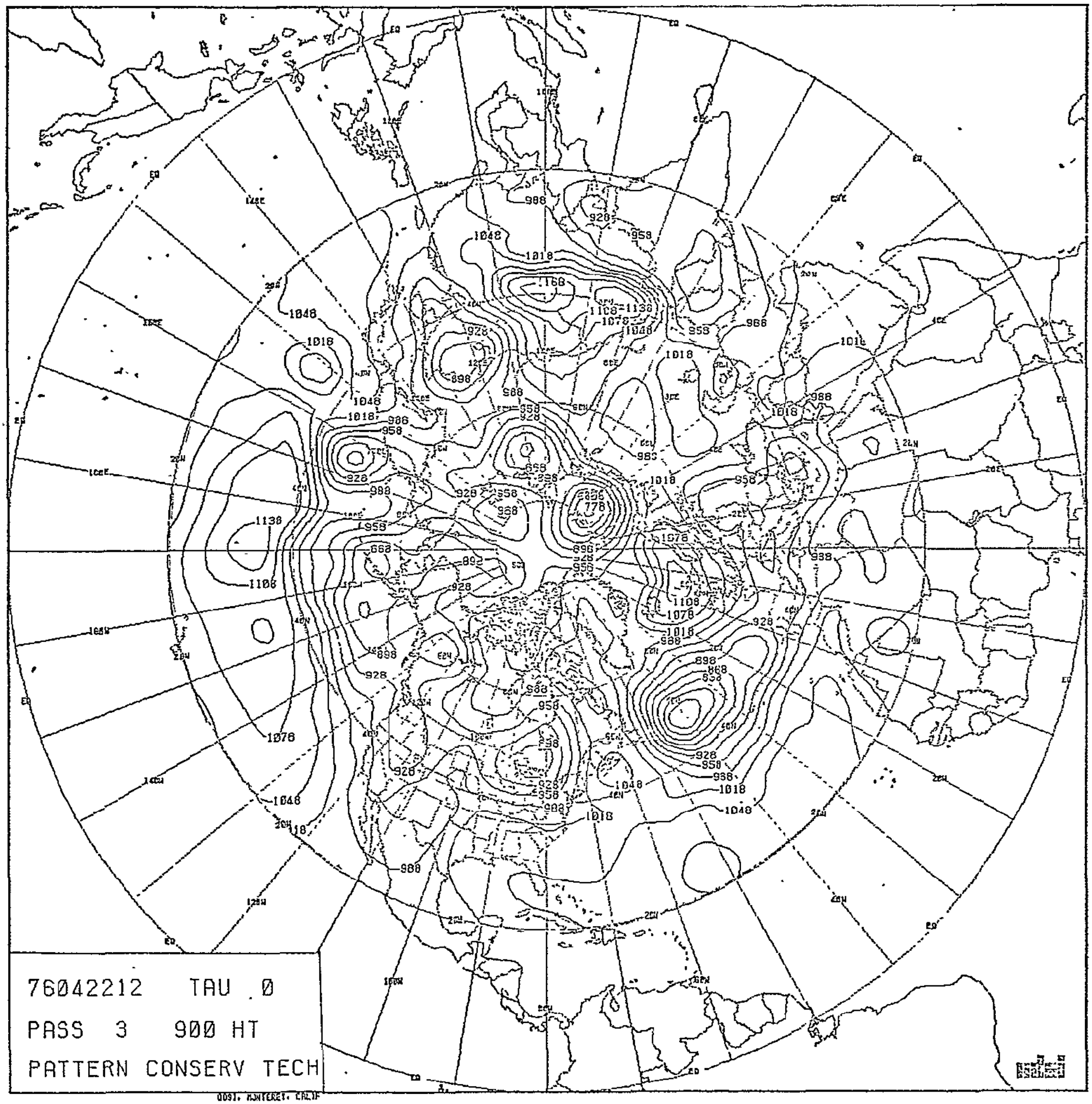

FIGURE II-35: ODSI 900mb HEIGHT ANALYSIS WITHOUT DATA 4/22/76 1200Z

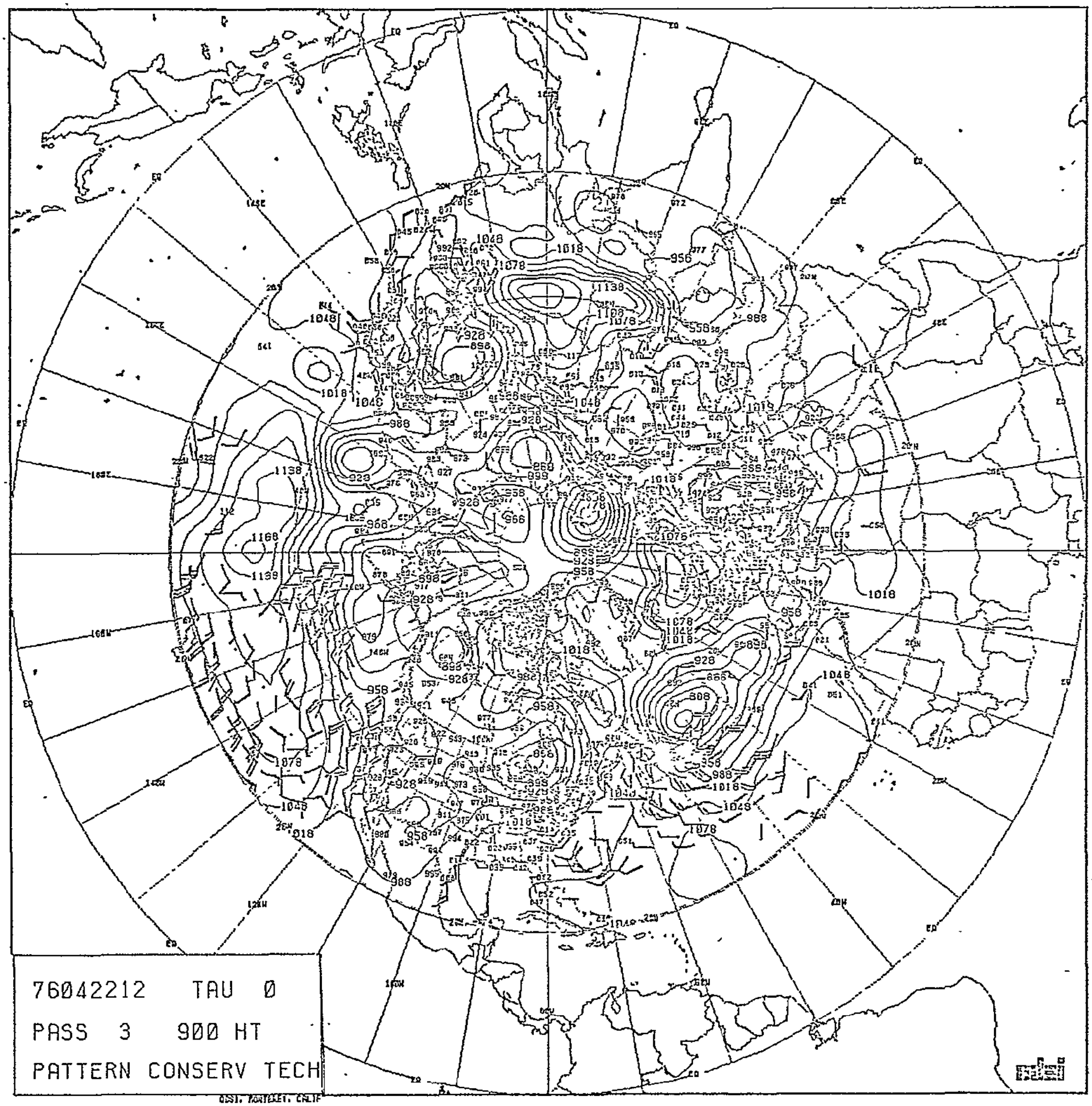

FIGURE II-36: ODSI 900mb HEIGHT ANALYSIS
WITH DATA 4/22/76 1200Z

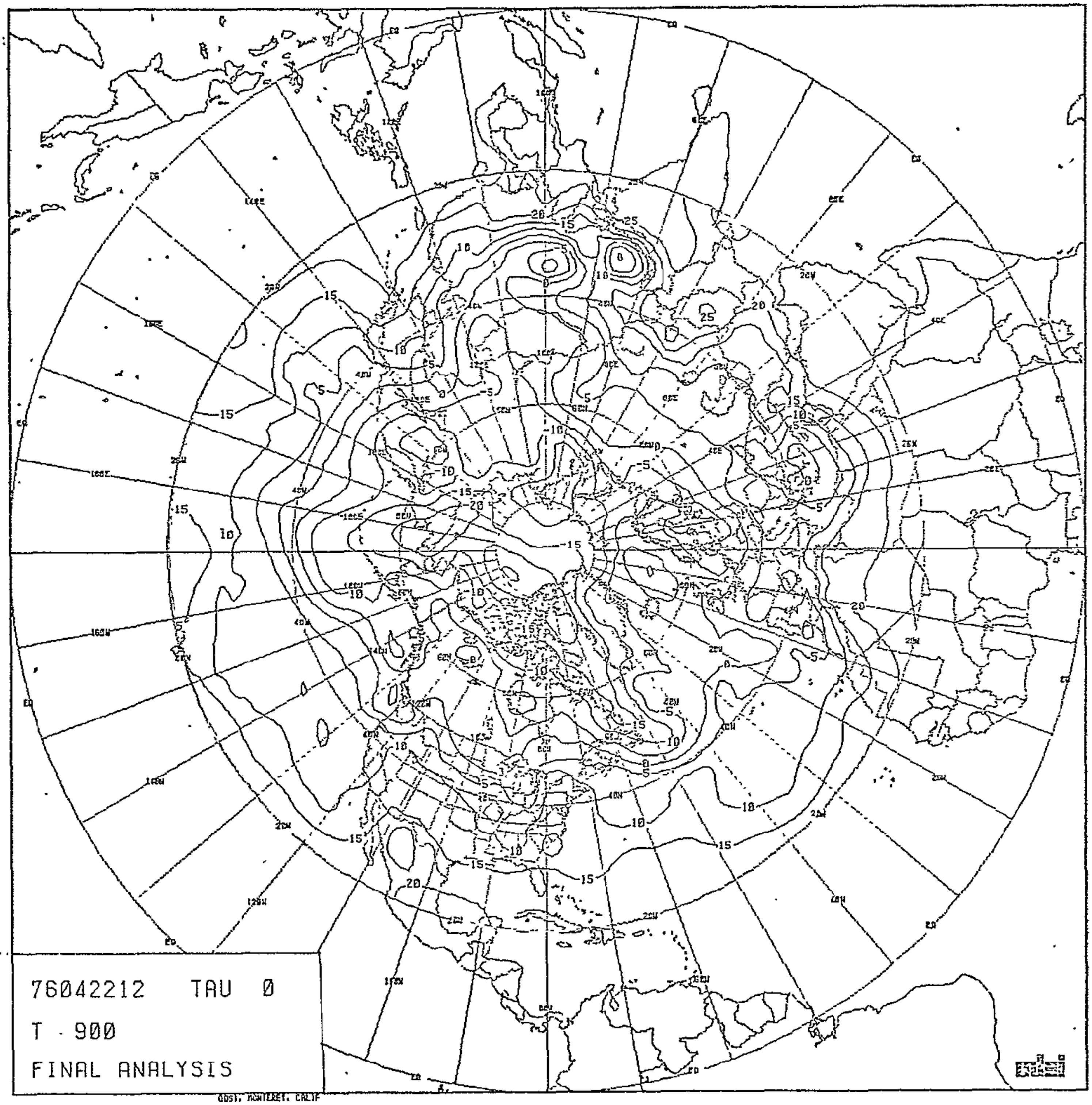

FIGURE II-37: ODSI 900mb RETRIEVED TEMPERATURES
4/22/76 1200Z

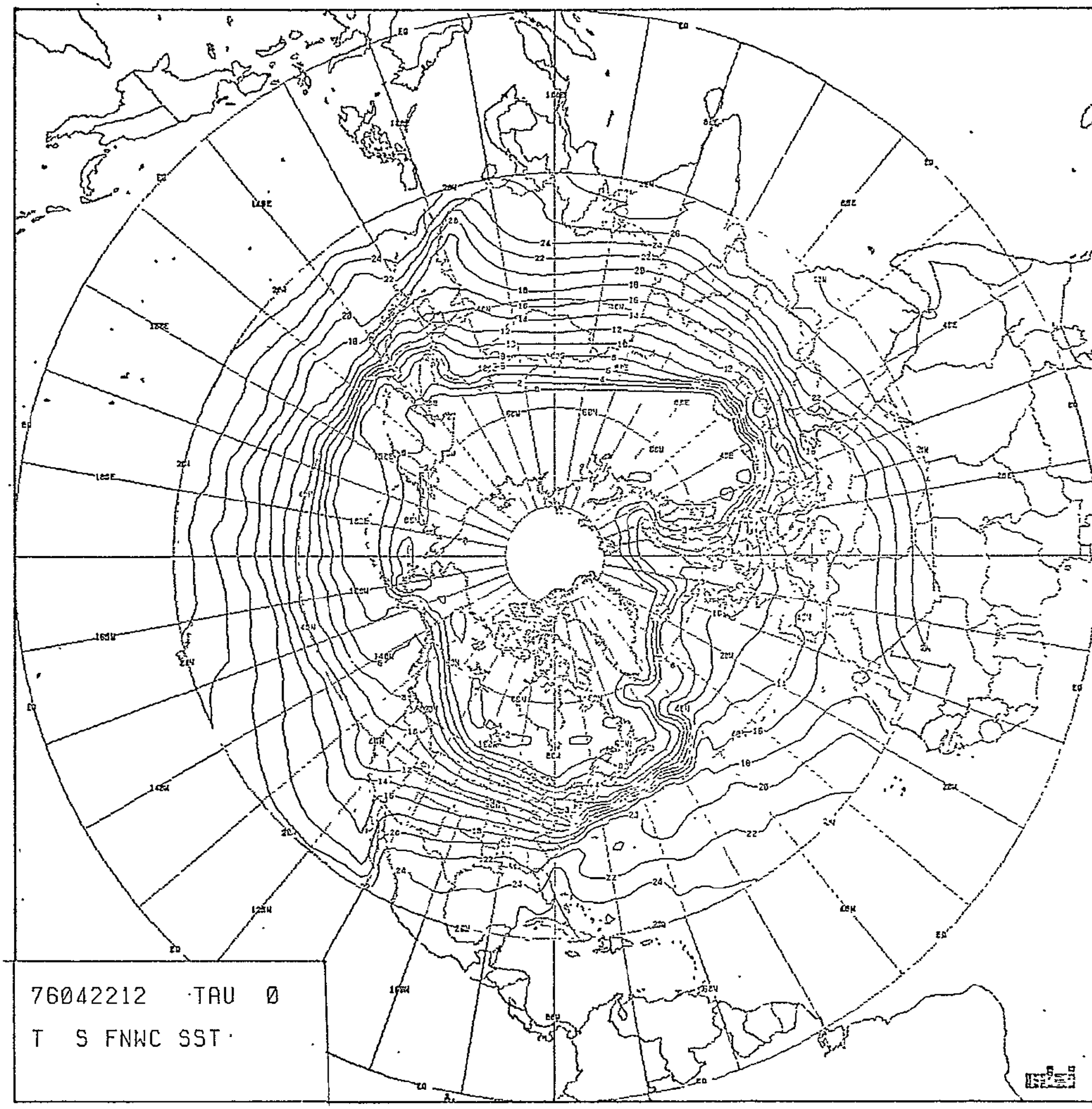

FIGURE II-38: FNWC SEA SURFACE TEMPERATURE ANALYSIS 4/22/76 1200Z

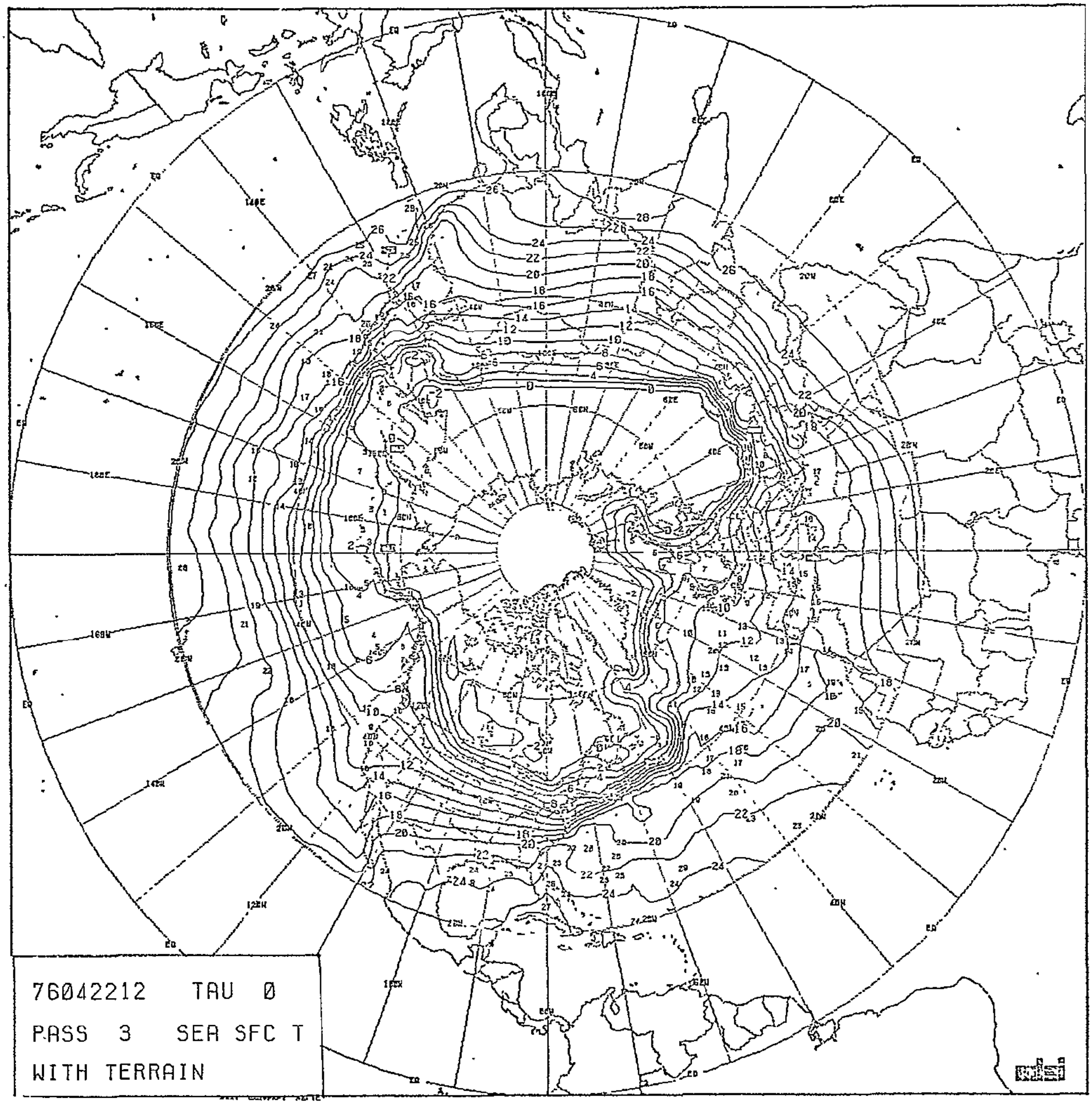

FIGURE II-39: ODSI SEA SURFACE TEMPERATURE ANALYSIS (63x63) 4/22/76 1200Z

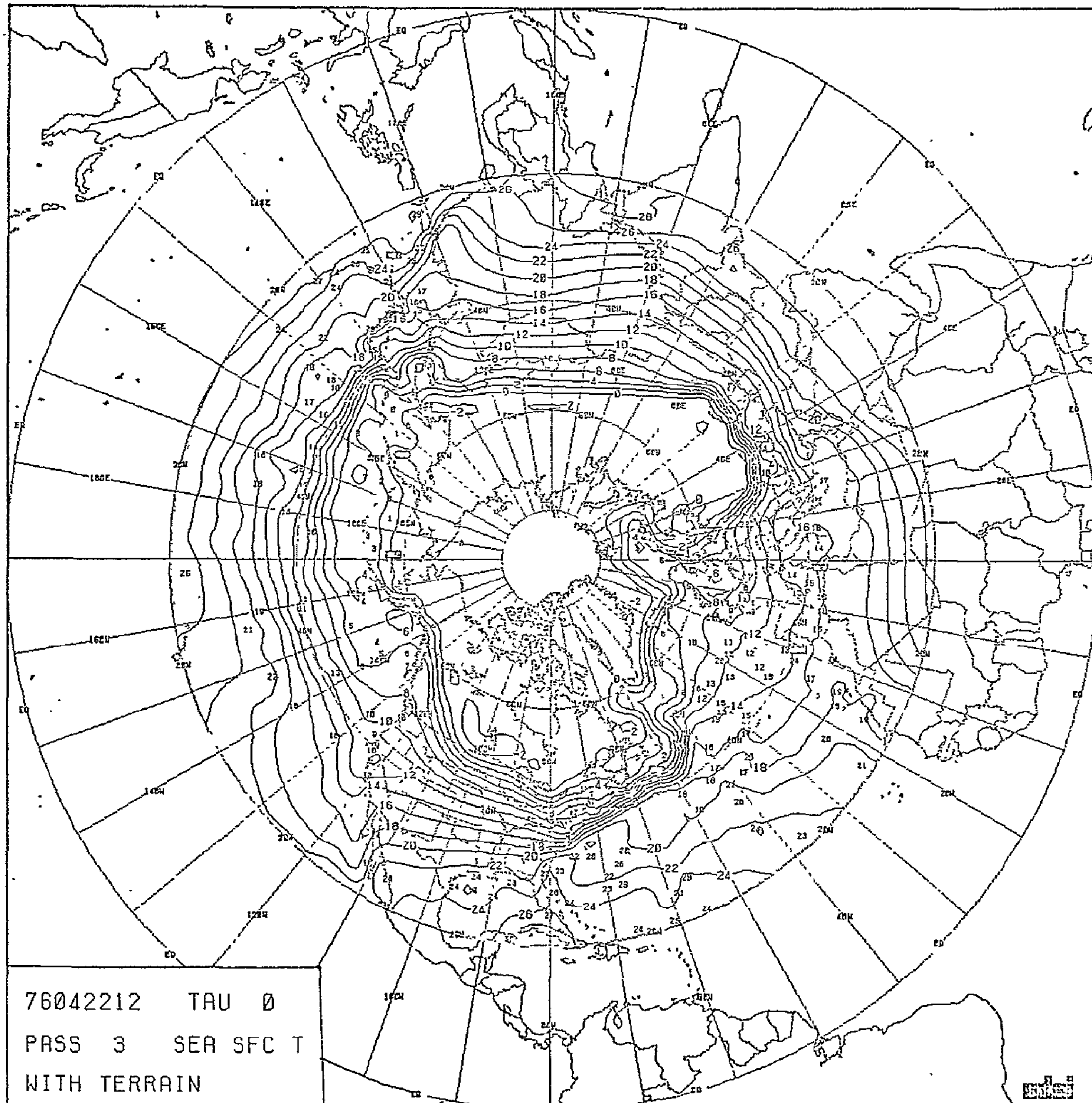

FIGURE II-40: ODSI SEA SURFACE TEMPERATURE ANALYSIS (187x187) 4/22/76 1200Z

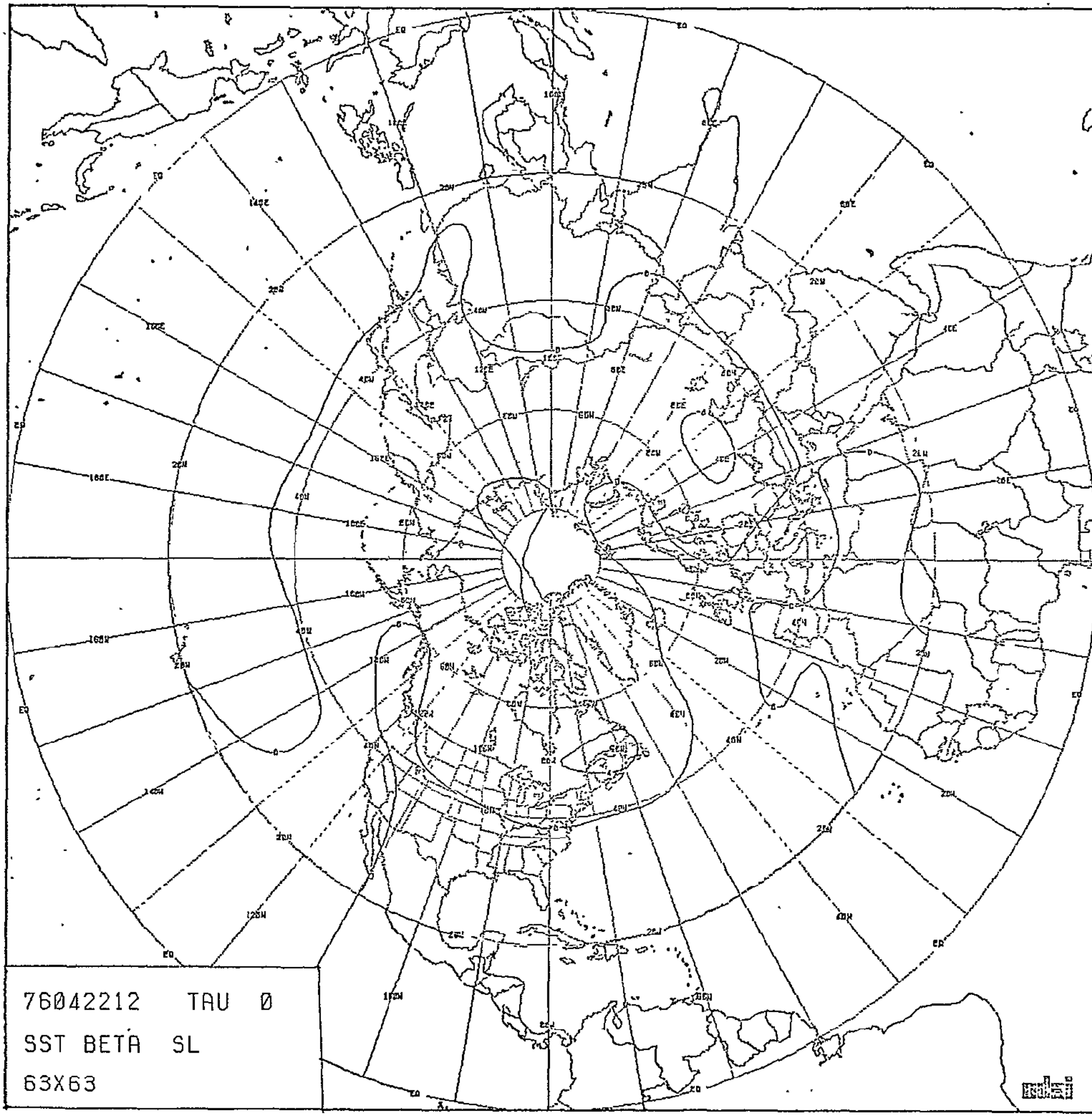

FIGURE II-41: ODSI SEA SURFACE TEMPERATURE
SL BETA (63x63) 4/22/76 1200Z

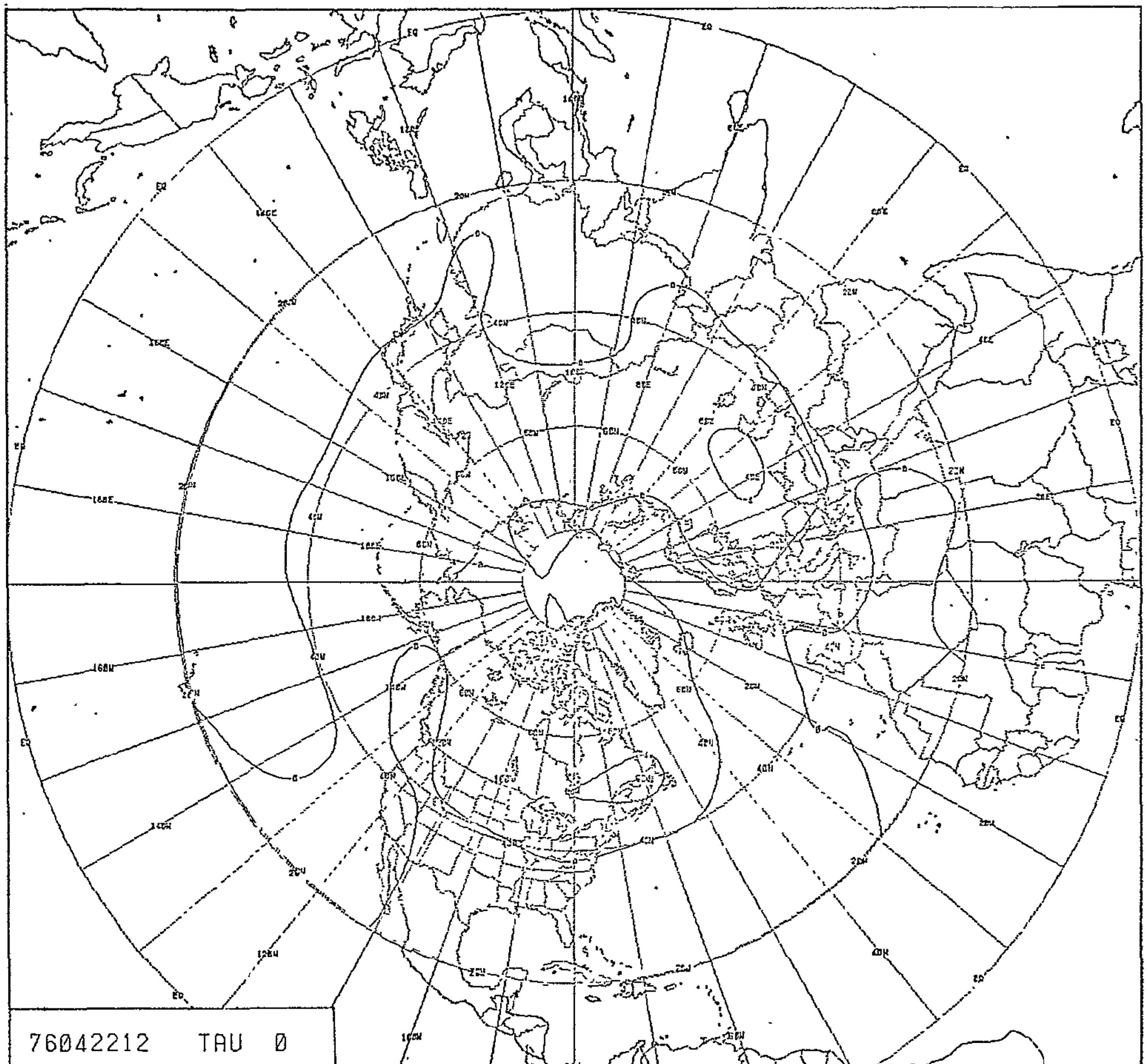

FIGURE II-42: ODSI SEA SURFACE TEMPERATURE SL
BETA (187x187) 4/22/76 1200Z

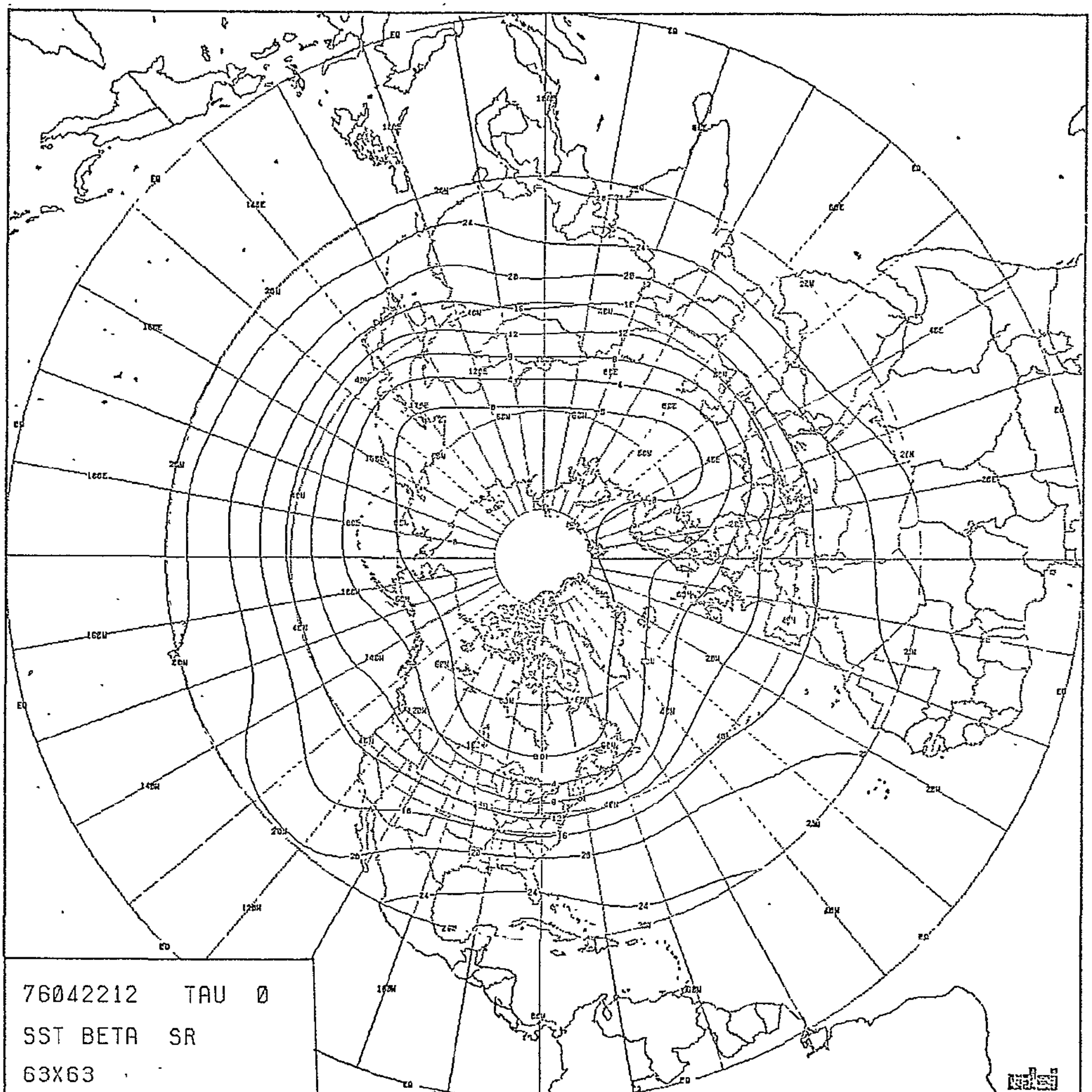

FIGURE II-43: ODSI SEA SURFACE TEMPERATURE SR BETA (63x63) 4/22/76 1200Z

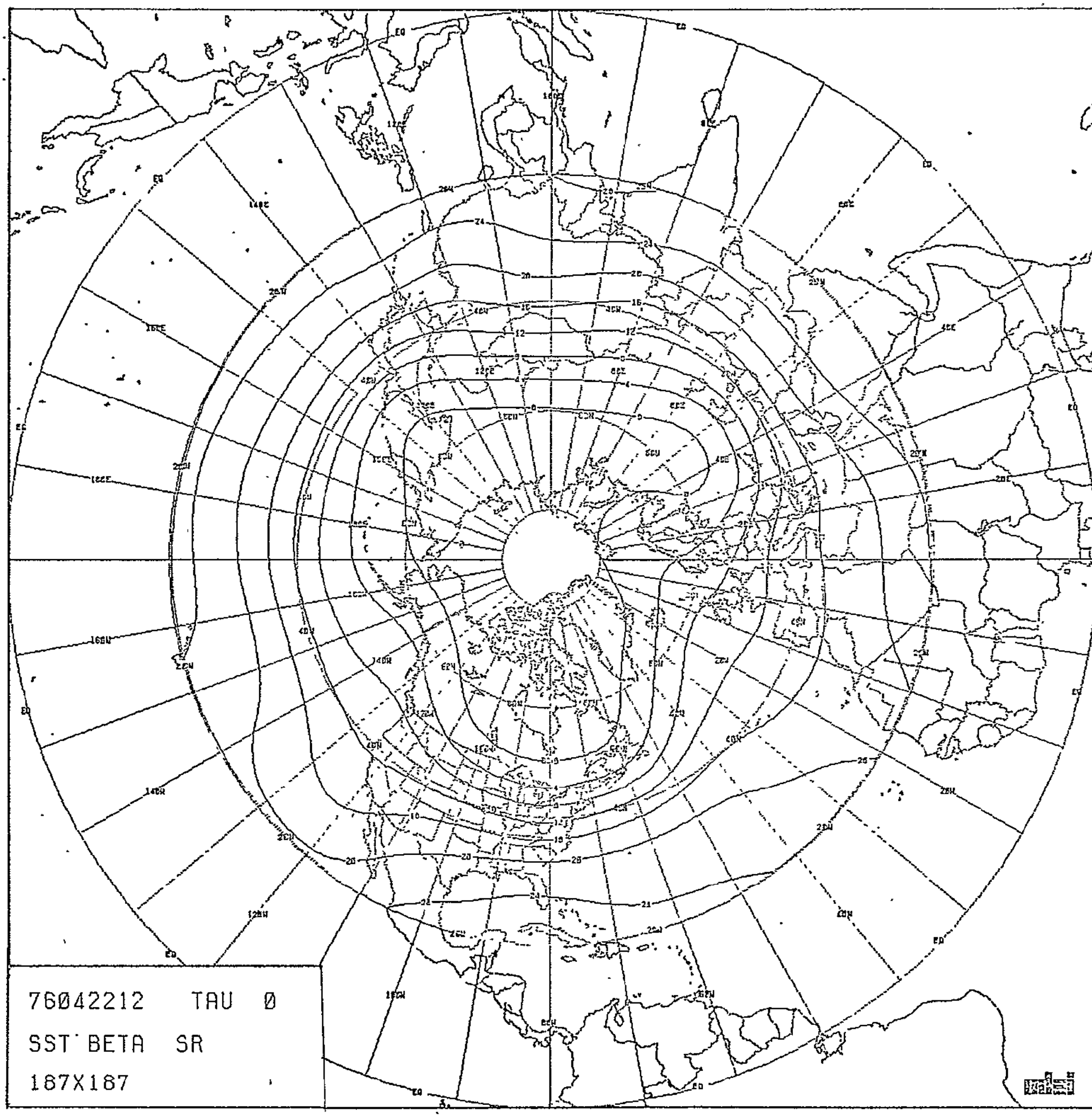

FIGURE II-44: ODSI SEA SURFACE TEMPERATURE
SR BETA (187x187) 4/22/76 1200Z

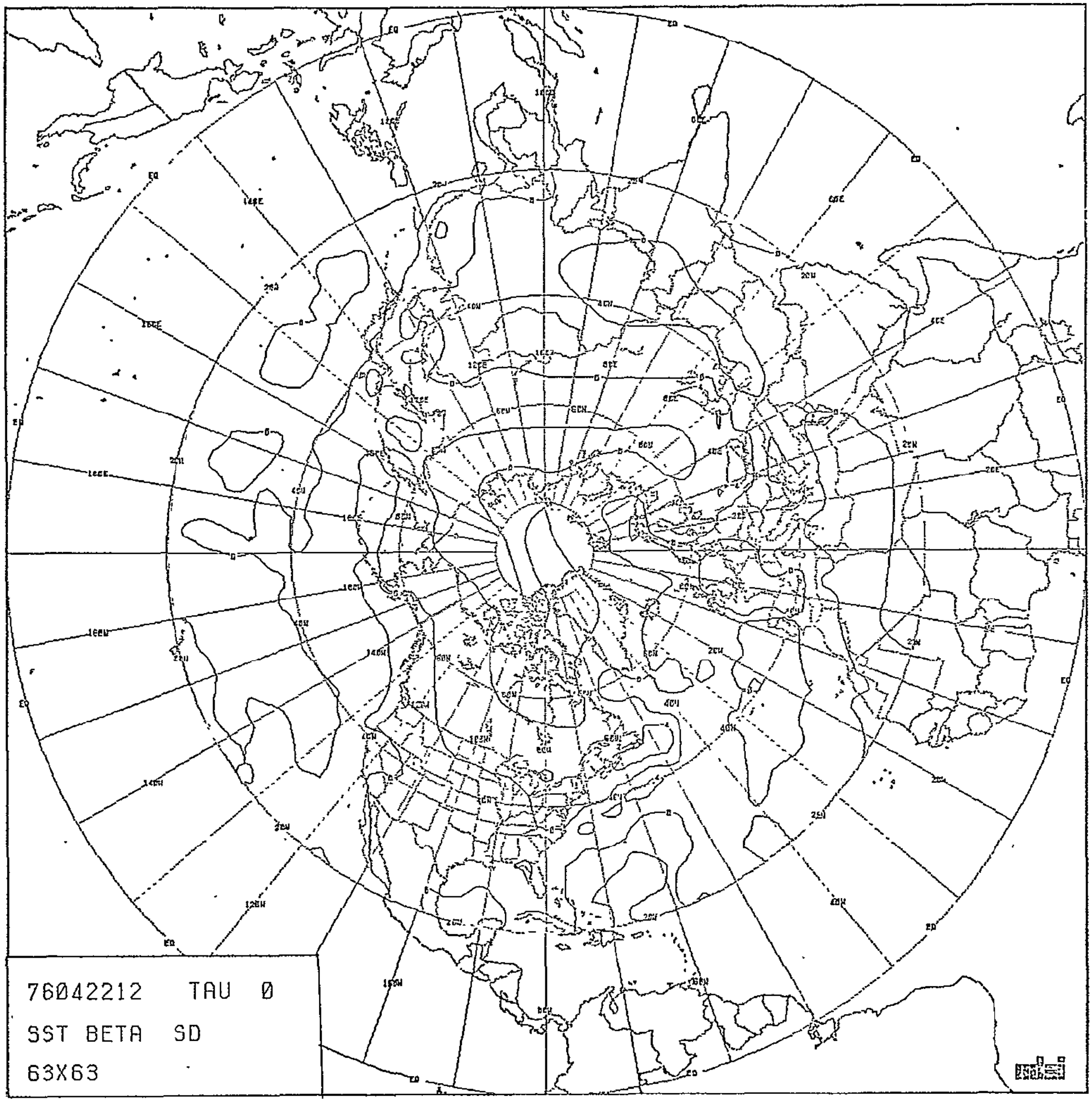

FIGURE II-45: ODSI SEA SURFACE TEMPERATURE
SD BETA (63x63) 4/22/76 1200Z

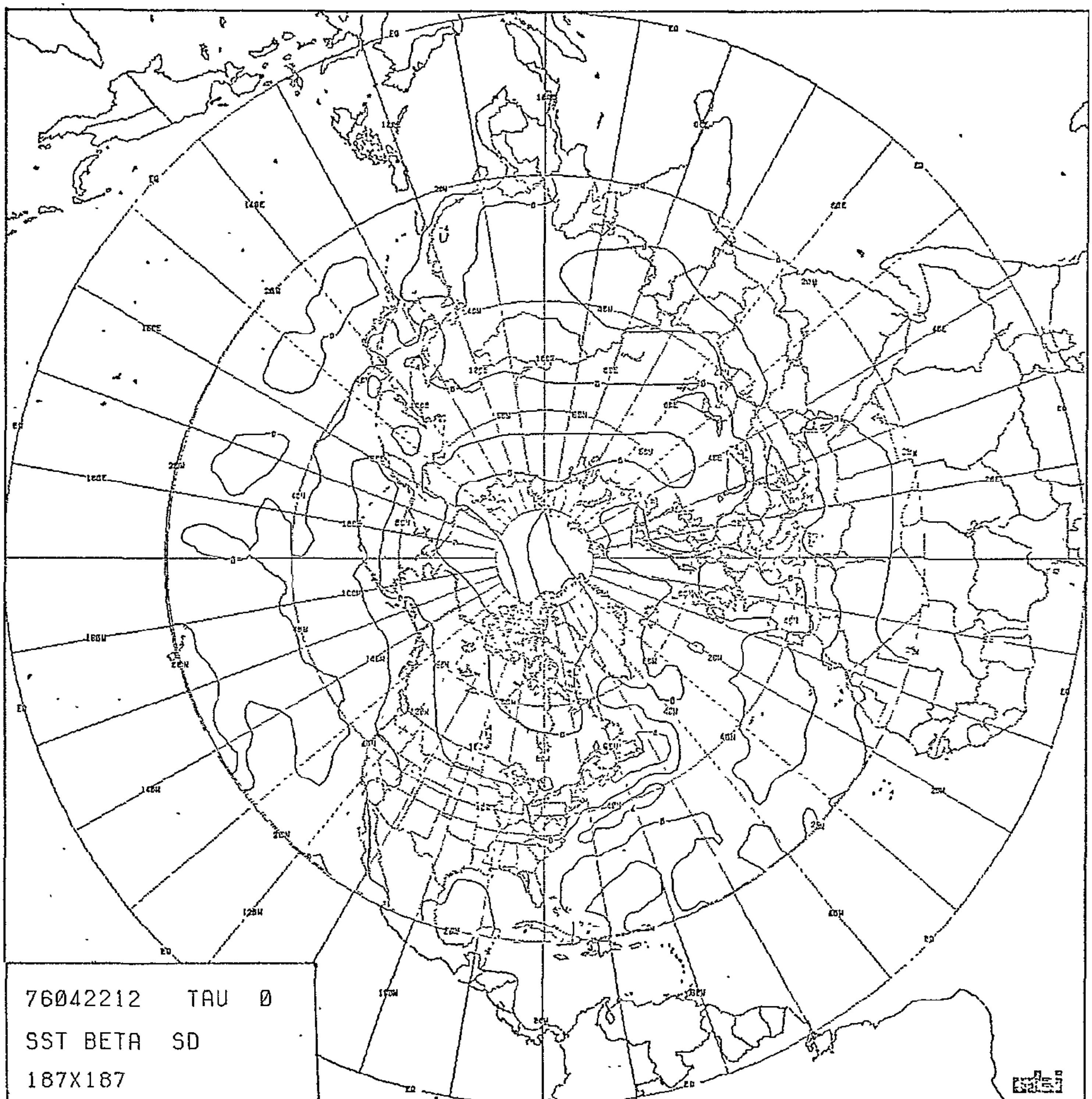

FIGURE II-46: ODSI SEA SURFACE TEMPERATURE
SD BETA (187x187) 4/22/76 1200Z

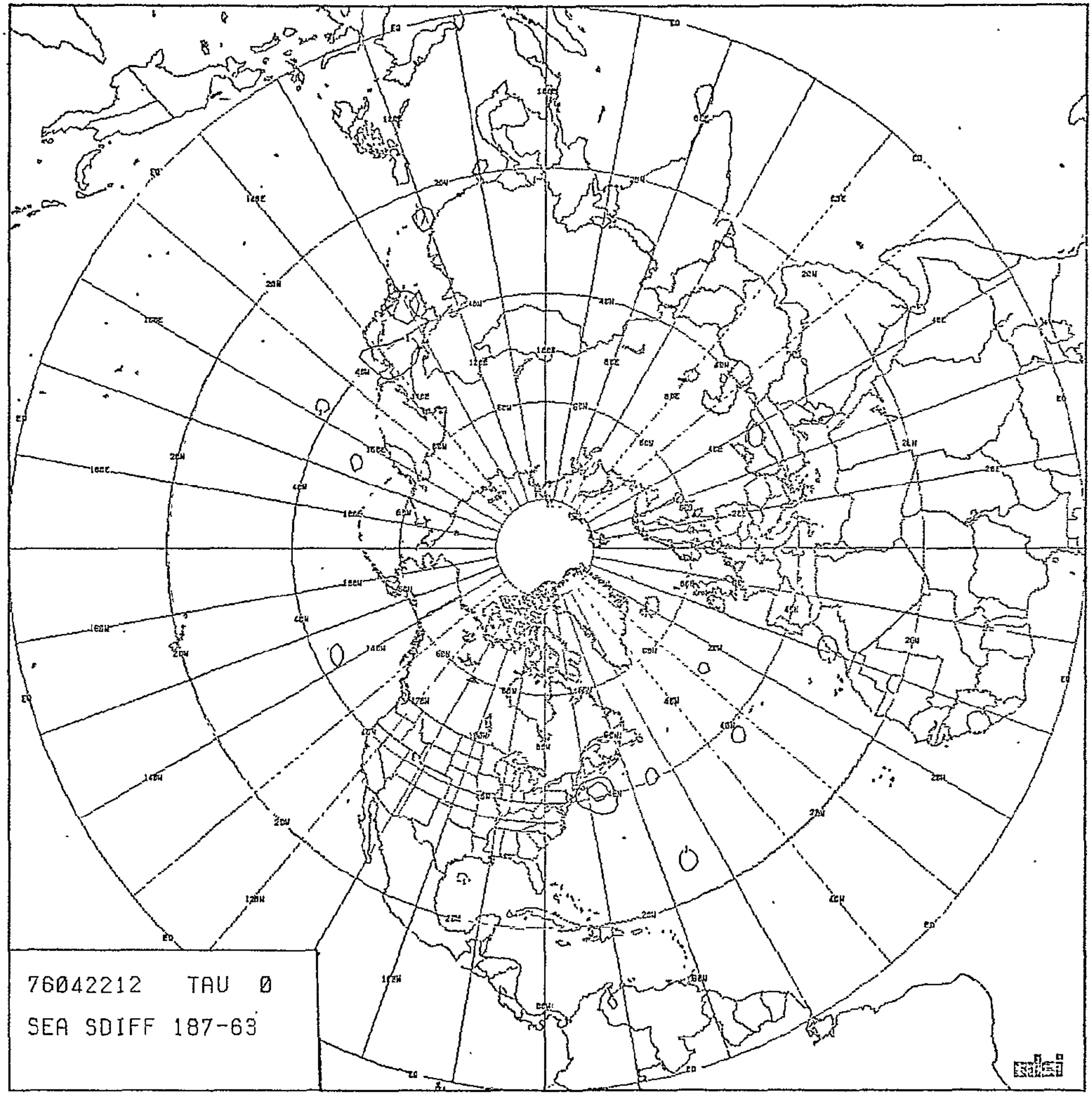

FIGURE II-47: ODSI SEA SURFACE TEMPERATURE
187 ANALYSIS-63 ANALYSIS
DIFFERENCE 4/22/76 1200Z
(1° contour interval)

III. FORECAST MODELING

This section describes the results, problem areas and solutions, both proposed and implemented, of the atmospheric prediction modeling effort. Section III-A gives a brief overview of the forecast models.

Section III-B describes the test results obtained. Included are a discussion of the forecast model terrain problem, a discussion of the results of a 24-hour forecast made with the 63 x 63, five sigma layer forecast model (PECHCV), and a discussion of the results of a 24-hour forecast made with the 63 x 63 ten sigma layer forecast model (PECHFV). Due to lack of sufficient computer resources, no forecasts were made with the 187 x 187 horizontal grid models.

A. Model Descriptions

The forecast model portion of this project involved developing a set of four hemispheric, atmospheric prediction models. The descriptors applied to these four models, which use a polar stereographic grid in the horizontal and a sigma coordinate in the vertical, are:

PECHCV - five sigma layers and a 63 x 63 horizontal grid
PECHFV - ten sigma layers and a 63 x 63 horizontal grid
PEFHCV - five sigma layers and a 187 x 187 horizontal grid
PEFHFV - ten sigma layers and a 187 x 187 horizontal grid.

Conservation forms of the difference equations based on the Arakawa technique are integrated using either a fifteen or five minute time step on a 381 km. or 127 km. grid (at 60°N) for the 63 x 63 or 187 x 187 models, respectively. Pressure gradient force terms are replaced by a single geo-potential gradient on local pressure surfaces to reduce in-consistent truncation error (Kurihara modification). Stress is applied at the lowest level. A nonlinear pressure smoothing is used to help control computational noise. The horizontal boundary conditions are rigid, insulated, slippery walls. Centered time differencing with time averaging of the pressure gradient force terms in the momentum equations is used. Robert' time filtering of the temperature and moisture solutions is used to preclude solution separation and to enhance solution stability.

The moisture and heat source/sink terms are modeled in a similar manner to those in the early Mintz and Arakawa general circulation model. Terms representing evaporation and large-scale condensation, sensible heat exchange, para-meterized cumulus convection and precipitation, and solar and terrestrial radiation are included. Dry convective adjustment precludes hydrostatic instability.

A detailed description of the forecast models can be found in Volume III of this final report entitled "PECHCV, PECHFV, PEFHCV and PEFHFV - A Set of Atmospheric, Primitive Equation Forecast Models for the Northern Hemisphere".

B. Test Results

1. Forecast Model Terrain

The specification of the gross terrain in a forecast model is necessary to ensure realism in the atmospheric flows being modeled. However, the terrain can cause problems by causing the generation of small scale disturbances and thereby inducing nonmeteorological features if it is not carefully specified. Figure III-1 shows the Northern Hemisphere terrain used in the test forecasts. This terrain has been limited to have a gradient less than 1500 meters per 63 x 63 grid interval and is further constrained to be "smooth" so as to create as little trauma in the forecast as possible.

Another problem associated with the inclusion of "realistic" terrain in the forecast model is the need to generate temperature and geopotential heights on pressure surfaces below the terrain at output time. Since no forecast has been generated at these levels, one must either extrapolate values from the sigma surfaces above or devise a more sophisticated method of obtaining values at these levels. Figure III-2 shows the temperature at 1000 mb from a twelve hour forecast made with zero terrain. As can be seen from the figure, the temperatures are quite reasonable since the lowest sigma surface is close to the 1000 mb level. Figure III-3 shows the temperatures at 1000 mb for the same twelve hour forecast period, but

with realistic terrain included. The feature that is immediately apparent is the intense cold region in the upper middle portion of the chart (the Himalayan region). This feature is, of course, not realistic, since it is caused by extrapolation from the high altitude sigma surfaces down to the 1000 mb level. If this field is used as a first guess for the analysis model, a very unrealistic analysis will result.

Obviously, a more sophisticated method of producing data on pressure surfaces below the terrain is required. The method described below is a variation of the one in use at FNWC and basically uses the standard heights and temperatures of pressure surfaces and modifies them according to the conditions at $\sigma = 1.0$. Define:

$$Z_{1.0} = \left(\frac{288.16}{6.5\text{x}10^{-3}}\right) \left[1 - \left(\frac{\pi}{1013.25}\right)^{\left(\frac{1.0}{5.2561}\right)}\right] \qquad \text{[III.1]}$$

$$S_{1.0} = \frac{T_{1.0}}{288.16 - Z_{1.0}(6.5\text{x}10^{-3})} - 1 \qquad \text{[III.2]}$$

$$Z_{SFC} = \left(\frac{288.16}{6.5\text{x}10^{-3}}\right) \left[1 - \left(\frac{P_s}{1013.25}\right)^{\left(\frac{1.0}{5.2561}\right)}\right] \qquad \text{[III.3]}$$

and

$$\bar{S} = \frac{Z_T}{Z_{1.0} - Z_{SFC}} - 1 \qquad \text{[III.4]}$$

where

$$T_{1.0} = 1.5\ T_{0.9} - 0.5\ T_{0.7} \qquad \text{[III.5]}$$

Then if

$$Z_{1.0} - Z_{SFC} < 500 \qquad [III.6]$$

the height and temperature at standard level L is given by:

$$Z(L) = [Z_{STD}(L) - Z_{SFC}]\ [1 + S_{1.0}] \qquad [III.7]$$

and

$$T(L) = T_{STD}(L)\ [1 + S_{1.0}] \qquad [III.8]$$

Otherwise, by

$$Z(L) = [Z_{STD}(L) - Z_{SFC}]\ [1 + \frac{1}{2}(3\bar{S} - S_{1.0})] \qquad [III.9]$$

and

$$T(L) = T_{STD}(L)[1 + \bar{S}] \qquad [III.10]$$

where $Z_{STD}(L)$ and $T_{STD}(L)$ are the standard height and temperature, respectively, of the standard pressure level, L.

Figure III-4 shows the temperature at 1000 mb for the same forecast as Figure III-3, but the reduction method described above was used to produce temperatures below the terrain where required. Note that the intense cold region under the Himalayas has disappeared and numerous other small features are more realistic.

2. Five Layer (PECHCV) Forecast

As explained in Section II-B, the period 4/21/76 12 Z through 4/23/76 12 Z was chosen as the test period for the analysis and forecast models. Figure II-1 shows the analysis and forecast sequence that was made for this period. A bootstrap analysis was made for 4/21/76 12 Z followed by forecast model initialized analyses for the rest of the period on a twelve hour cycle.

The analysis for 4/22/76 12 Z was used as the initial condition for a 24-hour forecast verifying at 4/23/76 12 Z. The set of Figures III-5 through III-26 presents the results of this forecast for surface pressure and 500 mb height along with the FNWC forecast for the same period for comparison. Also presented are the 24-hour actual changes, forecast changes, error charts and differences between the two forecasts.

As can be seen from the figures, the forecast is of mediocre quality since some systems that greatly intensified were not predicted to do so and some others, while more or less correct in intensity, were not moved correctly. However, other systems were forecast correctly. Also, the 500 mb height forecast is considerably better than the surface pressure forecast (which is to be expected) since it is much easier to predict the open wave motion at 500 mb than to predict the highly cellular structure of the surface

pressure field. Also, as might be expected, the quality of the FNWC forecast is somewhat better since it is the result of many years of model "engineering" and fourth-order differences in the forecast model.

As was pointed out in Section II, this case was chosen since it covers a very meteorologically active period with rapid movement of systems and intense cyclogenesis and, therefore, severely tests the performance of any forecast model. There are still numerous problems in the analysis procedure and particularly in the forecast model - analysis model interaction. Progress is currently being made on these problems and better analyses and forecasts should result.

3. Ten Layer (PECHFV) Forecast

A 24-hour forecast was made with the ten sigma layer forecast model (PECHFV) for the same 24-hour period (4/22/76 12Z to 4/23/76 12Z) as the five sigma layer model (PECHCV). The same analysis was used, with the difference being the finer resolution in the vertical. There are also some minor computational differences between the two forecast models as explained in Volume III.

Figures III-27 through III-36 show the surface pressure and 500 mb height forecasts, forecast change and error charts and a comparison with the FNWC and the five layer forecasts.

Very little difference exists between the five and ten sigma layer forecasts. In fact, the ten layer forecast is possibly not quite as good as the five layer forecast. This is somewhat surprising since one would expect better depiction of the vertical structure of the atmosphere and, certainly, better definition of the near surface region with increased vertical resolution. This was the first 24-hour forecast made with this model (in other than a checkout mode). There is still some tuning to be done, so it is quite possible that some improvement in the forecast will result. On the other hand, increased vertical resolution may not make much difference when coupled with a fairly coarse horizontal resolution.

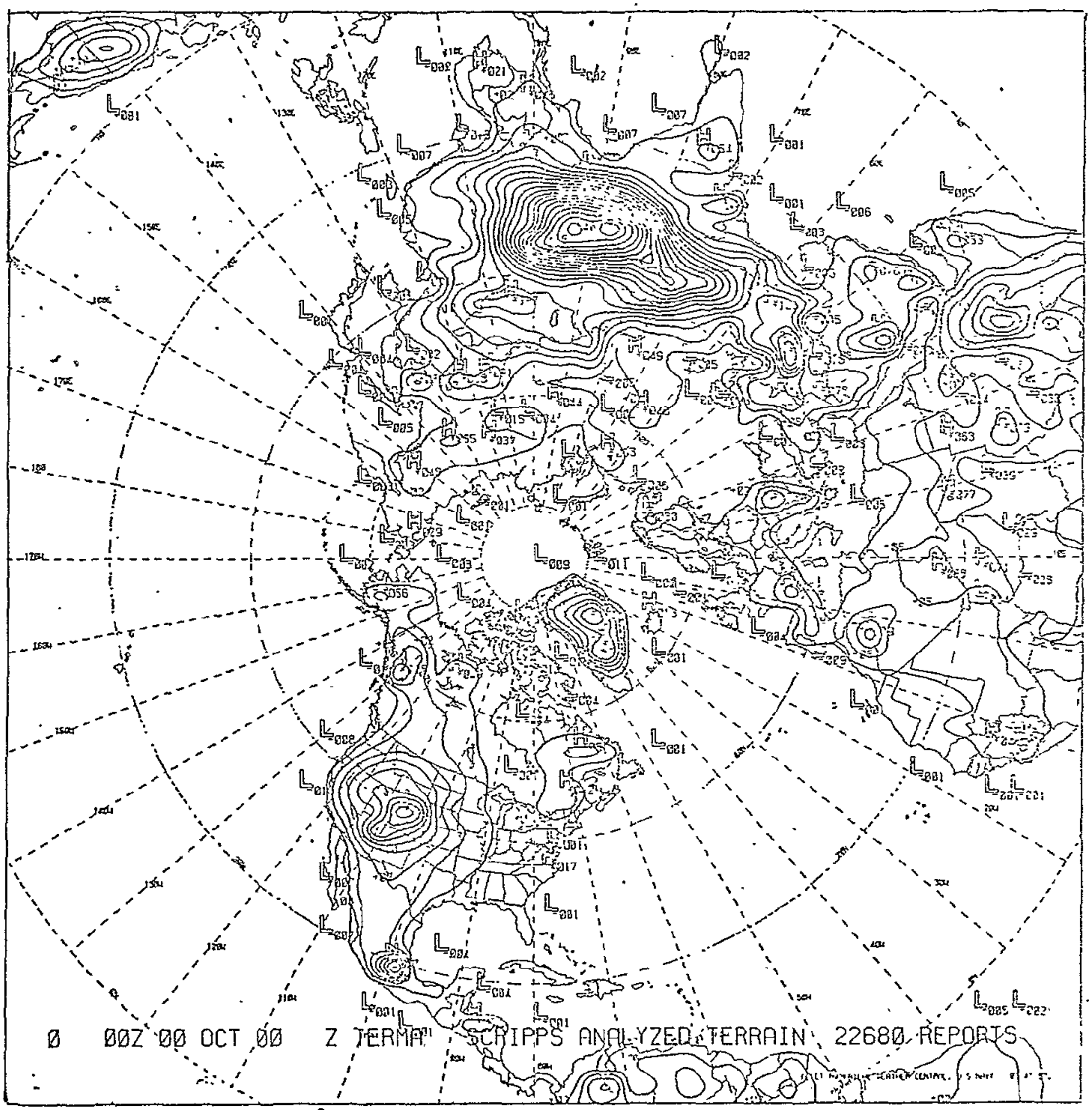

FIGURE III-1: NORTHERN HEMISPHERE 1500 m/d TERRAIN

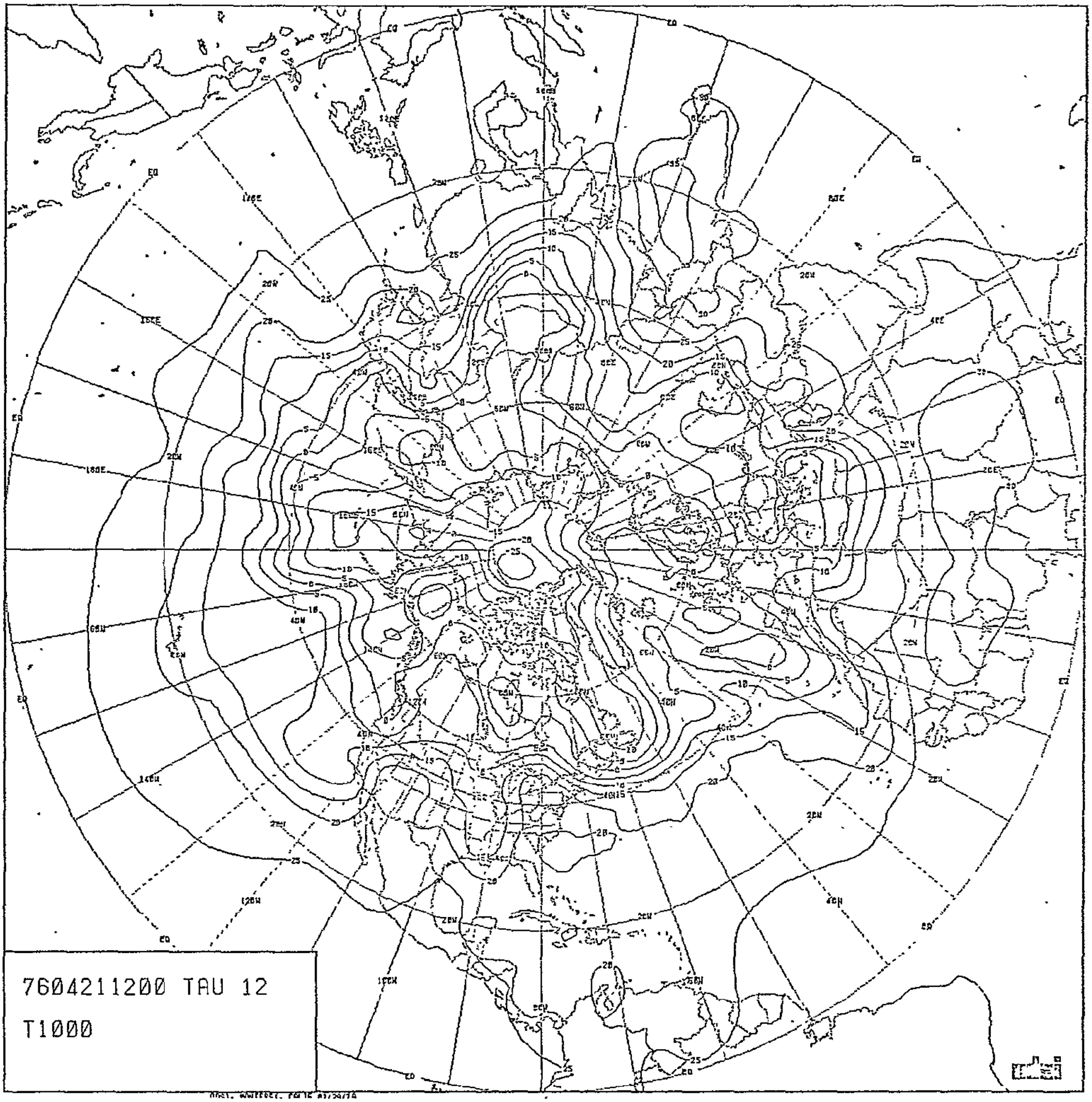

FIGURE III-2: ZERO TERRAIN FORECAST
4/22/76 1200Z

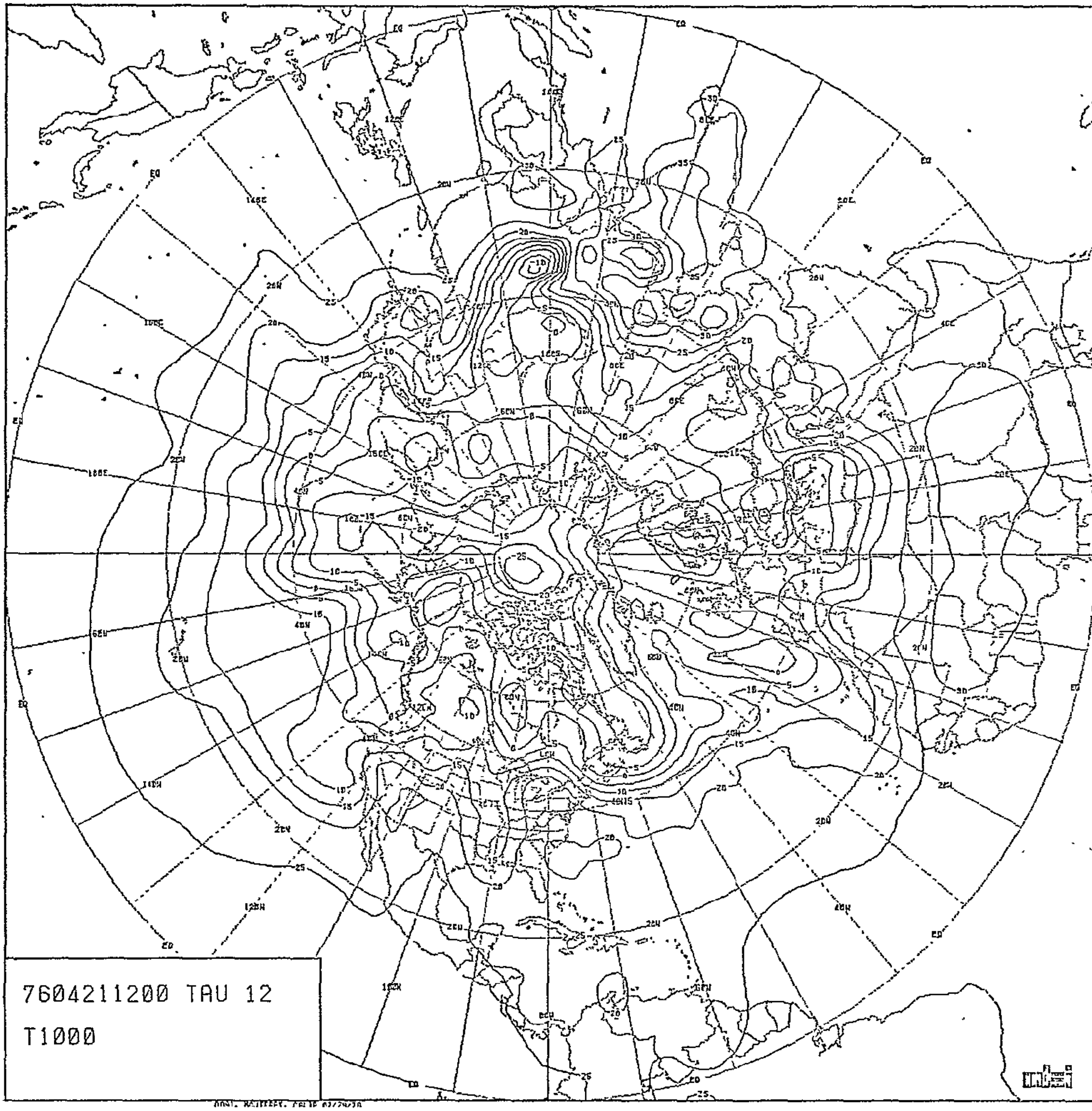

FIGURE III-3: 1500 m/d TERRAIN FORECAST
(EXTRAPOLATION BELOW SURFACE)
4/22/76 1200Z

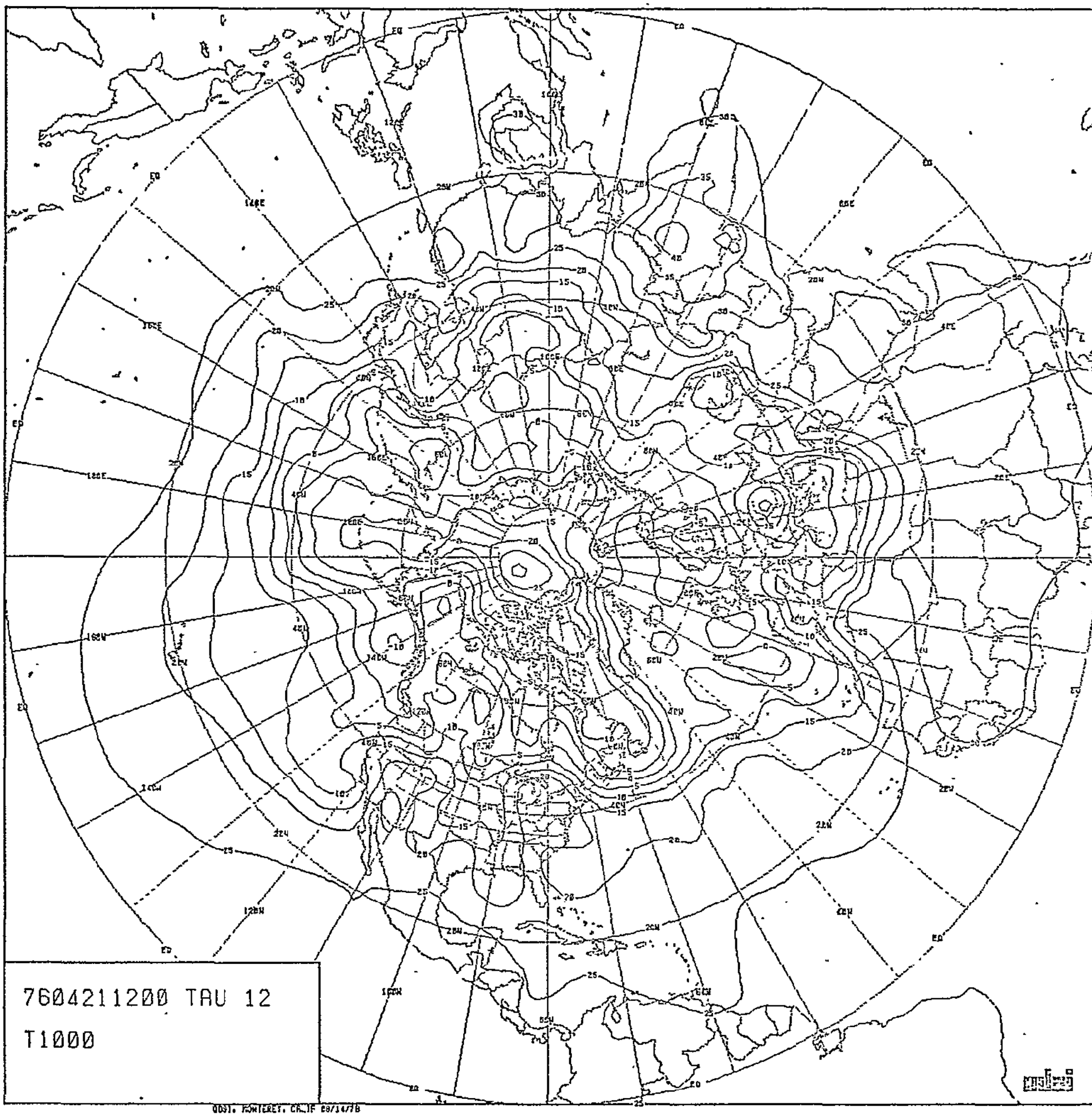

FIGURE III-4: 1500 m/d TERRAIN FORECAST
(ALTIMETRY BELOW SURFACE)
4/22/76 1200Z

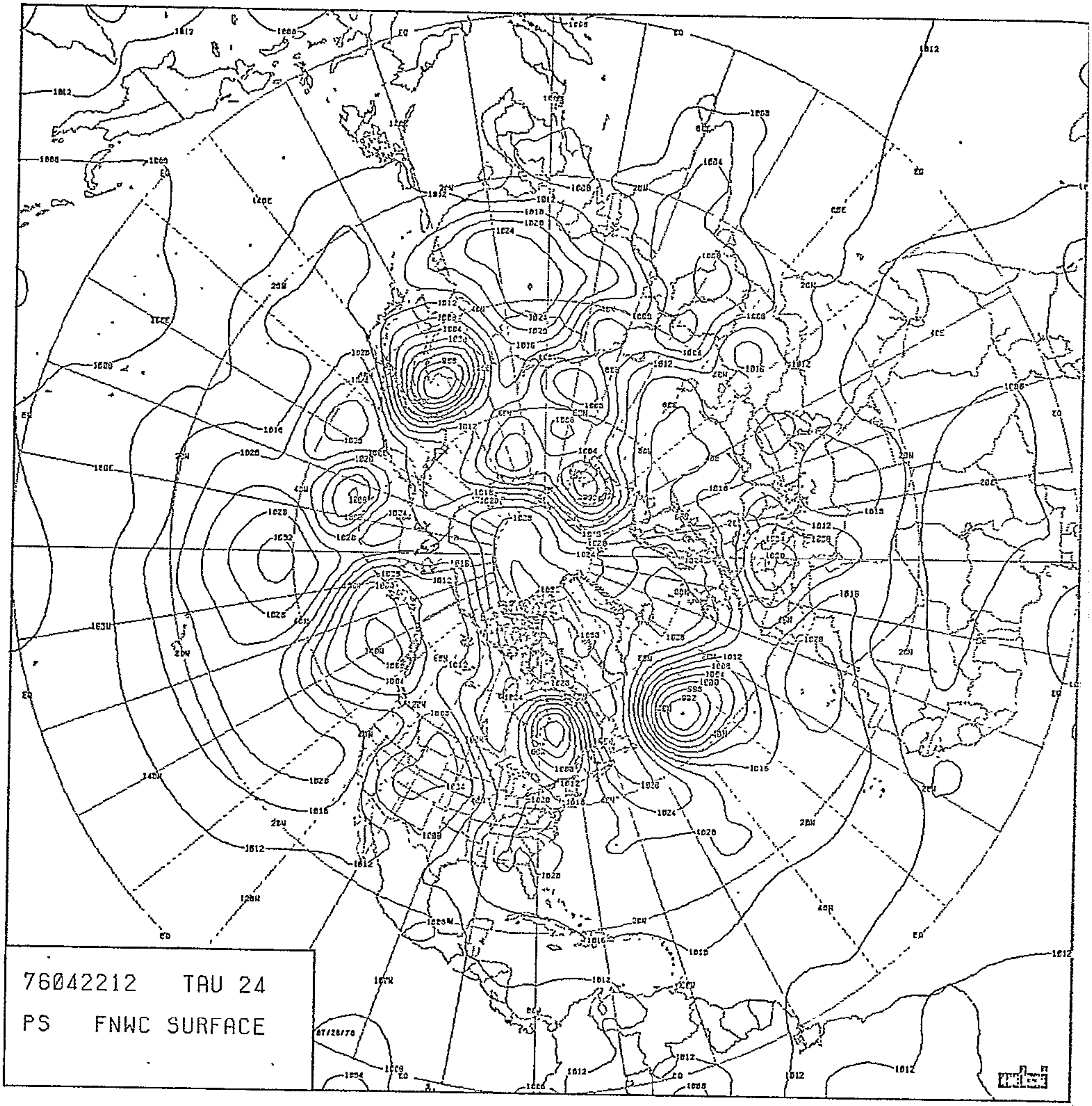

FIGURE III-5: FNWC 24-HOUR SURFACE FORECAST
VERIFYING 4/23/76 1200Z

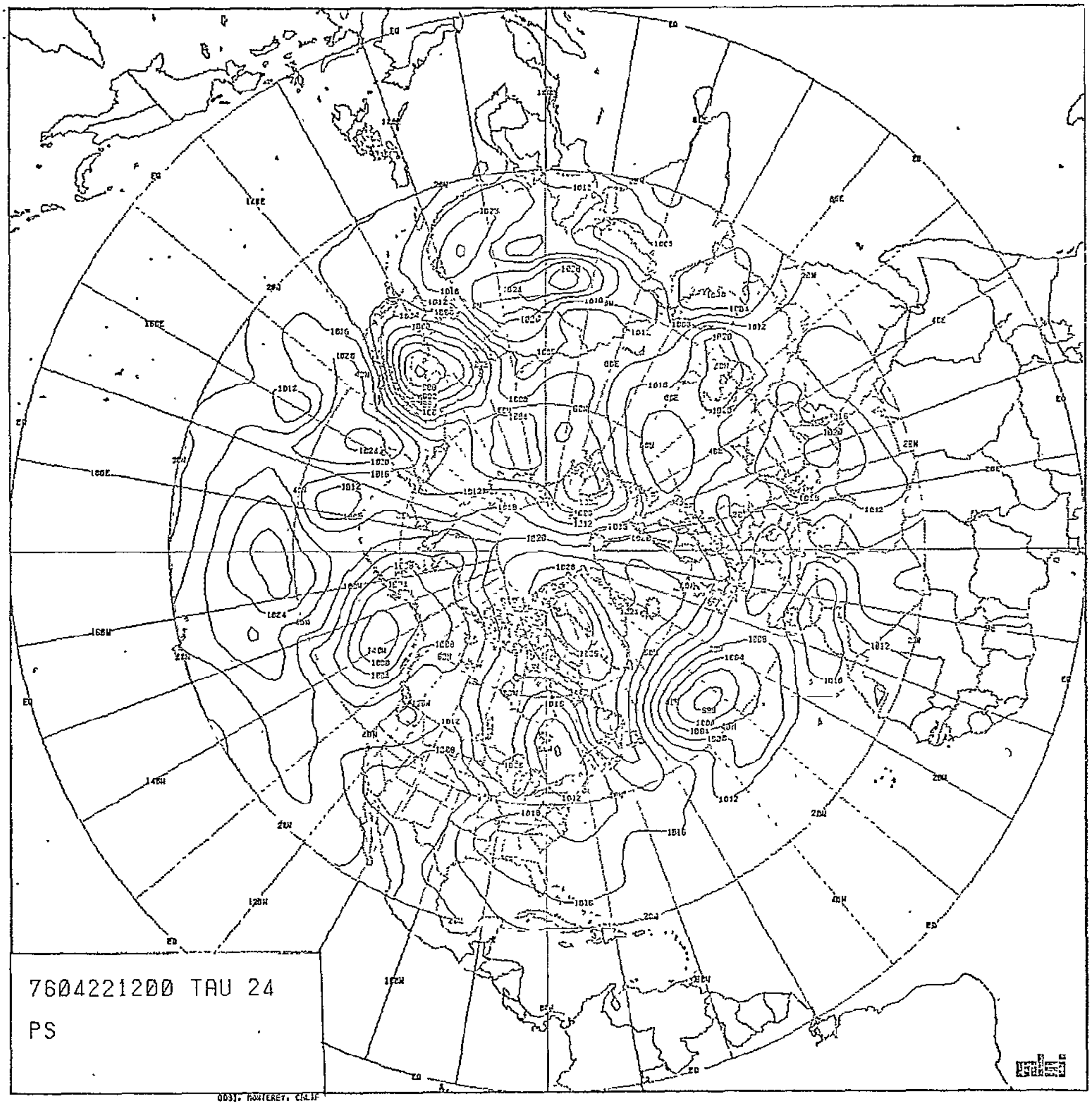

FIGURE III-6: ODSI 24-HOUR SURFACE FORECAST
VERIFYING 4/23/76 1200Z

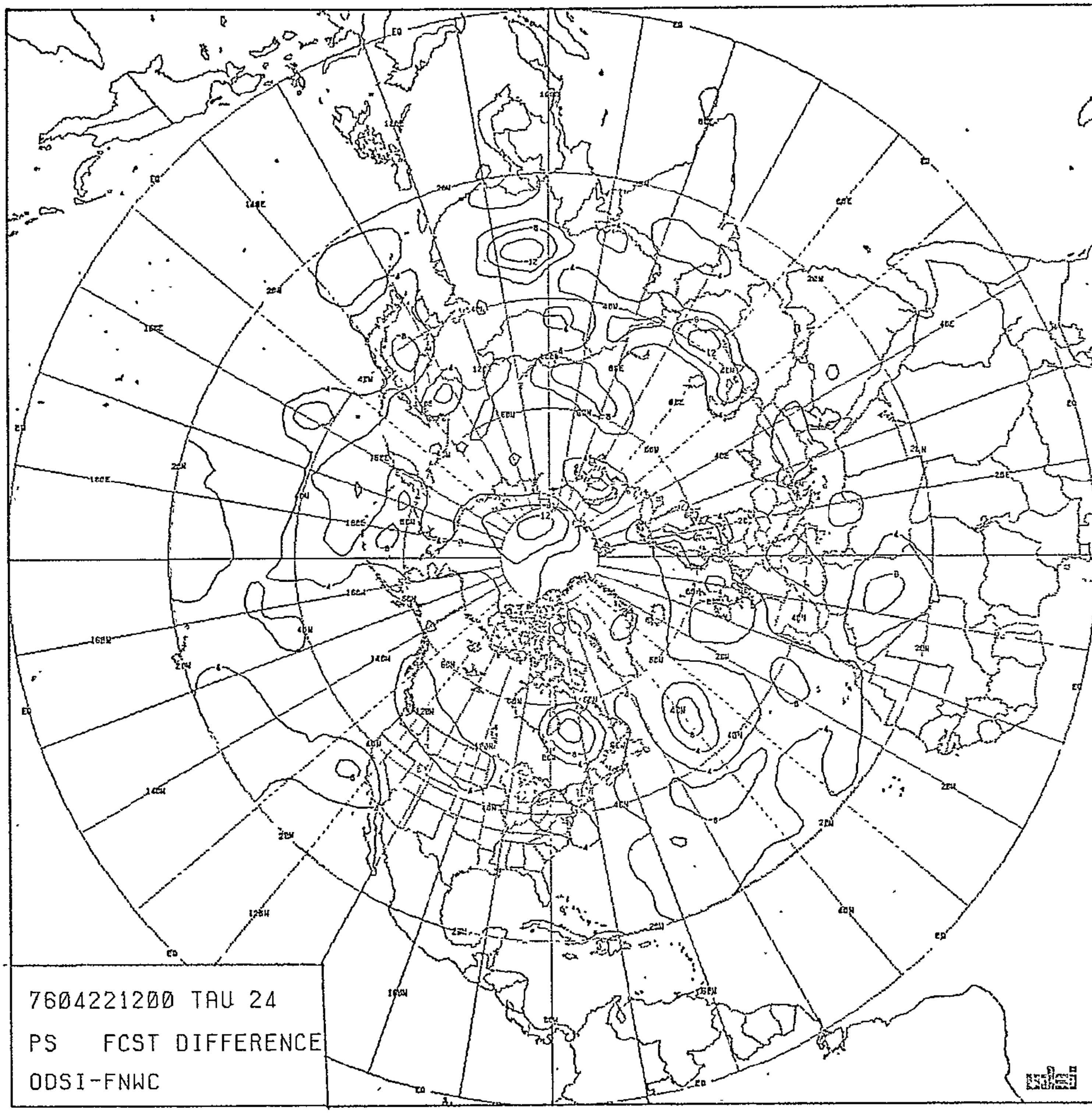

FIGURE III-7: ODSI-FNWC SURFACE FORECAST DIFFERENCE 4/23/76 1200Z

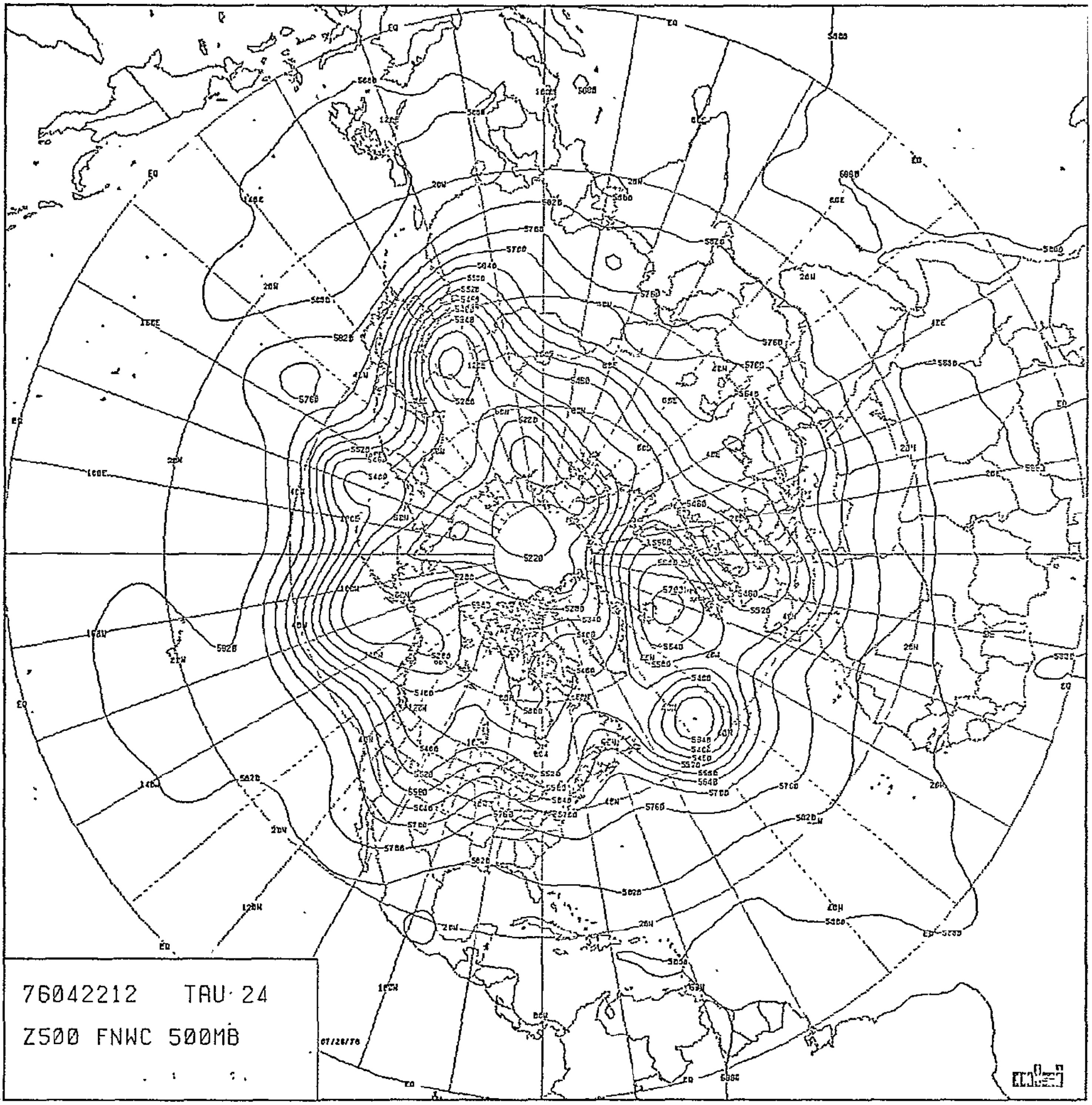

FIGURE III-8: FNWC 24-HOUR 500mb FORECAST
VERIFYING 4/23/76 1200Z

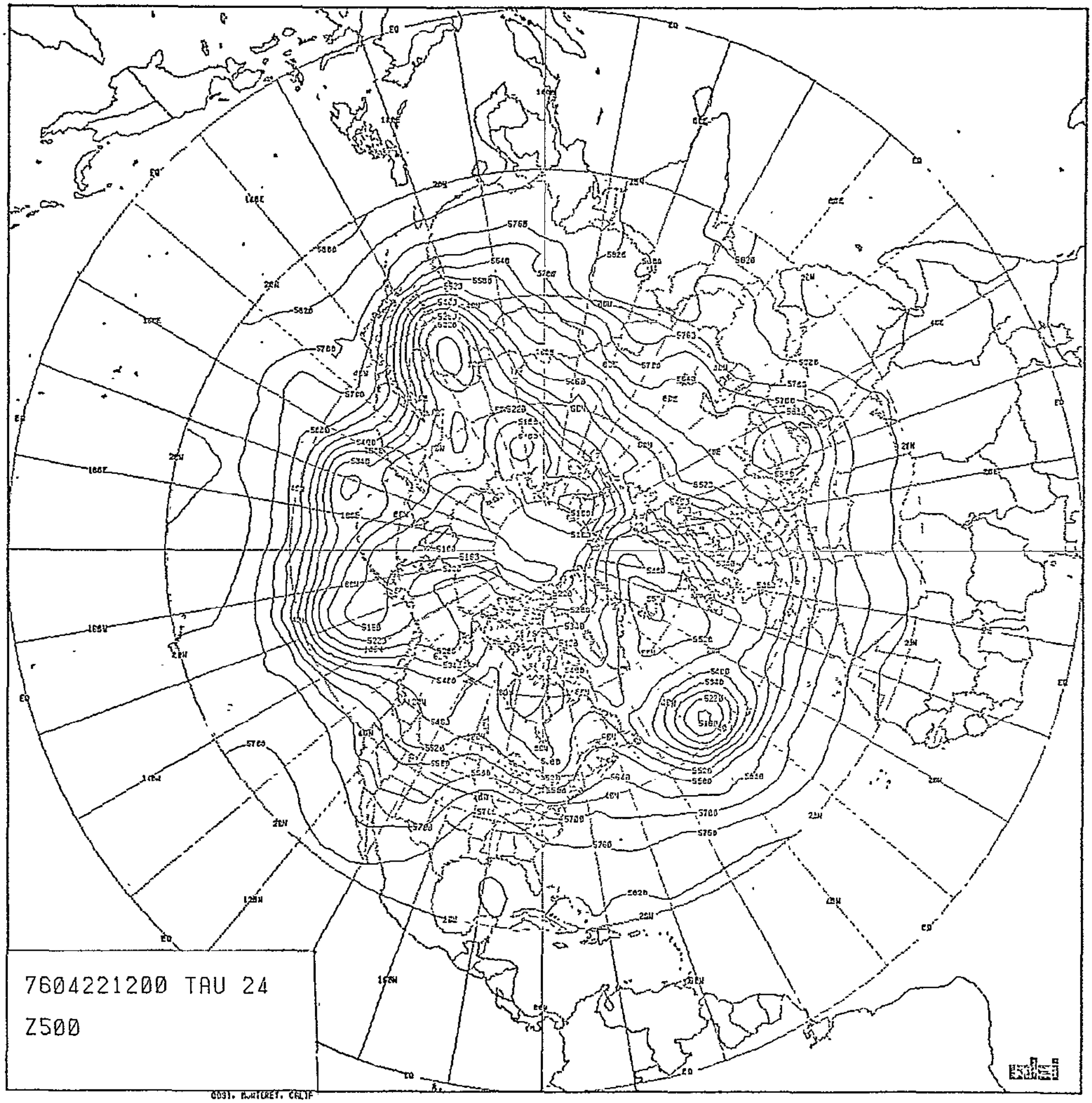

FIGURE III-9: ODSI 24-HOUR 500mb FORECAST
VERIFYING 4/23/76 1200Z

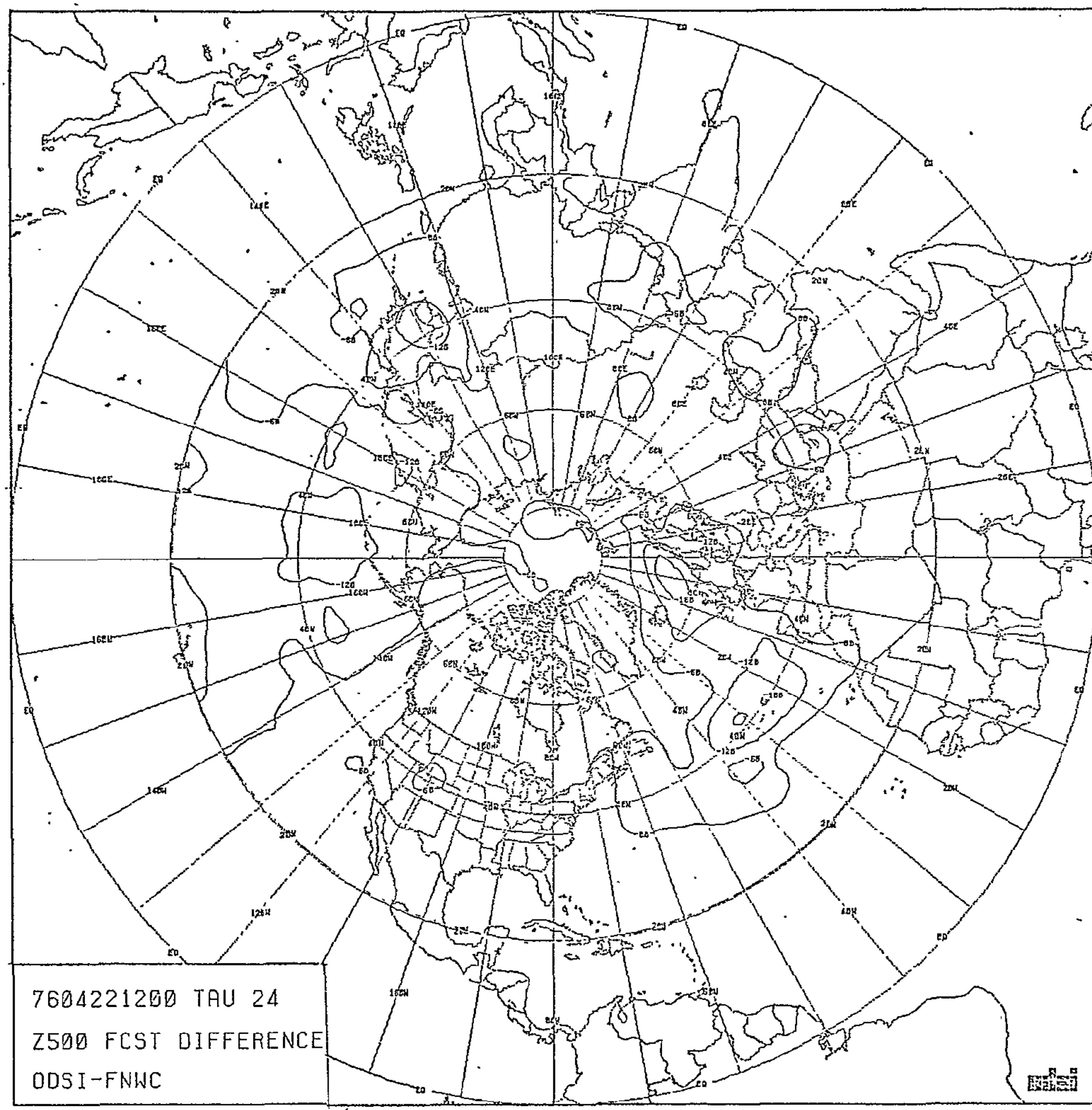

FIGURE III-10: ODSI-FNWC 500mb FORECAST DIFFERENCE 4/23/76 1200Z

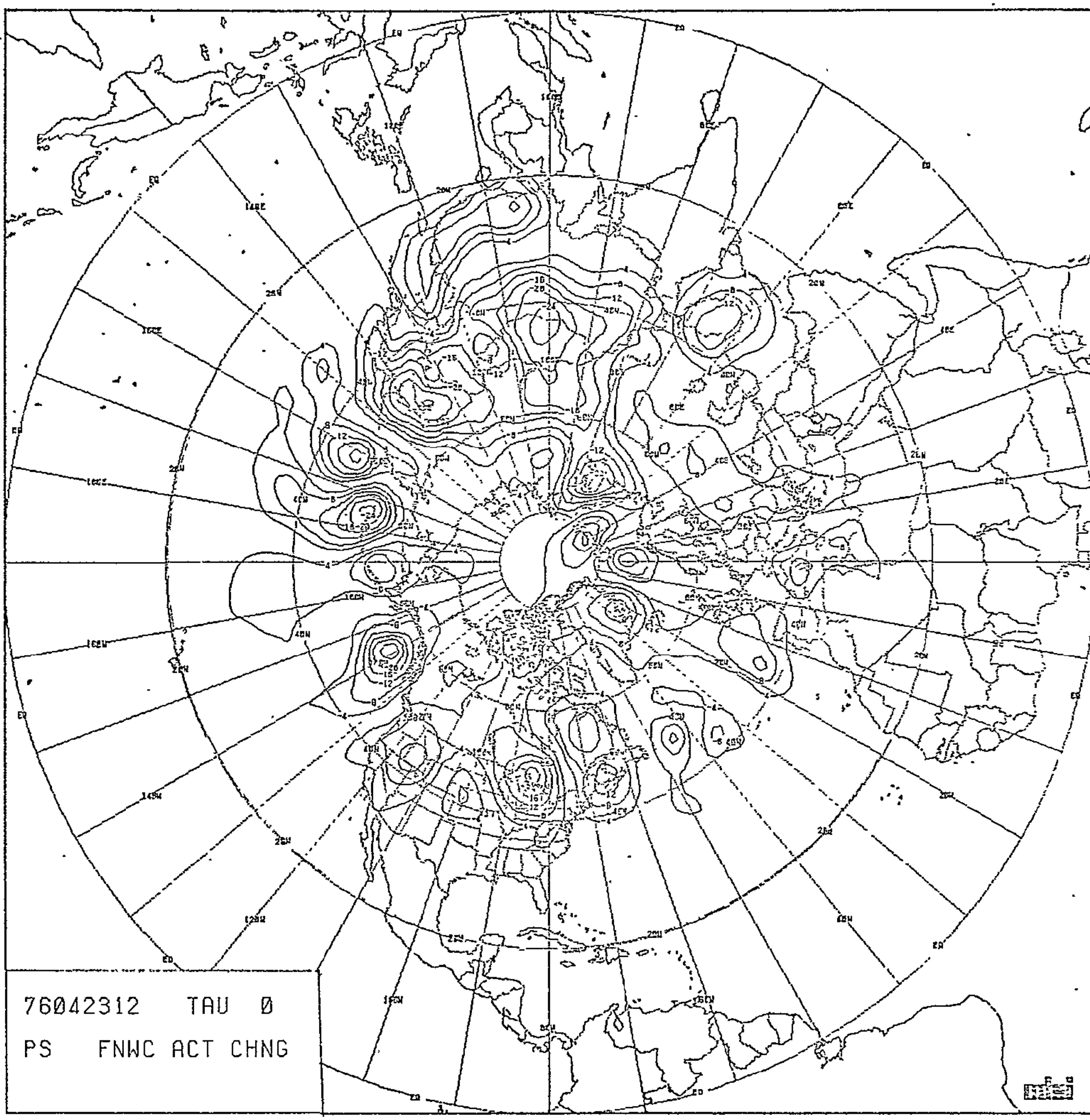

FIGURE III-11: FNWC 24-HOUR SURFACE ACTUAL
CHANGE VERIFYING 4/23/76
1200Z

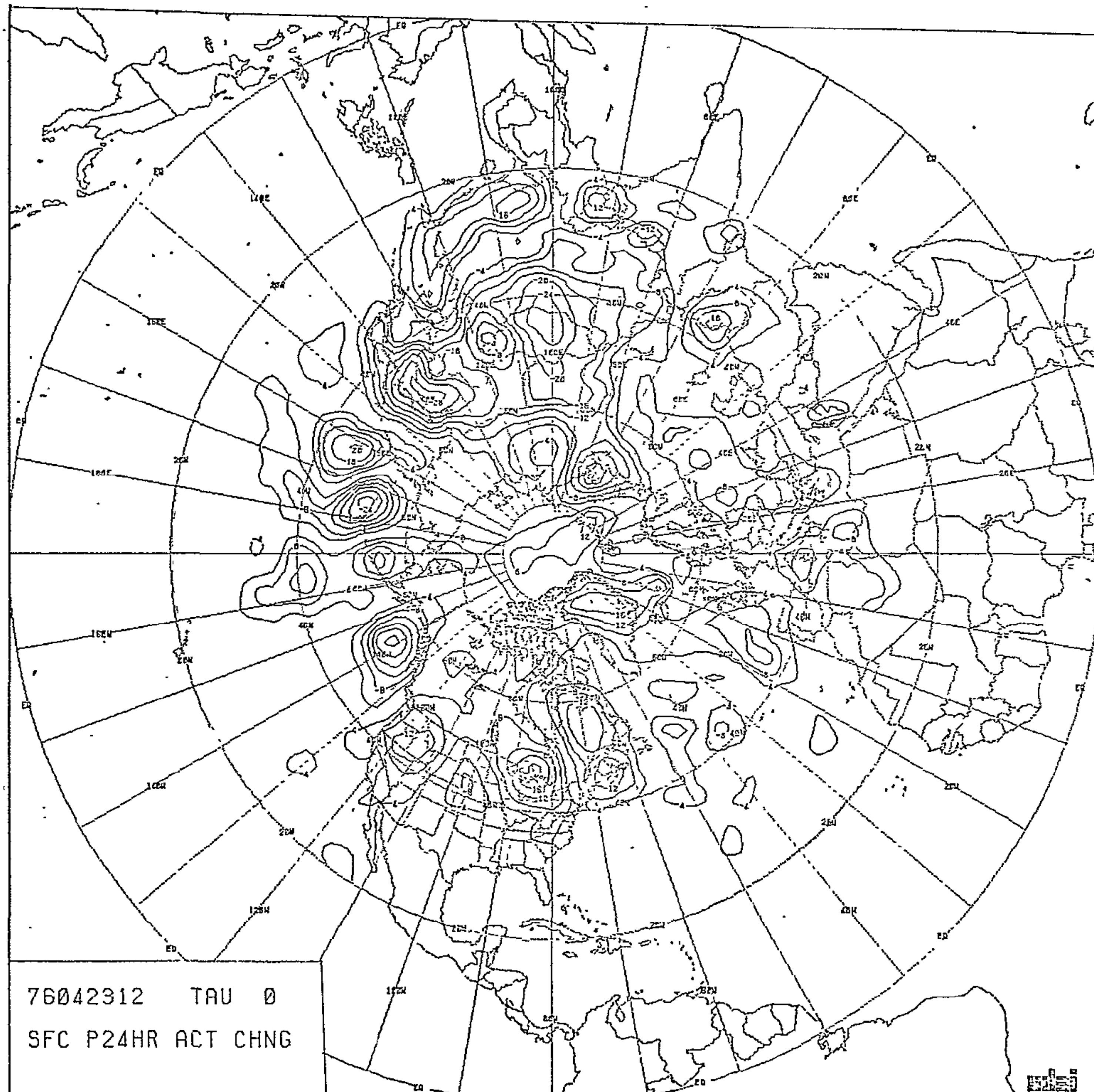

FIGURE III-12: ODSI 24-HOUR SURFACE ACTUAL CHANGE VERIFYING 4/23/76 1200Z

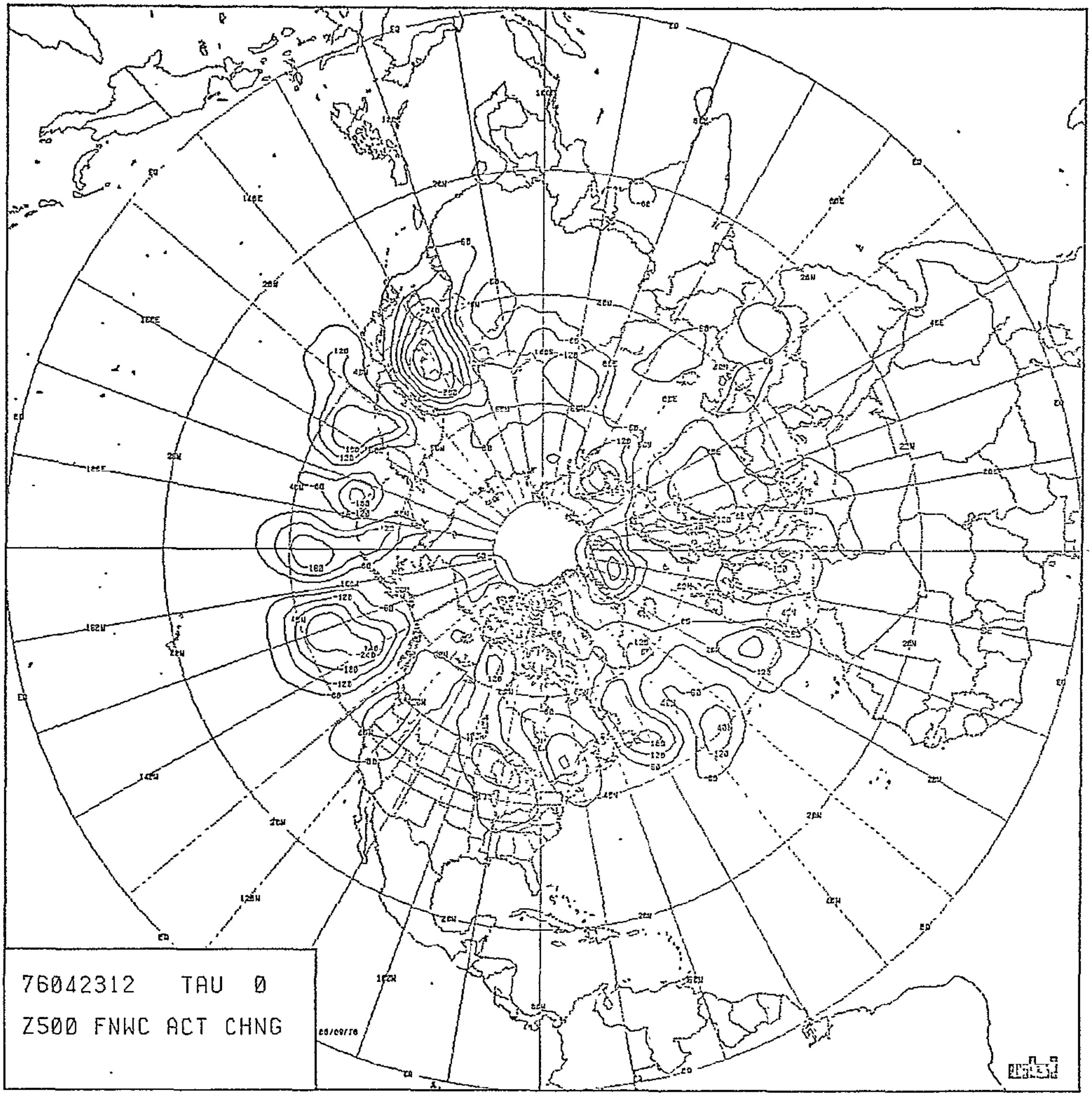

FIGURE III-13: FNWC 24-HOUR 500mb ACTUAL CHANGE VERIFYING 4/23/76 1200Z

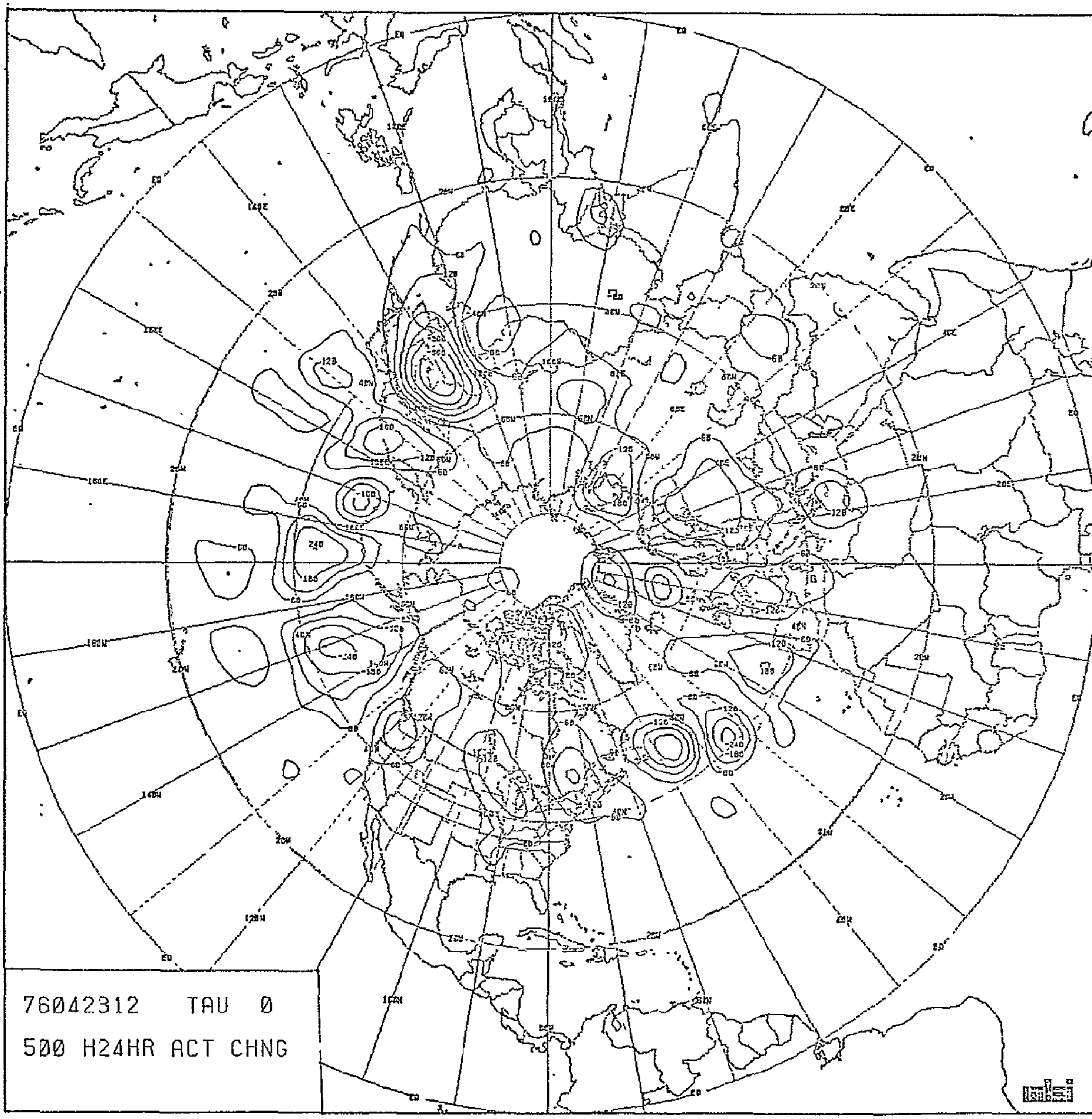

FIGURE III-14: ODSI 24-HOUR 500mb ACTUAL CHANGE VERIFYING 4/23/76 1200Z

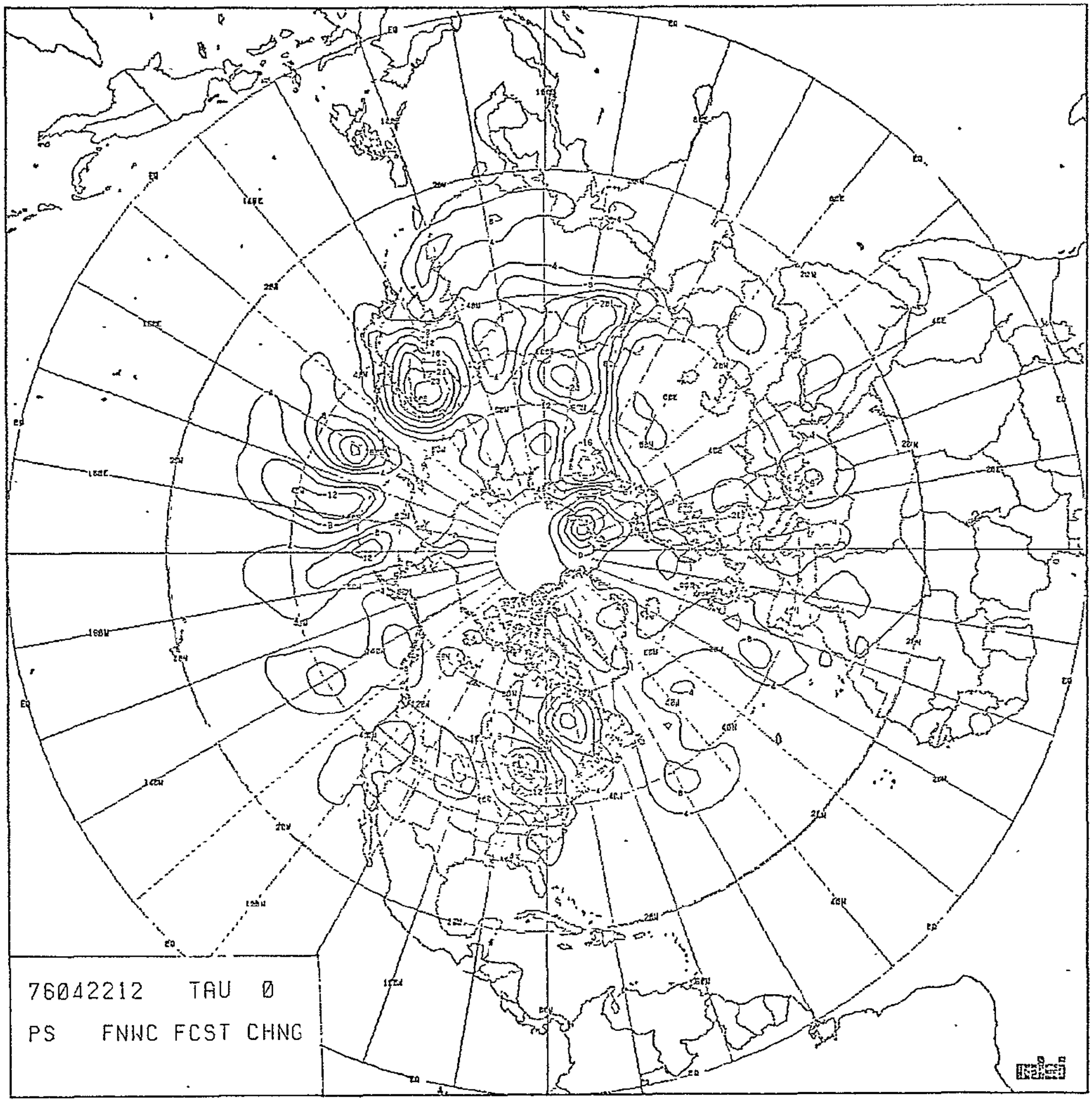

FIGURE III-15: FNWC 24-HOUR SURFACE FORECAST CHANGE VERIFYING 4/23/76 1200Z

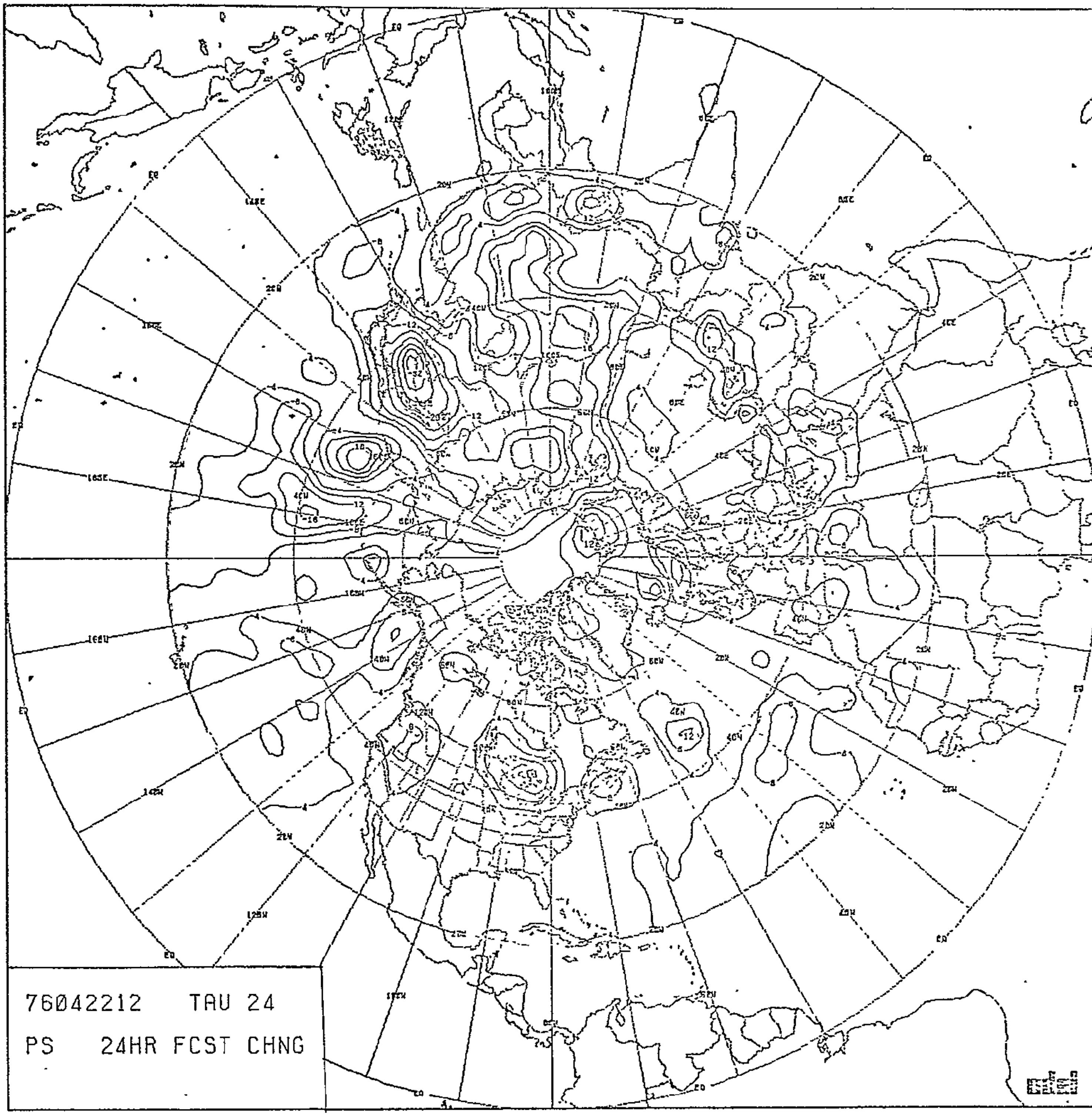

FIGURE III-16: ODSI 24-HOUR SURFACE FORECAST
CHANGE VERIFYING 4/23/76 1200Z

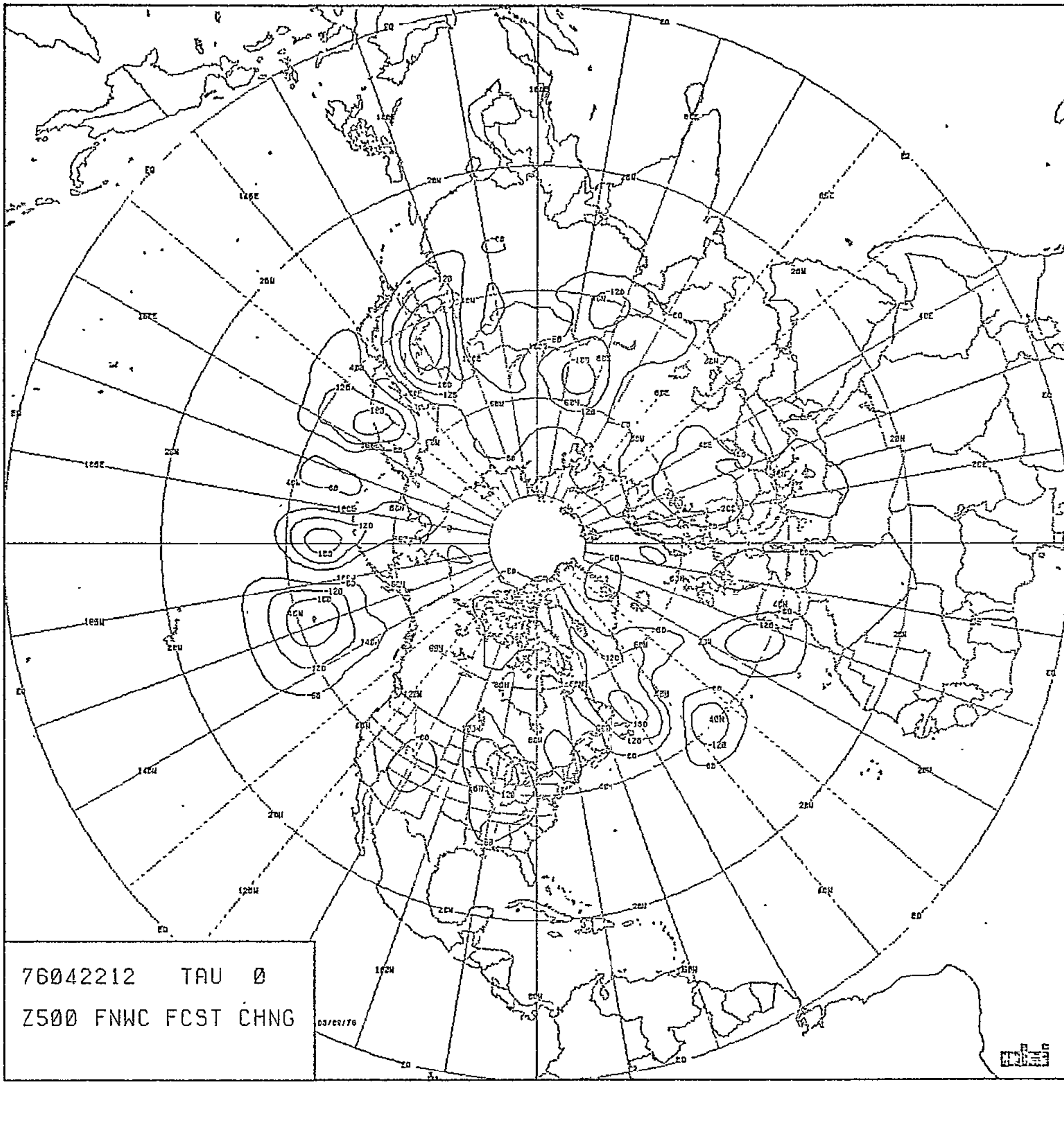

FIGURE III-17: FNWC 500mb SURFACE FORECAST CHANGE VERIFYING 4/23/76 1200Z

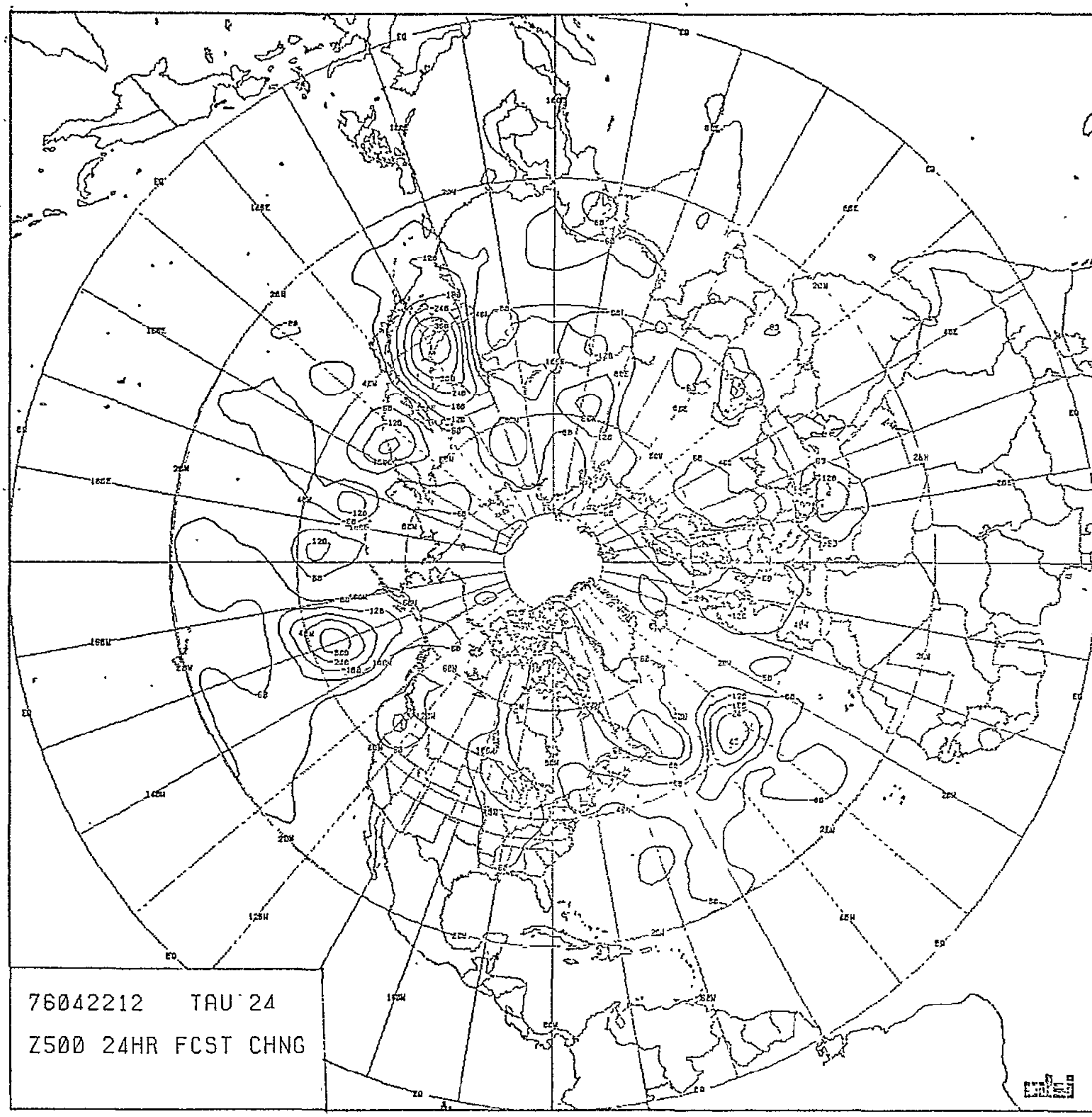

FIGURE III-18: ODSI 500mb SURFACE FORECAST CHANGE VERIFYING 4/23/76 1200Z

C-2

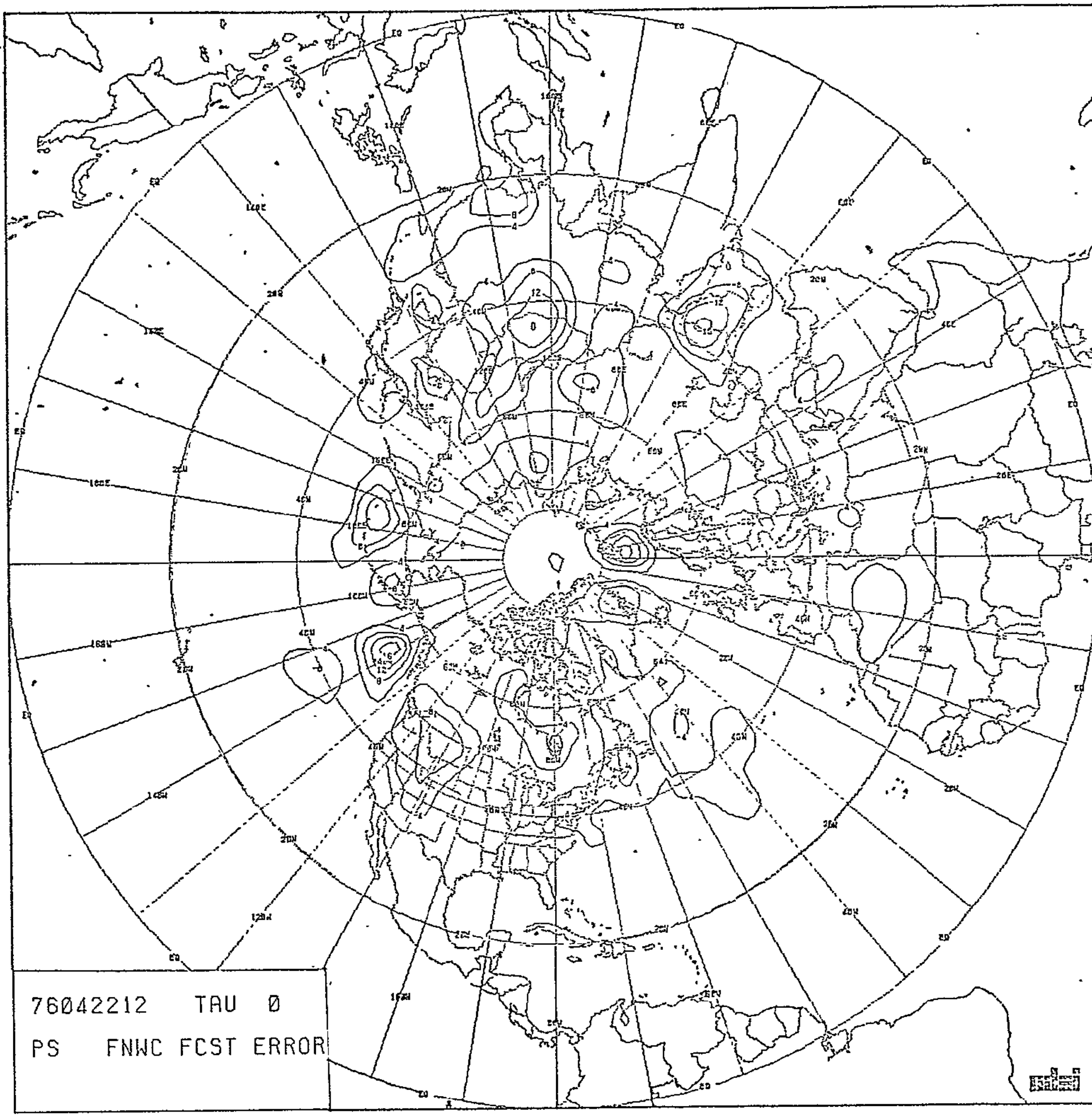

FIGURE III-19: FNWC 24-HOUR SURFACE FORECAST ERROR VERIFYING 4/23/76 1200Z (VERIFICATION FNWC ANALYSIS)

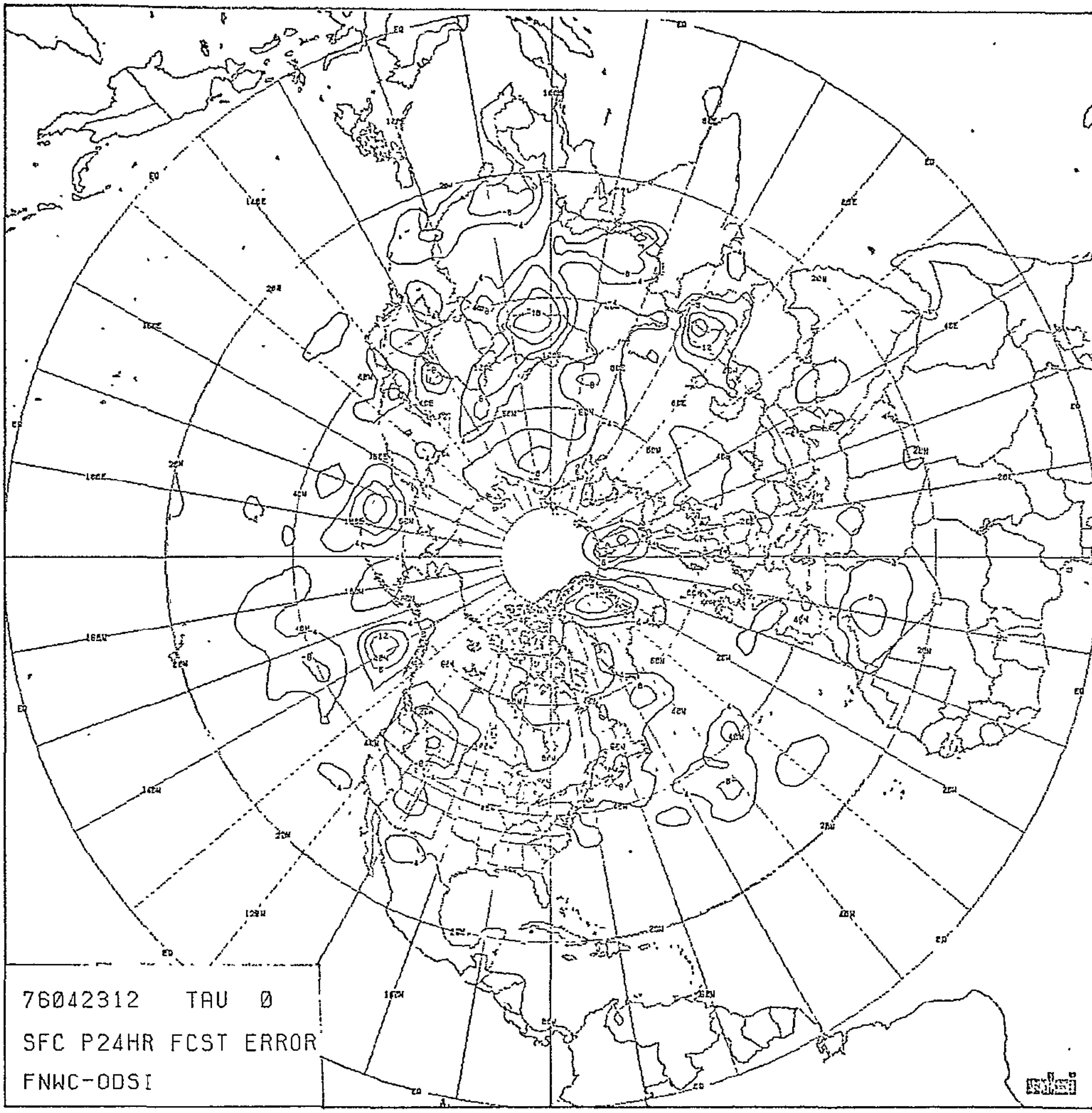

FIGURE III-20: FNWC 24-HOUR SURFACE FORECAST ERROR VERIFYING 4/23/76 1200Z (VERIFICATION ODSI ANALYSIS)

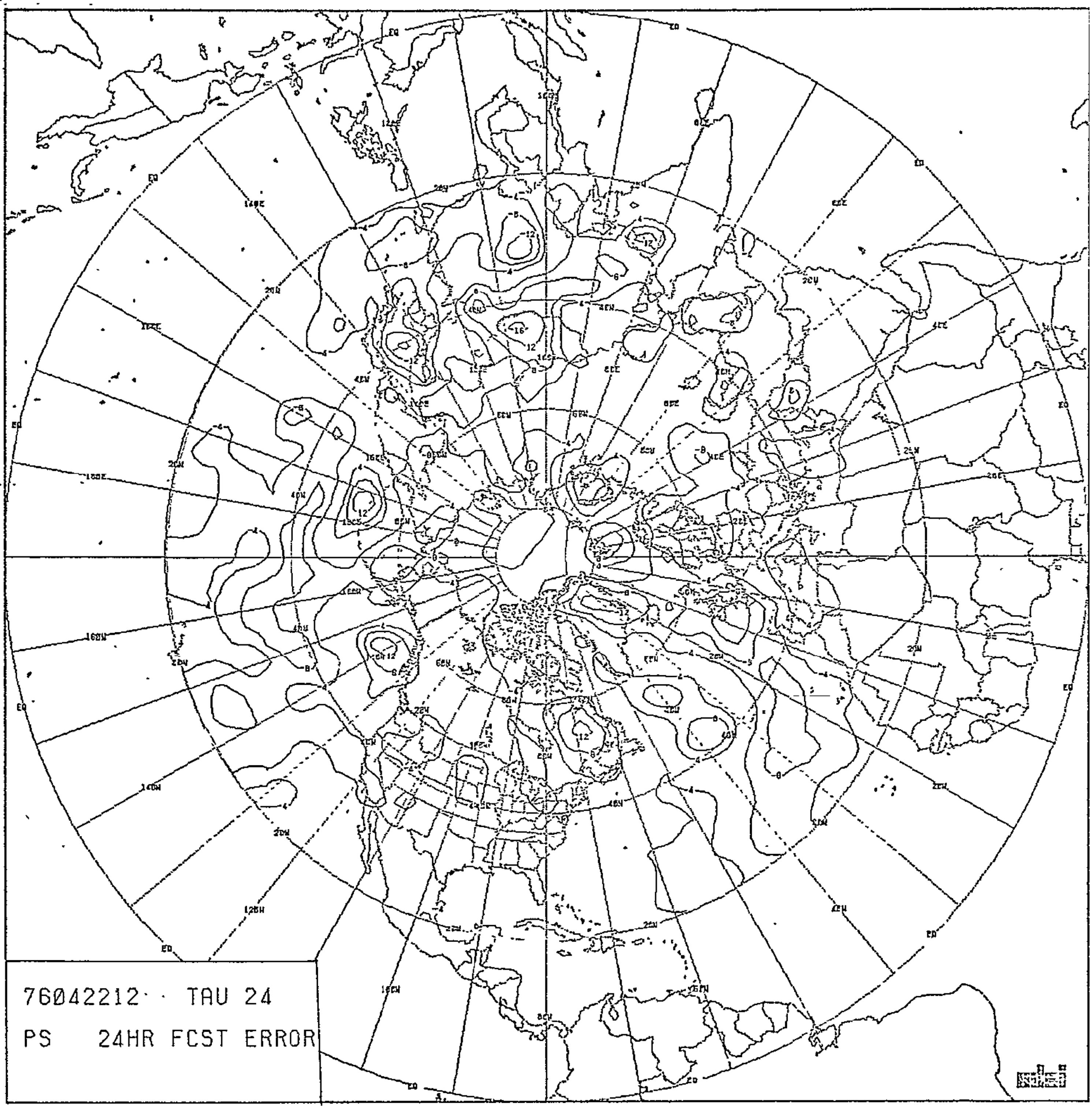

FIGURE III-21: ODSI 24-HOUR SURFACE FORECAST ERROR VERIFYING 4/23/76 1200Z (VERIFICATION ODSI ANALYSIS)

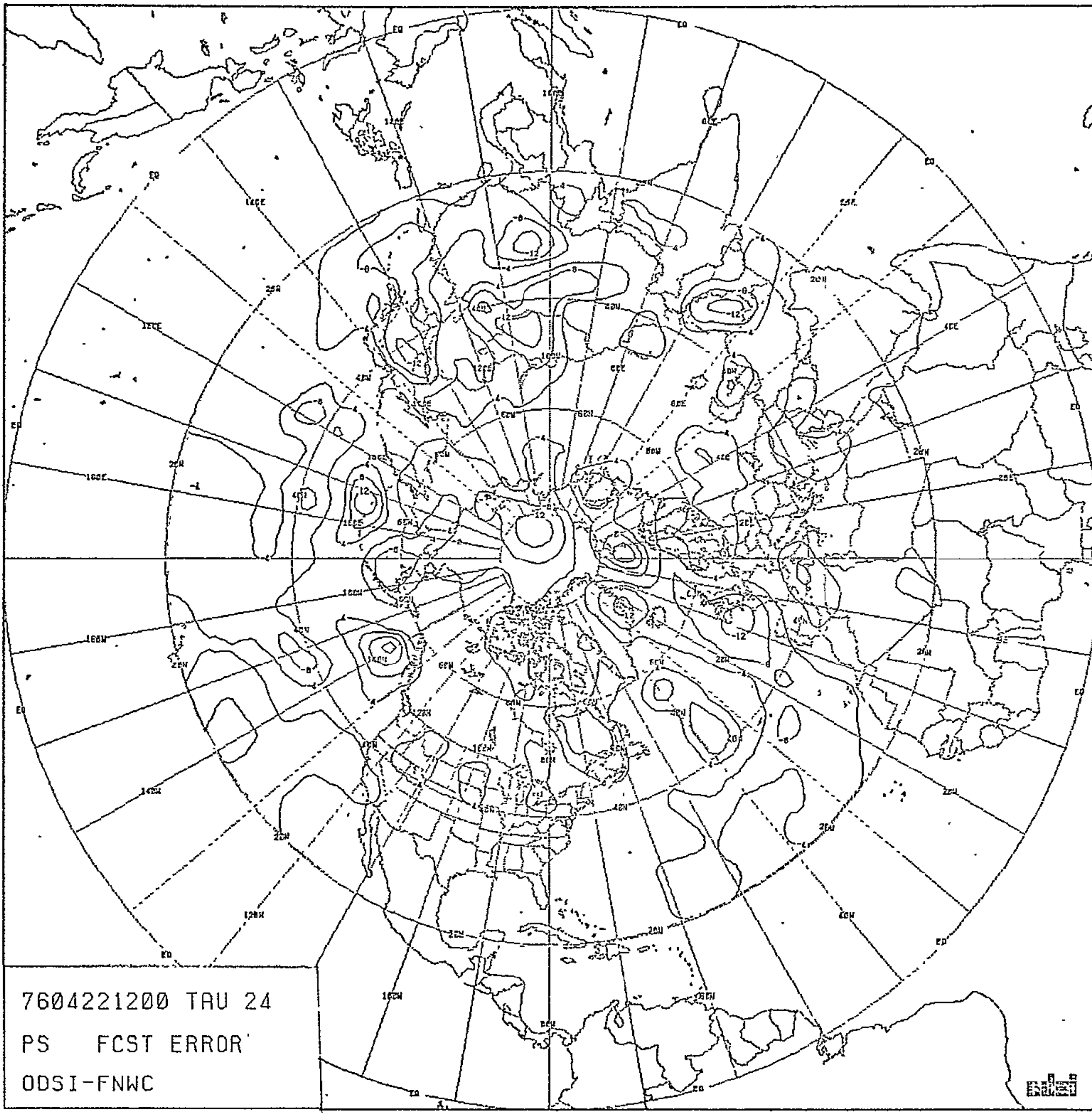

FIGURE III-22: ODSI 24-HOUR SURFACE FORECAST ERROR VERIFYING 4/23/76 1200Z VERIFICATION FNWC ANALYSIS)

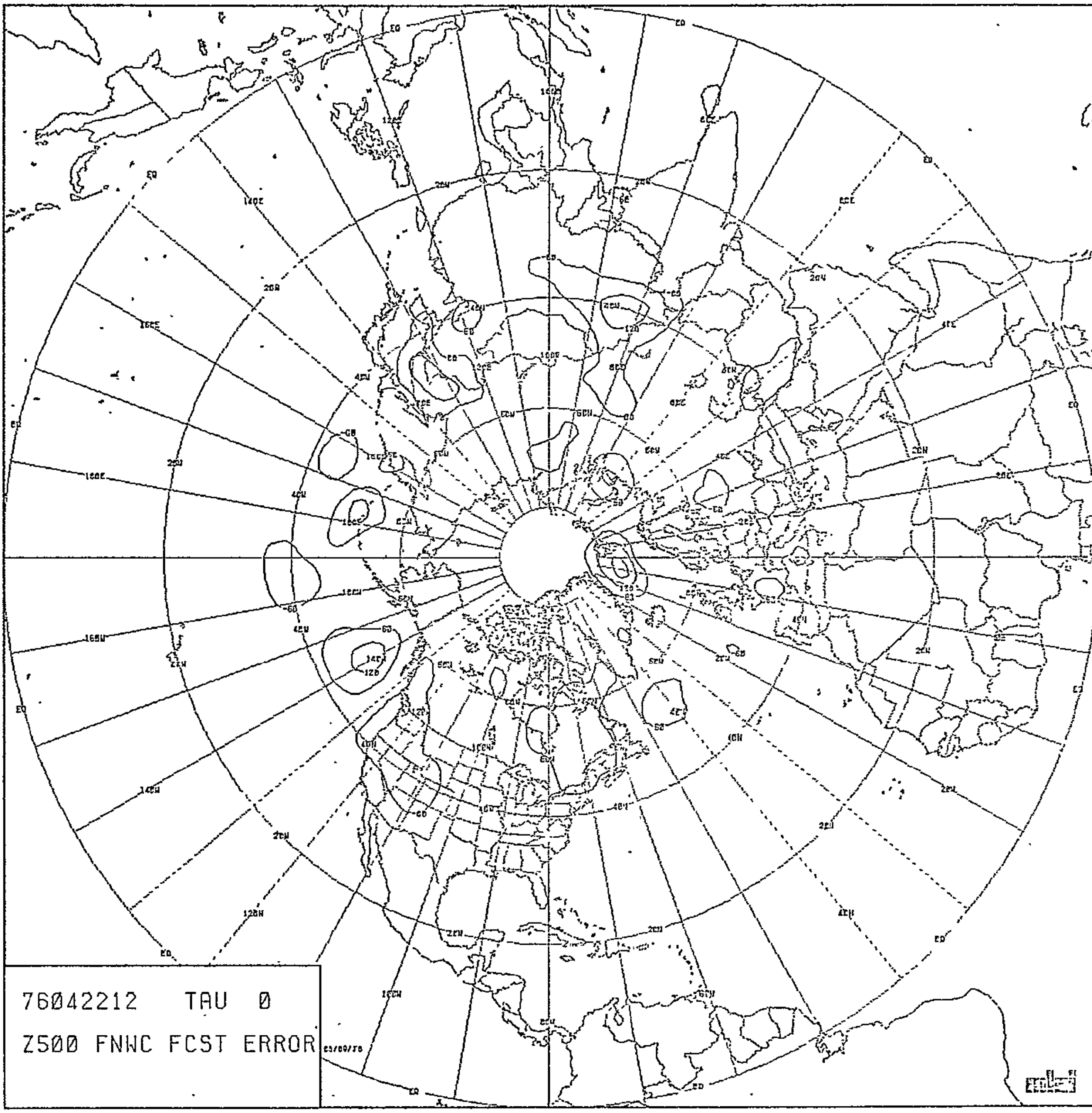

FIGURE III-23: FNWC 24-HOUR 500mb FORECAST ERROR VERIFYING 4/23/76 1200Z (VERIFICATION FNWC ANALYSIS)

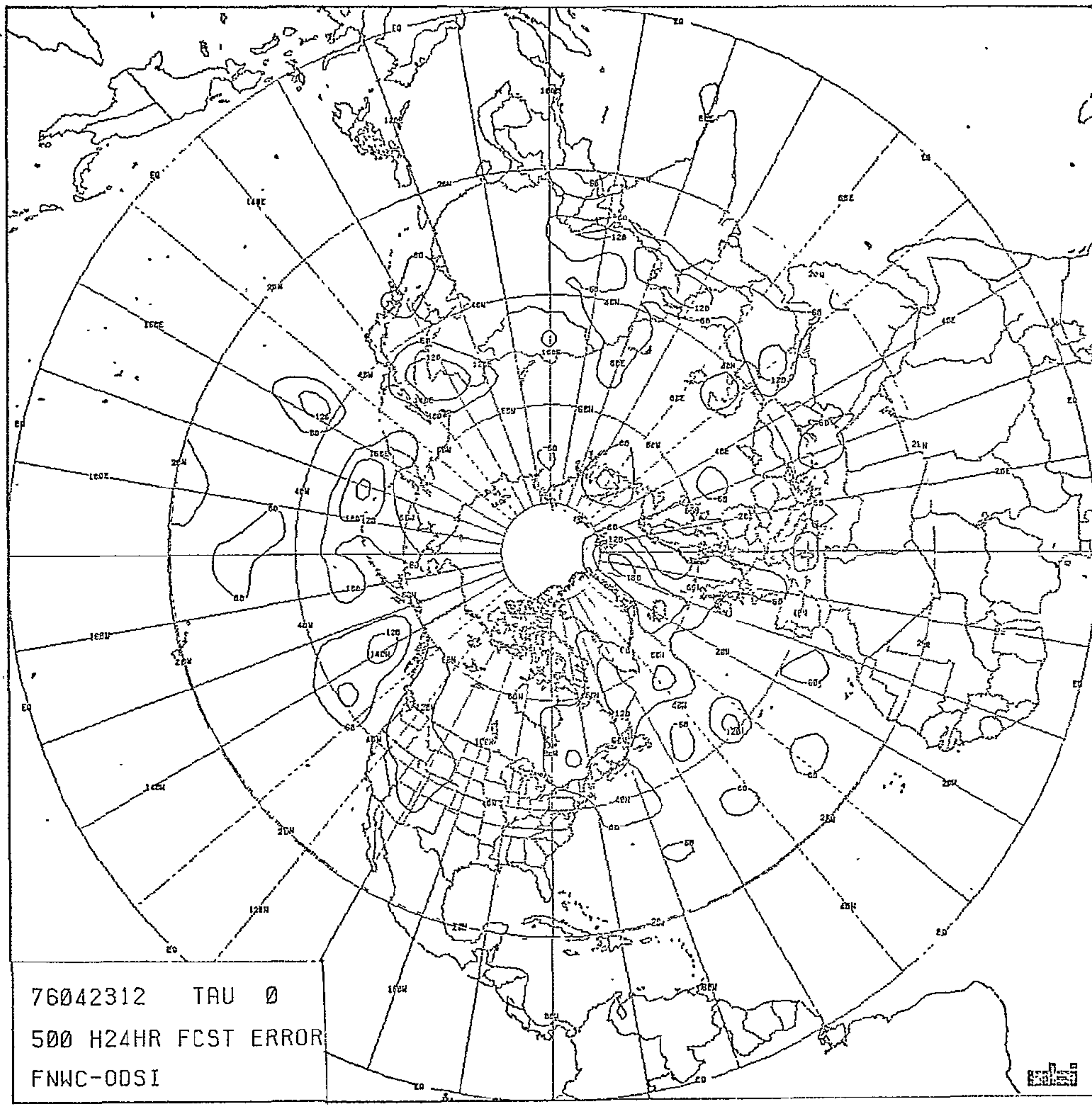

FIGURE III-24: FNWC 24-HOUR 500mb FORECAST ERROR VERIFYING 4/23/76 1200Z (VERIFICATION ODSI ANALYSIS)

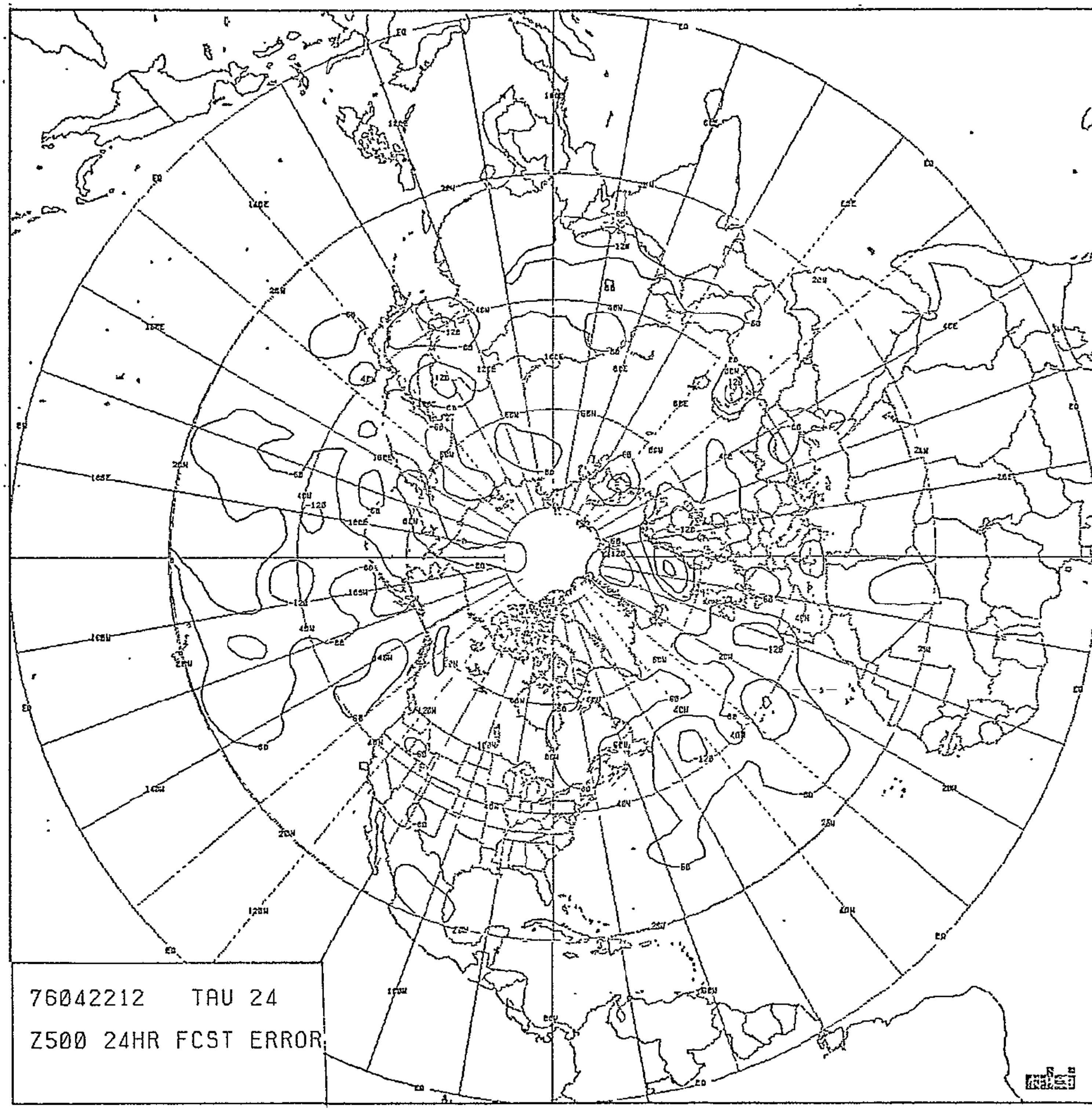

FIGURE III-25: ODSI 24-HOUR 500mb FORECAST ERROR VERIFYING 4/23/76 1200Z (VERIFICATION ODSI ANALYSIS)

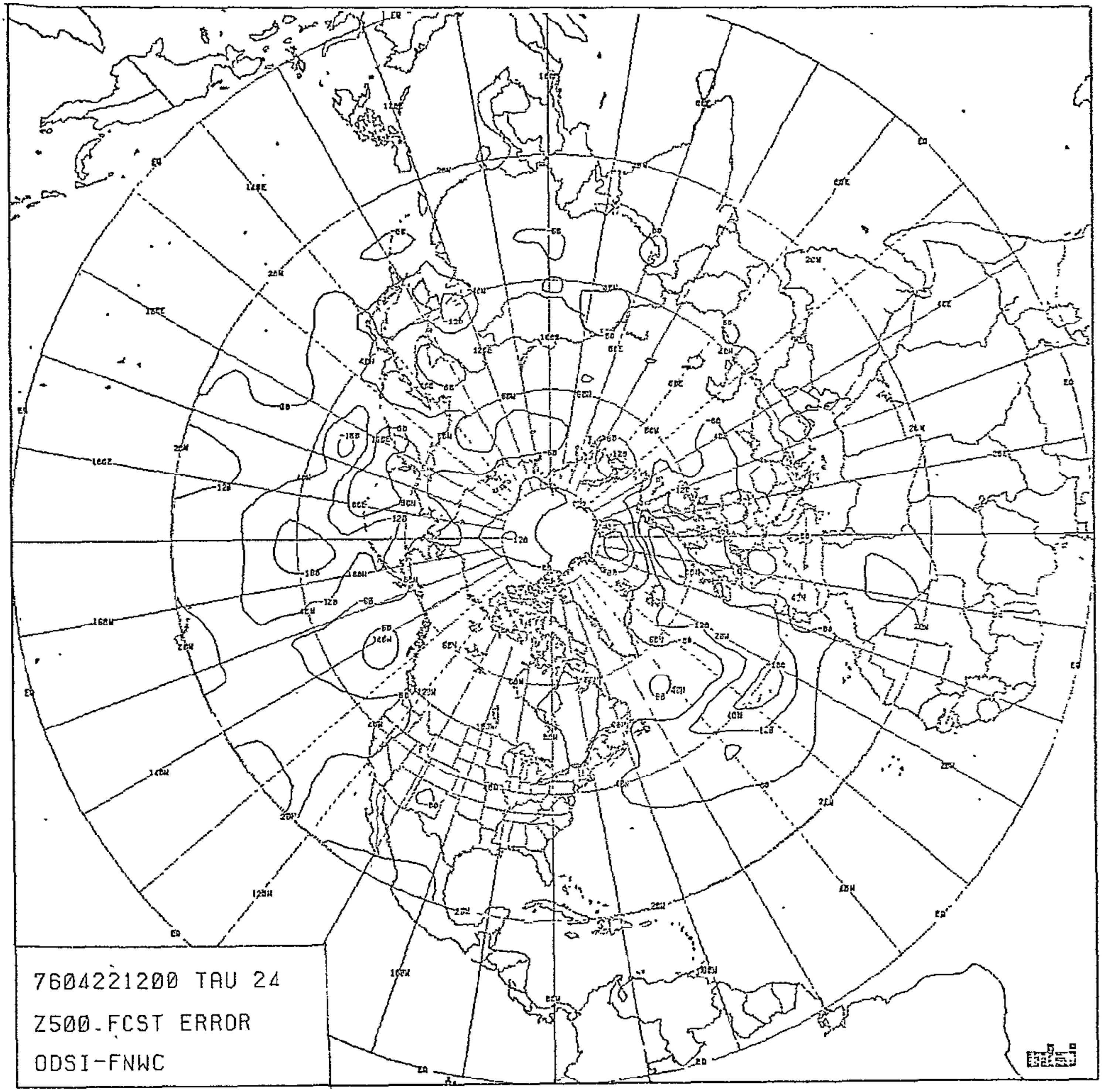

FIGURE III-26: ODSI 24-HOUR 500mb FORECAST ERROR VERIFYING 4/23/76 1200Z (VERIFICATION FNWC ANALYSIS)

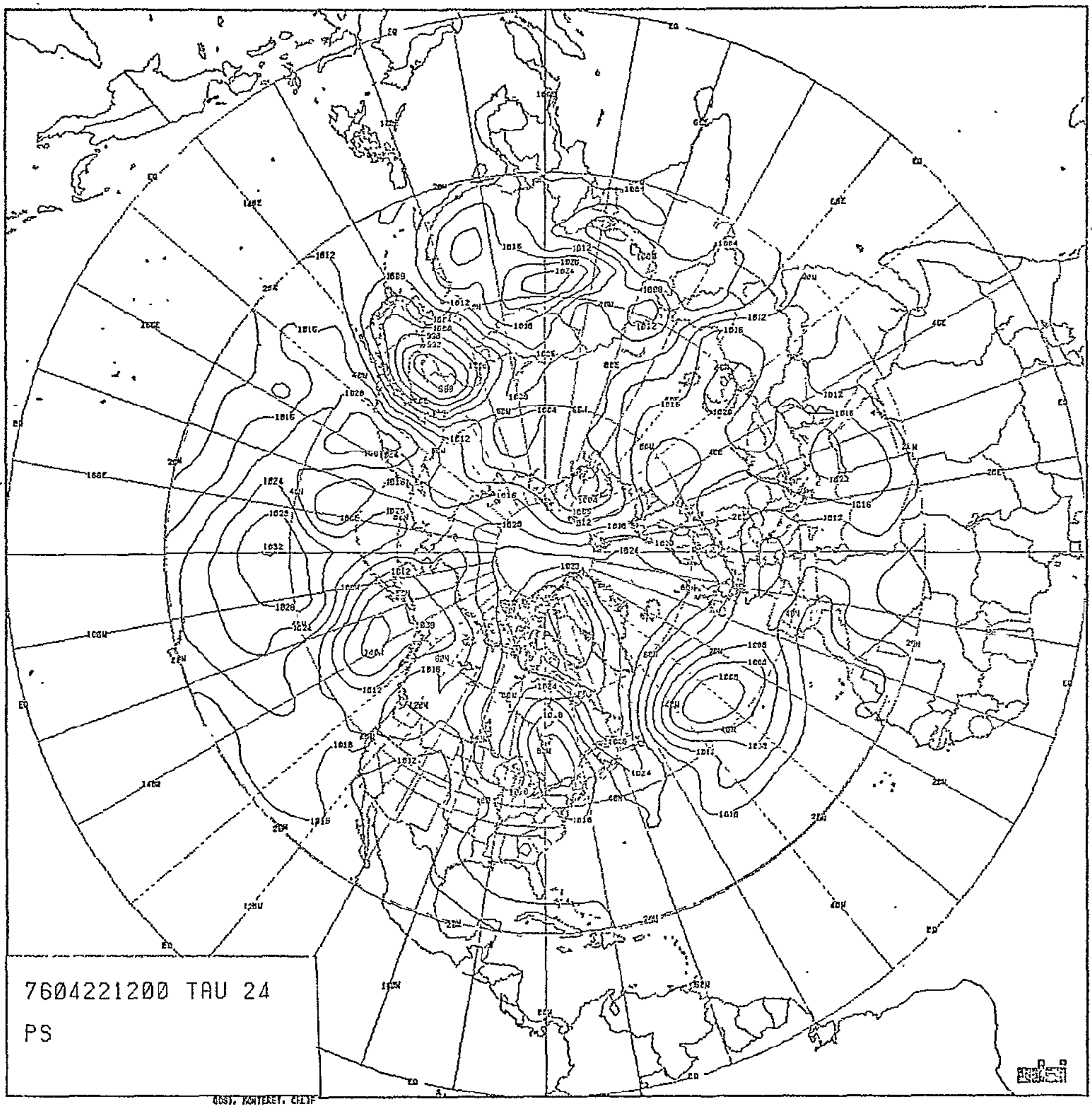

FIGURE III-27: ODSI 24-HOUR SURFACE FORECAST (PECHFV) VERIFYING 4/23/76 1200Z

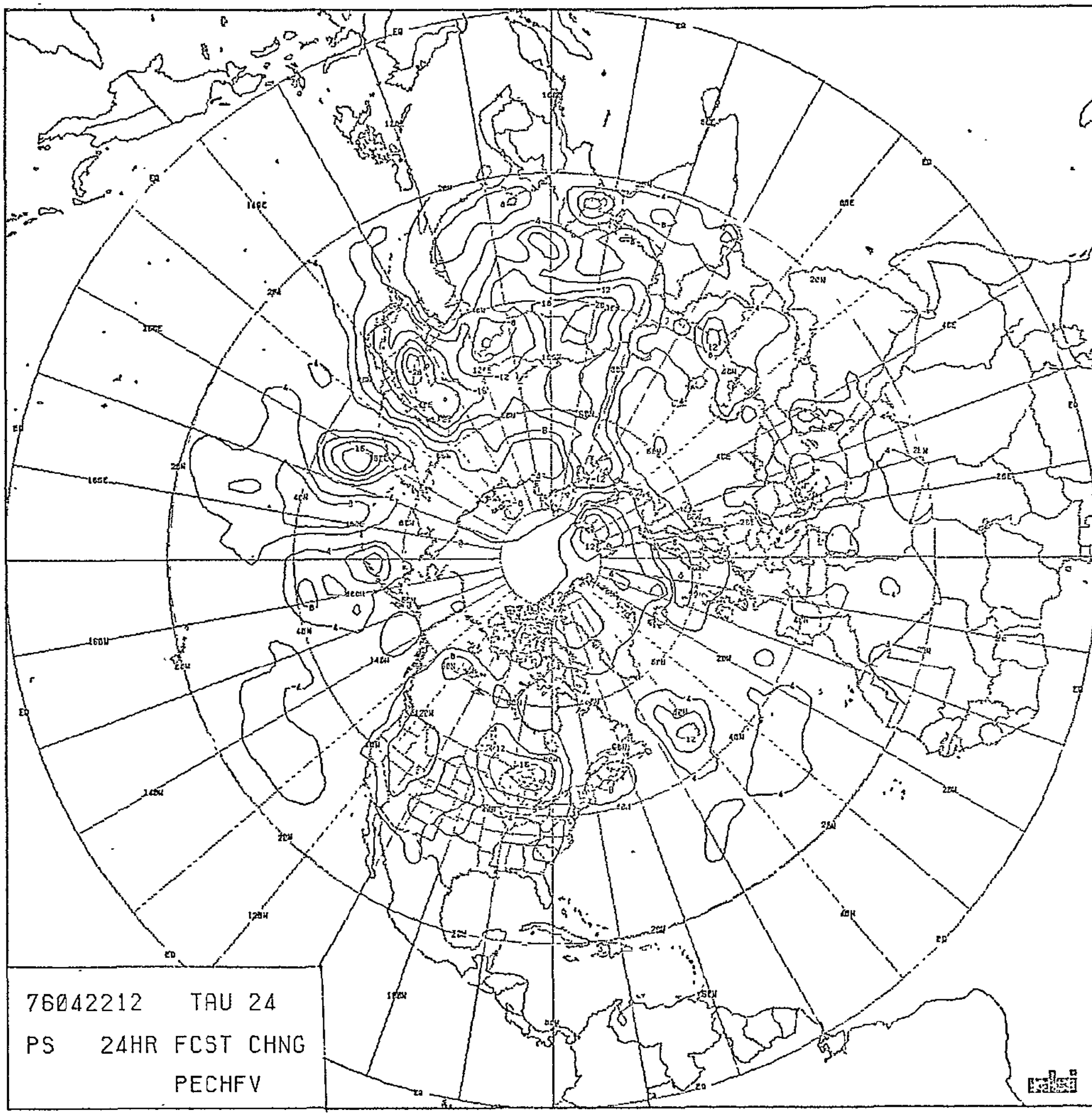

FIGURE III-28: ODSI 24-HOUR SURFACE FORECAST CHANGE (PECHFV) VERIFYING 4/23/76 1200Z

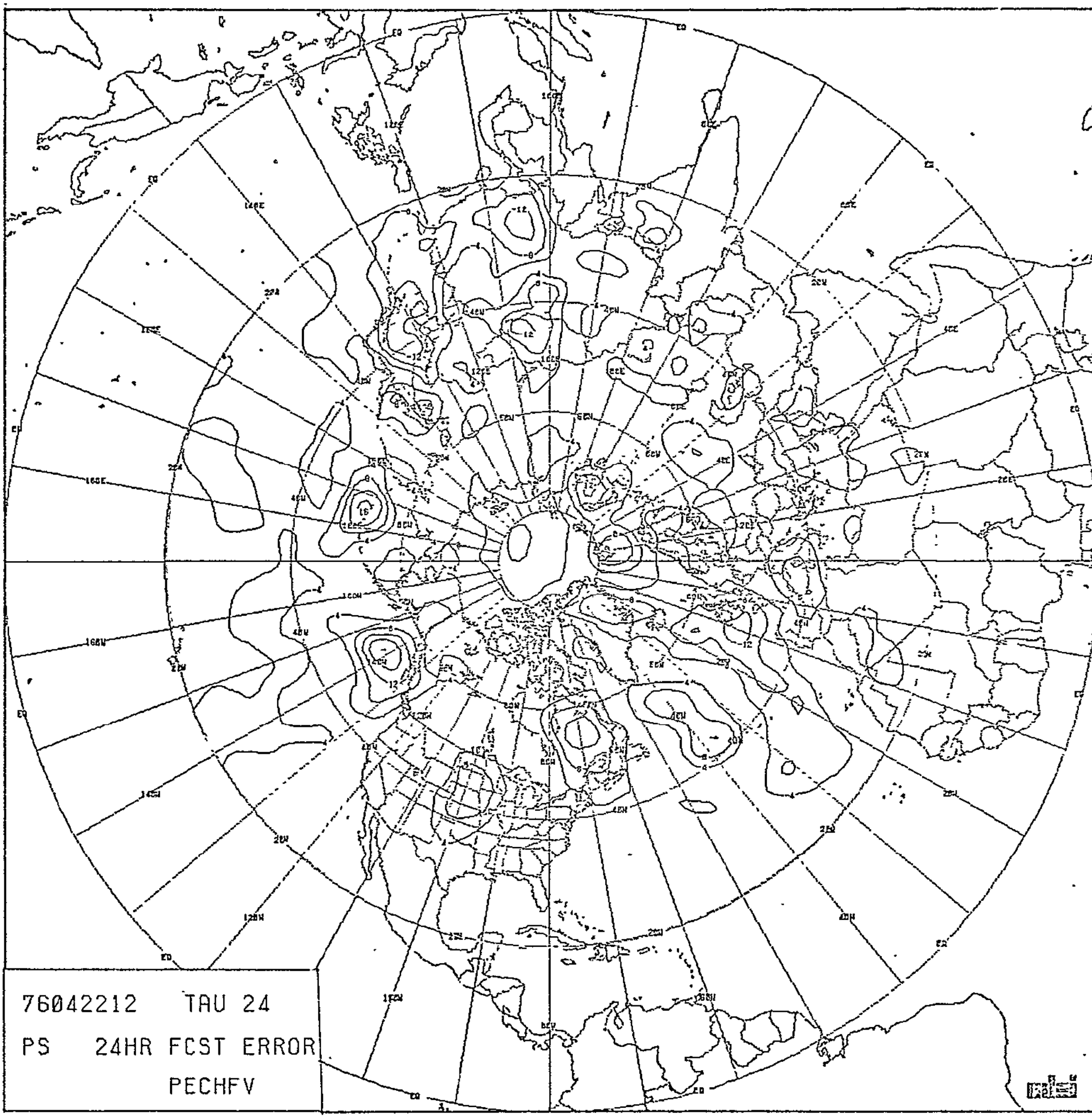

FIGURE III-29: ODSI 24-HOUR SURFACE FORECAST ERROR (PECHFV) VERIFYING 4/23/76 1200Z (VERIFICATION ODSI ANALYSIS)

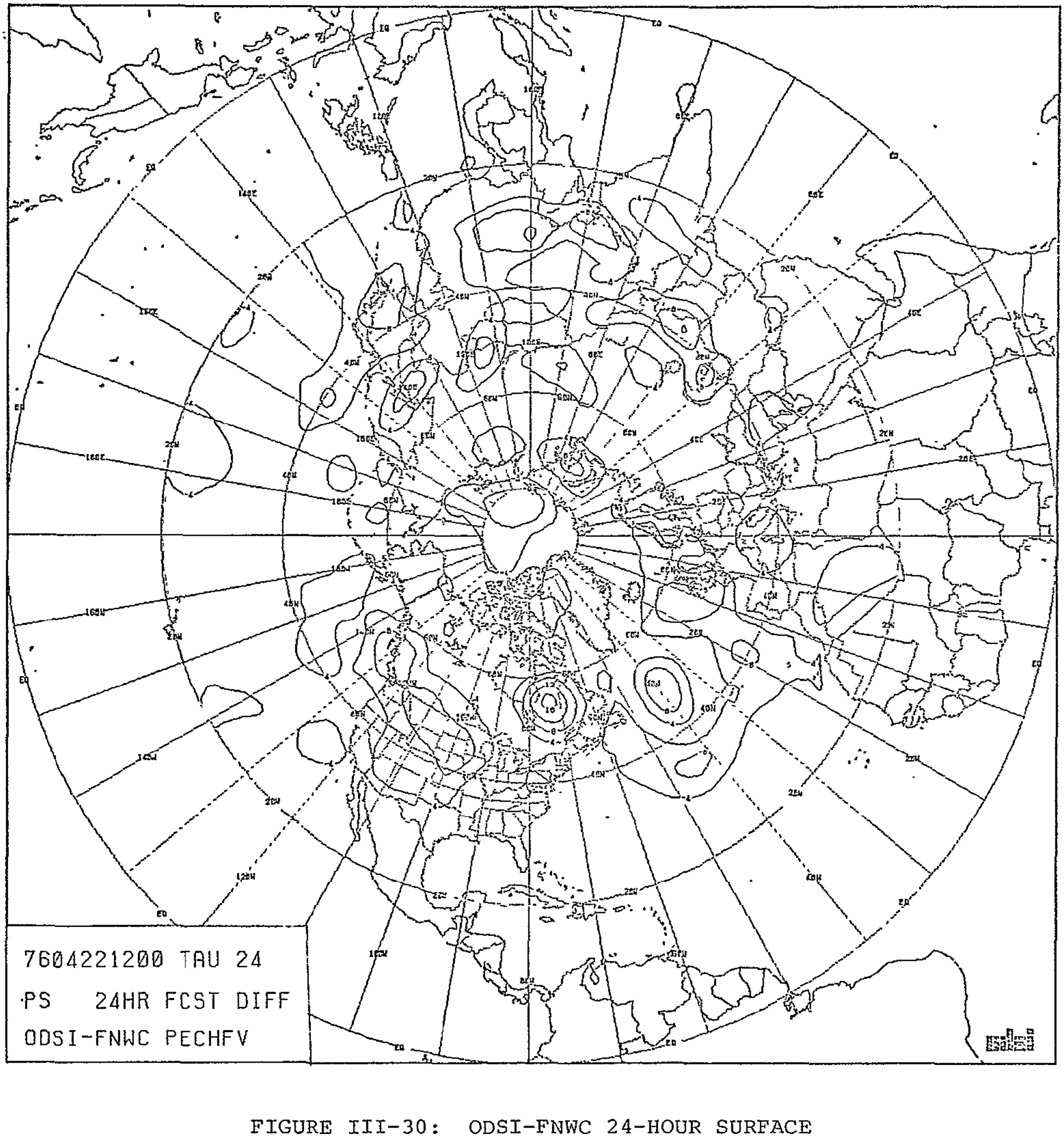

FIGURE III-30: ODSI-FNWC 24-HOUR SURFACE FORECAST DIFFERENCE (PECHFV) 4/23/76 1200Z

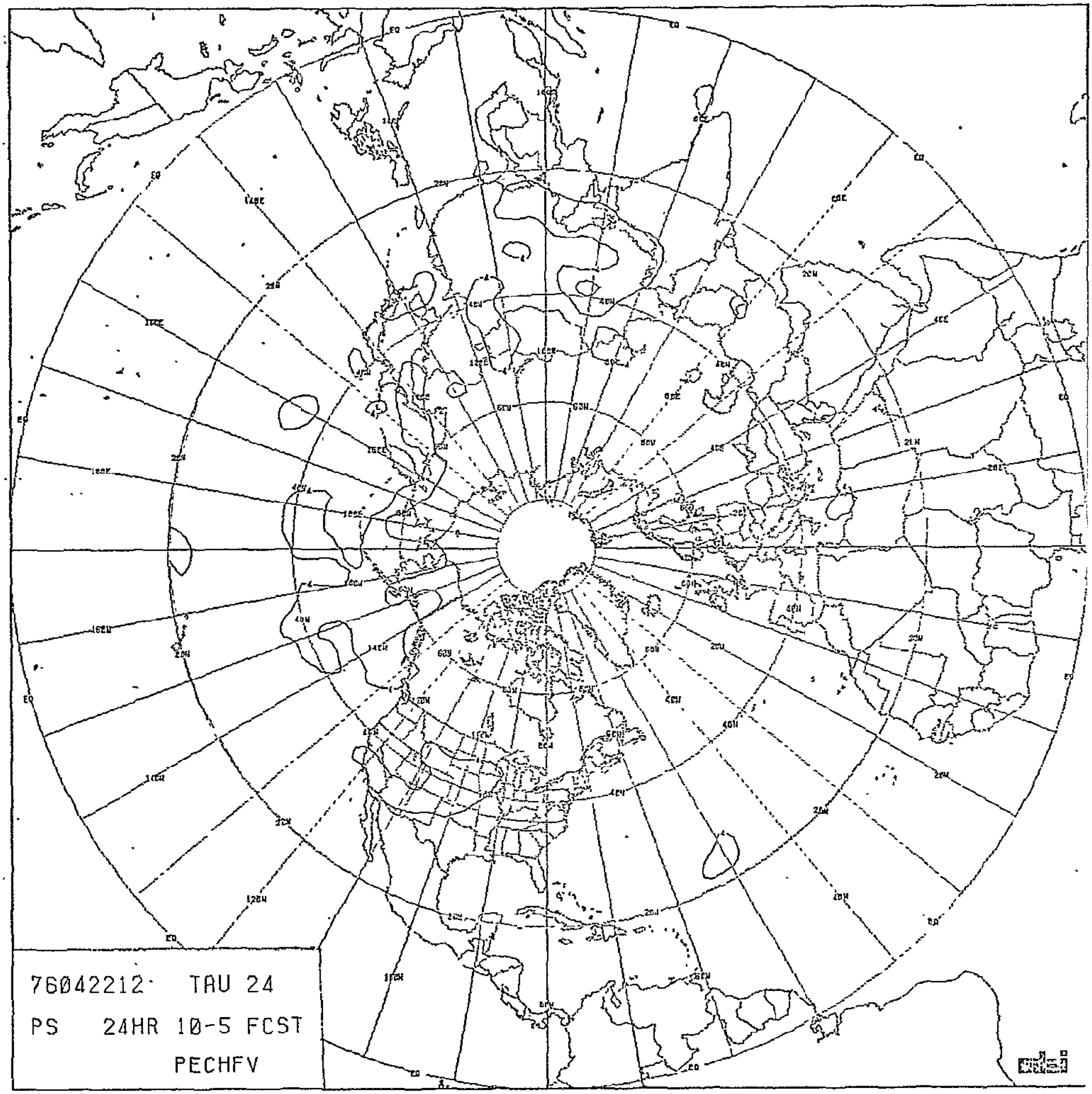

FIGURE III-31: ODSI TEN LEVEL (PECHFV)-
FIVE LEVEL (PECHCV) SURFACE
FORECAST DIFFERENCE 4/23/76
1200Z

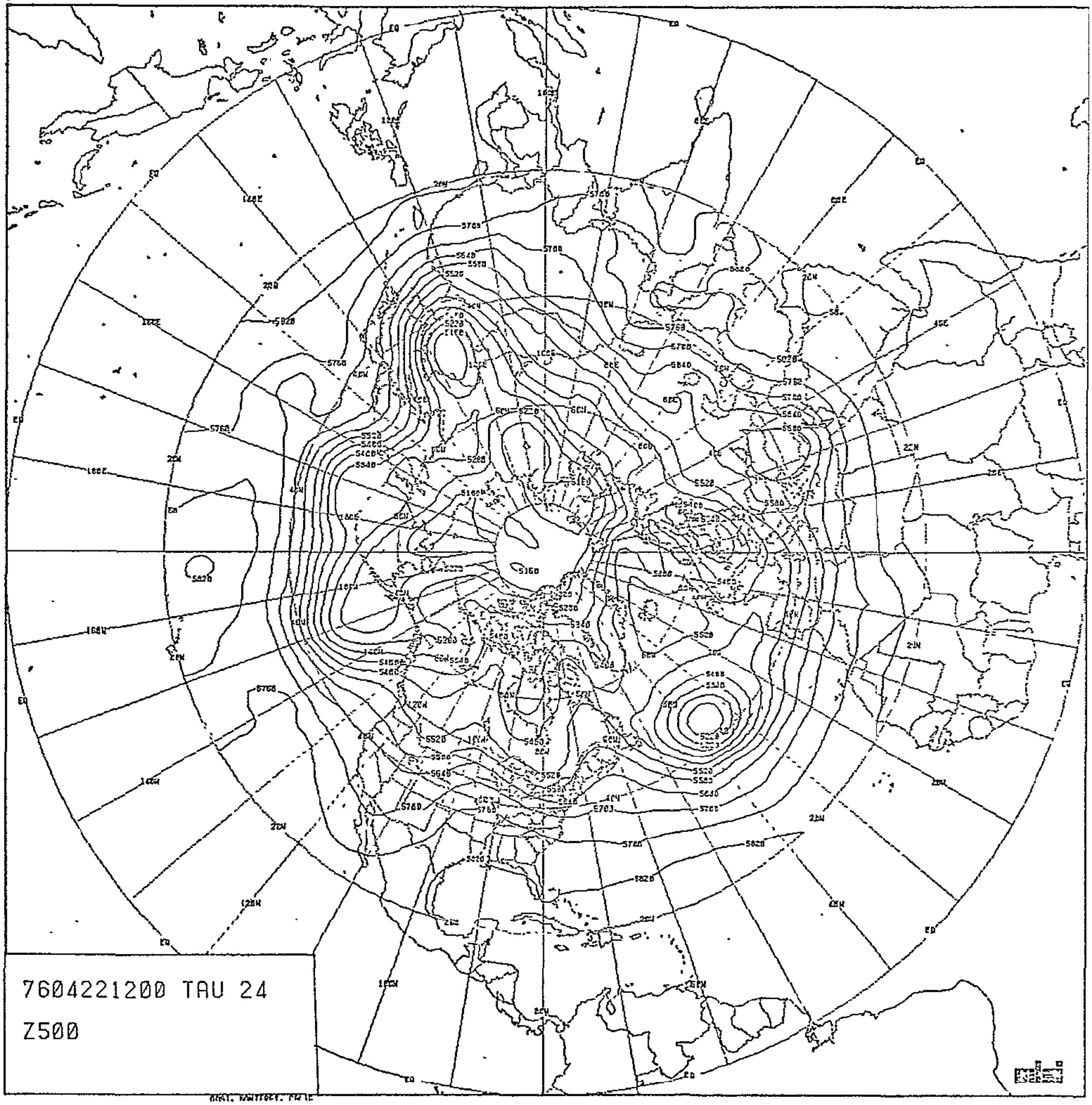

FIGURE III-32: ODSI 24-HOUR 500mb FORECAST
(PECHFV) VERIFYING 4/23/76
1200Z

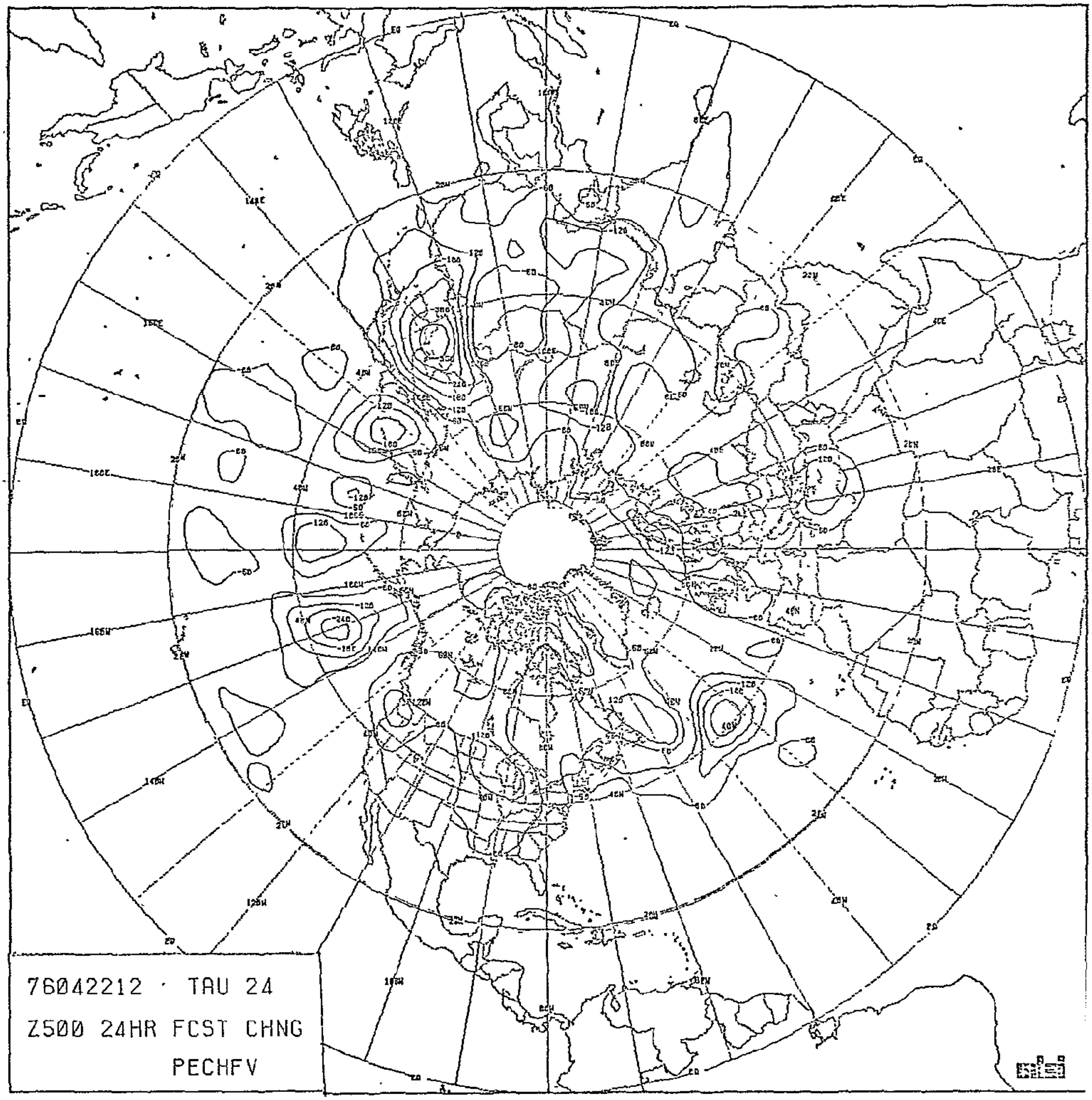

FIGURE III-33: ODSI 24-HOUR 500mb FORECAST CHANGE (PECHFV) VERIFYING 4/23/76 1200Z

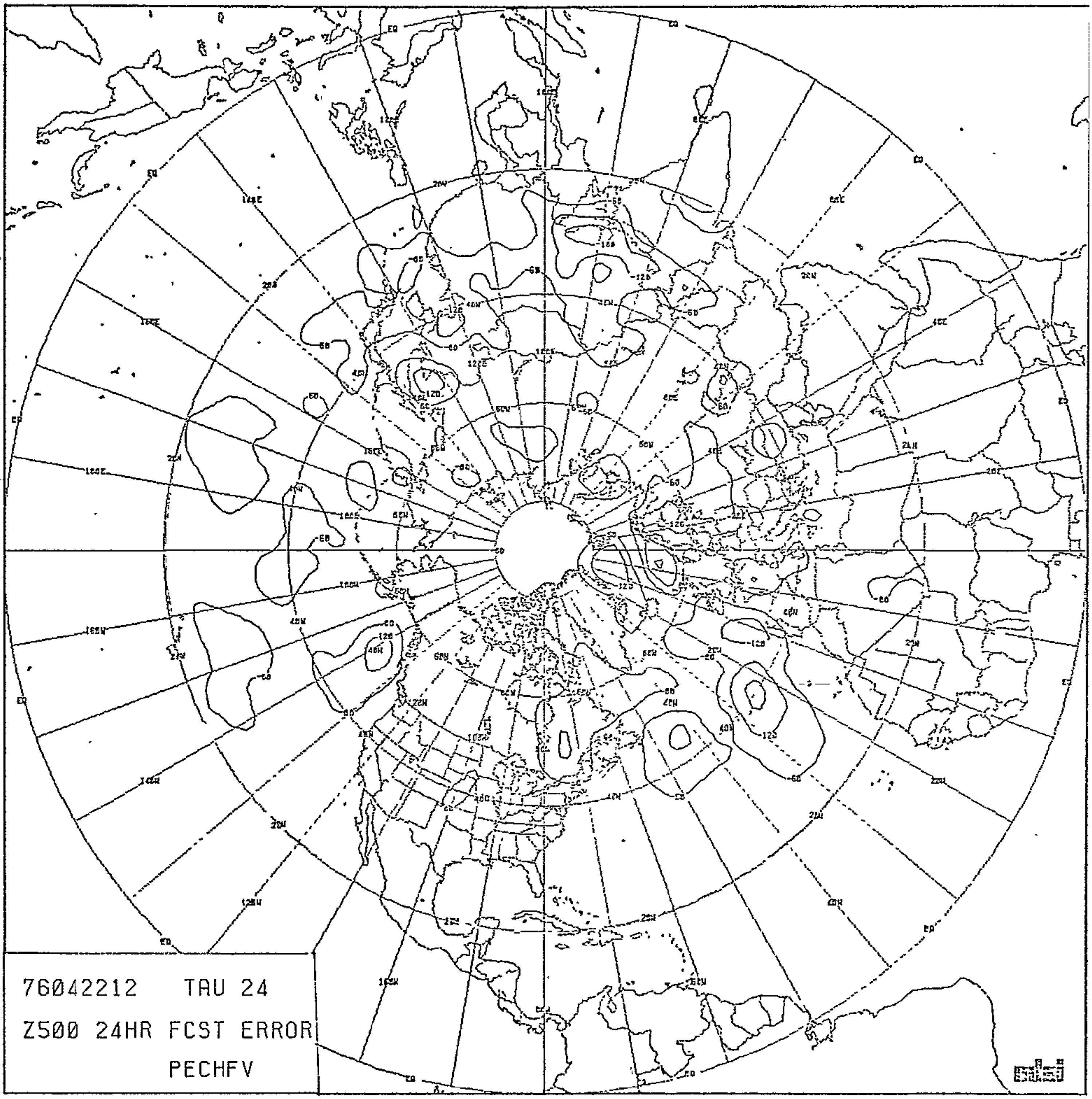

FIGURE III-34: ODSI 24-HOUR 500mb FORECAST ERROR (PECHFV) VERIFYING 4/23/76 1200Z (VERIFICATION ODSI ANALYSIS)

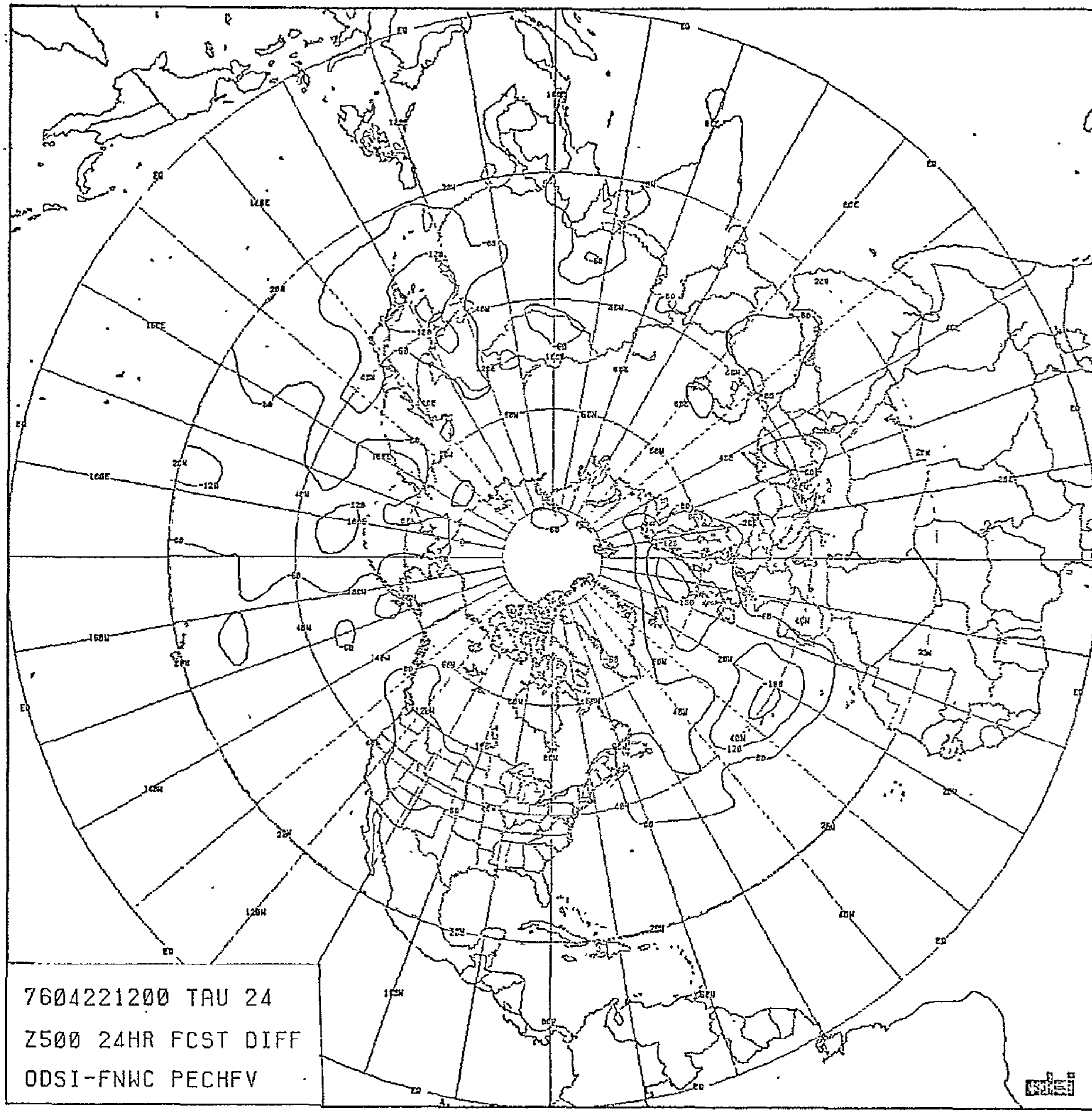

FIGURE III-35: ODSI-FNWC 24-HOUR 500mb FORECAST DIFFERENCE (PECHFV) 4/23/76 1200Z

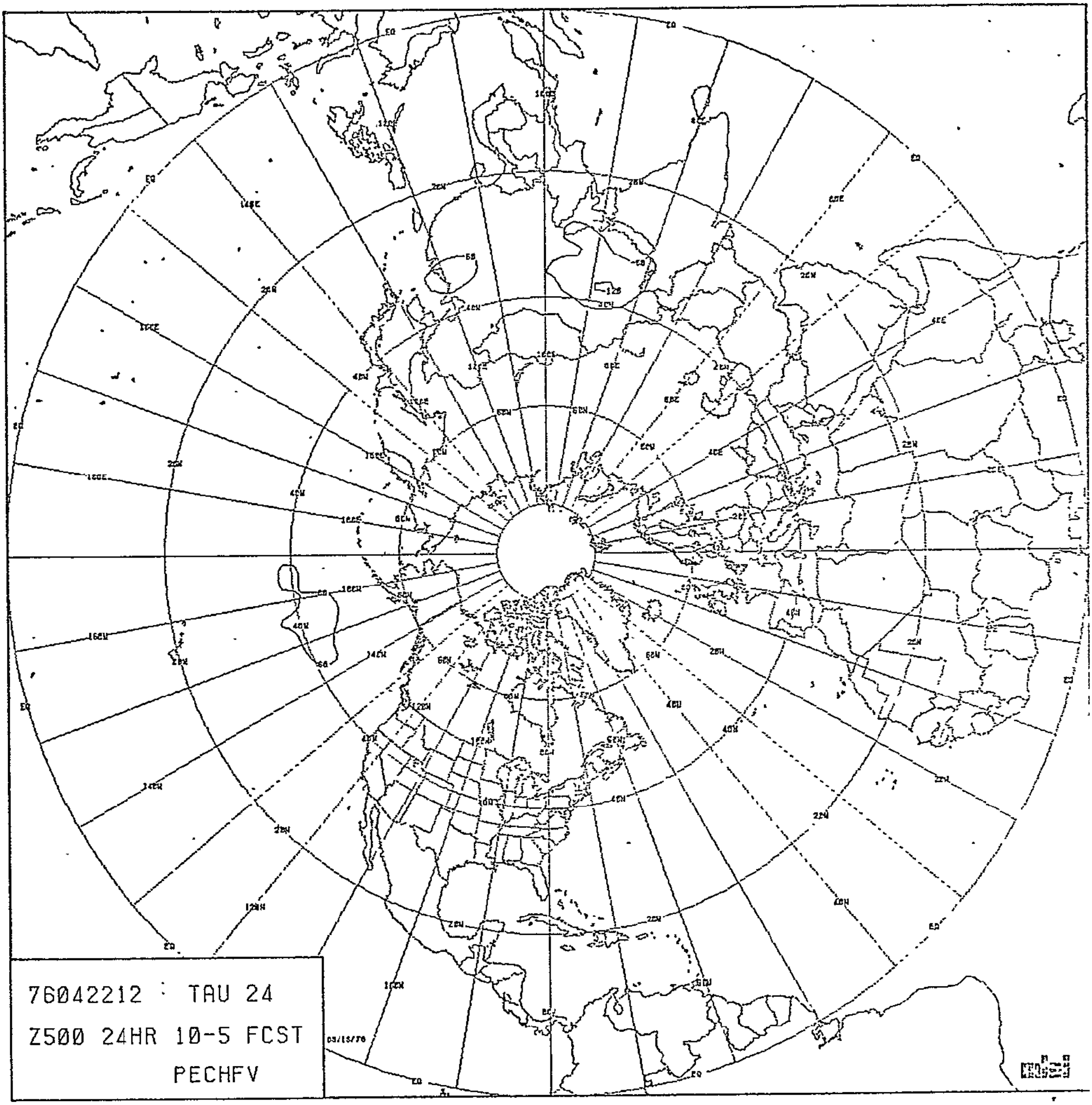

FIGURE III-36: ODSI TEN LEVEL (PECHFV)-
FIVE LEVEL (PECHCV) 500mb
FORECAST DIFFERENCE
4/23/76 1200Z

IV. SUMMARY

As part of the SEASAT program of NASA, a set of atmospheric analysis and prediction models was developed for ECON, Inc. under Contract NASW-2558, Modification 5. The analysis models developed consisted of hemispheric coarse mesh (63 x 63) and fine mesh (187 x 187) models which include, in addition to sea surface temperature and sea level pressure analyses, twelve levels of temperature, height and wind analysis. The set of forecast models developed consist of the hemispheric, primitive equation models listed below:

- PECHCV - five sigma layers and a 63 x 63 grid
- PECHFV - ten sigma layers and a 63 x 63 grid
- PEFHCV - five sigma layers and a 187 x 187 grid
- PEFHFV - ten sigma layers and a 187 x 187 grid.

These analysis and prediction models are intended to be test vehicles to evaluate the impact of SEASAT data on the analysis-forecast process for numerical weather prediction systems of this type. Due to the open-ended nature of model development, the models should not be considered as completed, but, rather as solution elements at this point in time and subject to change. In fact, work is continuing on the development and testing of these models for NASA under contract to JPL.

Due to insufficient computer resources during the contract period, the high resolution (187 x 187) analysis and forecast models were not excercised. Complete test results will be published at a later date when all of the analysis and prediction models have been tested. A meteorologically active period (4/21/76 12Z through 4/23/76 12Z) was chosen as the test period for the analysis and prediction models. Rapid movement of systems and intense cyclogenesis occurred during this period and, thus, a severe test of model performance was offered.

The first forecasts obtained were disappointing, but considering the severity of the test and the lack of tuning through repetitive use of the analysis-forecast model combination, not too bad. Numerous problem areas were discovered and discussed above, and solutions were proposed for these problems. The report on the complete analysis and forecast model tests will reflect many of these proposed solutions.

In summary, the goal of developing a model context for assessing the impact of SEASAT data on the analysis-forecast cycle of numerical weather prediction has been largely realized in this contractual effort. The models will be developed further in ongoing contractual efforts in order to identify and examine some of the limiting factors in short-range weather prediction.